Development and Evaluation of a Permeation Plug Release Vessel (PPRV) for the Release of Perfluoromethylcyclohexane (PMCH) in Underground Mine Tracer Gas Studies

Edmund Chime Jong

Dissertation submitted to the Faculty of Virginia Polytechnic and State University in partial fulfillment of the requirements for the degree of

Doctor of Philosophy
in
Mining Engineering

Kramer D. Luxbacher, Chair
Zach Agioutantis
Michael E. Karmis
Inoka E. Perera
Erik C. Westman

December, 18, 2013
Blacksburg, VA

Keywords: tracer gas, underground mine ventilation, perfluoromethylcyclohexane (PMCH)

Abstract

Development and Evaluation of a Permeation Plug Release Vessel (PPRV) for the Release of Perfluoromethylcyclohexane (PMCH) in Underground Mine Tracer Gas Studies

Edmund Chime Jong

The use of sulfur hexafluoride (SF_6) as a tracer gas for analyzing underground mine ventilation systems has been practiced for over 30 years. As a result, the methods used to release, sample, and analyze SF_6 are well accepted. Although improvements are still being made to enhance the analysis of this tracer, the overall technique remains largely the same. However, as the complexity and size of underground mine ventilation networks increase, coupled with steadily rising SF_6 background levels, the ability of a single gas to function as a convenient, rapid means of analysis diminishes. The utilization of multiple tracer gases can mitigate these problems by allowing for a more comprehensive evaluation using multi-zone techniques. A well-documented alternative in HVAC studies to SF_6 as a tracer are perfluorocarbon tracers (PFT). Many PFTs exist as volatile liquids at room temperature and pressure. This characteristic prevents a PFT from being released using the same technique as SF_6. This paper introduces a passive release method for PMCH. Details about the development of the permeation plug release vessel (PPRV) from creating a GC calibration curve for vapor PMCH to the final field evaluation are presented. The following study successfully developed a mine-scale PPRV. The PPRV is designed to passively deploy PMCH vapor at linear. An equation was derived in this study that allows the prediction of the release rate as a function of temperature and plug thickness. Details regarding the development of the PPRV from preliminary laboratory studies to final field evaluations are provided.

Acknowledgements

I would like to thank my advisor, Dr. Kray Luxbacher, for her guidance and support throughout the course of my graduate career. Dr. Luxbacher's kindness, understanding, and advice have shaped me into the student I am today. I wish to thank Dr. McNair who has shared his knowledge of gas chromatography above and beyond what was needed of him. He has been both a mentor and a friend to me throughout my career as a graduate student. I also appreciate the support of my committee members, Dr. Zach Agioutantis, Dr. Eranda Perera, Dr. Michael Karmis, and Dr. Erik Westman. These four people have graciously taken the time out of their exceptionally hectic schedules to serve on my committee. I wish to thank Dr. Russell Dietz, Brookhaven National Laboratory, who has been generous with his time and knowledge of perfluorocarbon tracers and Rudy Maurer Jr., Dyno Nobel, who has been instrumental in supplying the aluminum shells used in this study. I would like to thank both the operators of the field study site and the Laboratory for Interdisciplinary Statistical Analysis (LISA) for their support and guidance. Without the help of these two organization, the final iteration of this research project would not have been a success. I would like to express my appreciation for the opportunity given to me by the Department of Mining and Minerals Engineering at Virginia Tech and the National Institute for Occupational Safety and Health (NIOSH) to pursue my research. Finally, I could not have completed this research without the support of my fellow students, especially Kyle Brashear, Susanne Underwood, and Jamie Howard, my mother, my father, and especially my wife, Catherine. Without Catherine's help and support, this dissertation would not have come to fruition.

This publication was developed under Contract No. 200-2009-31933, awarded by the National Institute for Occupational Safety and Health (NIOSH). The findings and conclusions in this report are those of the authors and do not reflect the official policies of the Department of Health and Human Services; nor does mention of trade names, commercial practices, or organizations imply endorsement by the U.S. Government.

Table of Contents

List of Tables

List of Figures

Chapter 1: Introduction

A ventilation systems is an essential element of underground mining. Ventilation provides fresh air to workers, carries harmful gases out of the mine, and prevents the accumulation of hazardous fumes. These systems must be maintained on a regular basis to fulfill these tasks. Ventilation systems are maintained by verifying the operating compliance of air ways, ventilation fans, and ventilation controls. These components ensure that the necessary amount of ventilation is provided to all areas of the mine. Without the cohesive functioning of fans and controls operating at design specifications, the effectiveness of the ventilation system can be adversely affected. Design and placement of new ventilation components as well as the maintenance of existing components are determined from ventilation surveys (Hartman et al. 1997).

Mine ventilation surveys involve the collection of air flow data in key areas of the mine. These surveys are designed to check air velocities, air quantities, and pressures. Once complete, the data are used to either create or validate mine ventilation models. These models are used to evaluate the effectiveness of a mine ventilation system, plan for mine expansion, and prepare for future ventilation changes. The model's degree of accuracy depends on the quality of the survey data. Unfortunately, fully representative data are difficult to achieve due to the intricacies of underground airflow patterns. This problem is especially apparent in areas with complex geometries or in locations that are inaccessible by personnel. For example, when data are gathered in intricate ventilation branches, such as in longwall gobs and bleeders, the sheer number of possible flow paths makes planning a traditional survey very challenging. For surveys of an active mine, the dynamic nature of mines, including geologic conditions, equipment operations, personnel movements, and atmospheric changes, creates sources of error. During an emergency situation, the challenges when using traditional techniques are exponentially increased as accessibility to desired survey areas becomes drastically limited.

Surveys assist in the regular maintenance of ventilation systems. Environmental conditions, such as humidity, dust, ground movements, and water influx, stress the integrity of ventilation controls. As metals corrode and barriers degrade, ventilation controls will inevitably fatigue and fail. Visual inspections and regular maintenance are currently the most effective means to

prevent complete failures. Once a minor fault is discovered, such as a leak, the component can repaired before a failure occurs. However, even with regular inspections, minor leaks and re-circulations can be missed due to the sheer volume of items that must be examined. Tracer gas based surveys provide a viable supplement to traditional means in such cases.

Tracer gases have the unique ability to not only traverse inaccessible areas, but to also characterize complex flow patterns and small-scale flows such as leakage. One of the principal requirements of a tracer gas is that it has no significant natural background presence. As a result, if a significant concentration of tracer gas is detected in a location, then the ventilation flow must have a direct path to that location. This property is especially useful in the identification and quantification of leakage. If an emergency situation arises, traditional ventilation surveying techniques are severely limited as information about the ventilation system must be gathered remotely. Tracer gases in this type of situation can not only be readily deployed and analyzed from remote locations, but can also traverse collapsed entries as well as identify damaged ventilation controls. The mining industry has already used tracer gases for this purpose (Grot et al. 1995, Grot and Lagus 1991).

Sulfur hexafluoride (SF_6) has been used as the mining industry's standard and sole tracer gas for several decades. SF_6 has been very effective in accomplishing numerous underground tracer gas studies. However, the ability of SF_6 as a lone tracer is beginning to diminish as ventilation systems become more complex. The previous studies were confined to single area, or single zone, deployments of SF_6. Such deployments are only effective if the area being investigated can be confined to a single flow volume. If information is needed about the interaction between separate, independent flow volumes, then a multi-zone approach must be taken.

For example, many single zone releases of SF_6 have analyzed flow paths across gobs. Depending on the release location, these flow paths can only be determined for one direction. A completely separate tracer gas release must be executed in order to determine flow path for the other direction, which is costly and time consuming. The single tracer issue is further compounded by the increasing natural background levels of SF_6 thereby reducing its detection sensitivity. A solution to these problem is the addition of perfluoromethylcyclohexane (PMCH) as a

supplemental tracer gas to SF_6. PMCH has already been used in numerous multi-tracer studies across various disciplines. However, this approach is novel to the underground mining industry. As such, standardized operating protocols for the deployment of PMCH have not yet been established. The investigation presented in this paper provides and evaluates a means appropriate for a mine-scale release of PMCH.

Chapter 2: Literature Review

2.1 Tracer Gases

Tracer gases have been applied to a large variety of study areas that include commercial heating, ventilation, and air conditioning (HVAC) systems, atmospheric transport models, pollutant dispersion patterns, geological reservoir monitoring, and underground mine ventilation. Tracers are used in these studies to qualitatively or quantitatively characterize various types of suspended, turbulent flows such as atmospheric currents, air pollutant movements, reservoir leakage rates, and ventilation streams in locations where traditional practices are impractical or impossible to implement. In order to perform a flow characterization, a tracer gas, by definition, must be a substance that does not have a significant background presence in the region being investigated. In principle, this definition encompasses a large variety of gaseous compounds such as hydrogen, methane, carbon monoxide, and carbon dioxide. Although these aforementioned substances have been used as tracers in the past, the type and number of desired tracer gas properties have evolved over time.

Modern tracers must be gaseous at the desired operating temperature, non-toxic, non-allergenic, chemically inert, odorless, tasteless, non-flammable, non-explosive, easily transported, easily dispersed, easily sampled, quantified with high reliability, measured with repeatability, and economical to deploy (Collins et al. 1965, Grot and Lagus 1991). Sulfur hexafluoride (SF_6), halogenated compounds, and perfluorocarbons are examples of such substances, which are also, incidentally, the most commonly used tracer gases. The main advantage of these three tracer groups is afforded by a combination of their trace-level background presence and detectability at extremely low concentrations.

The low background presence of these tracers enhances detection sensitivity by limiting interference from background contamination. Therefore, a high signal to noise ratio can be achieved even at trace-level concentrations, such as in the parts per quadrillion (PPQ) by moles. These modern tracers, especially SF_6 and perfluorocarbons, are able to take advantage of this low background presence with enhanced detectability. This characteristic stems from these tracer

gases' high molecular electronegativity. Electronegativity allows detection and quantification using a gas chromatograph (GC) equipped with an electron capture detector (ECD). Tracer gases can also be detected with GCs outfitted with a mass spectrometer (MS) or any other detector based on electron capture (EC) such as a negative ionization chemical ionization mass spectrometer (NCI-MS). Although other detection methods are available, GC-ECD and NCI-MS provide the highest sensitivity for electronegative substances. A detailed summary of GC analytical systems with respect to tracer gas analysis is provided in a later section.

The GC-ECD is the most common analytical system due to repeatable detection limits in the parts per trillion (PPT) coupled with lower operating costs when compared to the GC-MS. This cost difference is derived from the fundamental operational differences between the two analytical platforms. The GC-ECD system, as opposed to the GC-MS, is designed to be quantitative but not qualitative. If a positive identification of the tracer gas is required, then the GC-MS system is preferred.

The added advantage of highly sensitive detectability with modern tracers enables the quantification of small-scale flows such as leakage as well as of large-scale ventilation systems. Additionally, less tracer gas is required to achieve the minimum detection threshold, which in turn facilitates greater usage efficiency and lower operating cost for tracer deployments. Trace-level detectability combined with the desired tracer properties provide these gases with excellent versatility as both a qualitative and quantitative flow analysis tool. This versatility is especially demonstrated by tracer gas investigations of ventilation systems.

Although an assortment of tracer gas survey techniques are available for surveying ventilation systems, the overall procedure can be generalized into three main parts: release, sampling, and analysis. The execution of each individual part, however, differ depending on the type of tracer gas study being performed. Two main types of tracer gas studies, continuous or pulse, are commonly performed. The continuous release method will be discussed first.

One of the benefits of using many tracer gases is that they exist as a gas throughout the desired operating conditions. Thus, a variety of release techniques may be used to deploy gaseous tracers

for the continuous release method. However, certain tracers, such as perfluorocarbons, can exist initially as a volatile liquid at normal temperature and pressure (NTP). As such, a specialized release systems must be utilized. Volatile liquid tracer release systems will be covered in detail in later sections. Gaseous tracers, alternatively, can be purchased in convenient, readily available, and standardized compressed gas cylinders. From this medium, many options are available for a controlled release. Three of the more popular release options are the differential weight method, the flow meter method, and the flow controller method.

The differential weight method is executed simply by weighing the gas cylinder before and after a release and noting the time allotted for the discharge. Thus, a release weight per unit time for the tracer can be computed. Although crude, this method can be effective if care is taken to provide a constant, continuous flow rate from the cylinder. The flow meter method utilizes an analog or a digital flow meter attached to the gas cylinder. The tracer gas is then released at a pre-determined volumetric flow rate, which can be translated to a mass flow rate if necessary. This method offers significantly more control and flexibility than the differential mass method but requires the acquisition of a suitable flow meter. The third method is the flow controller method. Flow controllers are sophisticated electronic regulators that allows for precise deployment of tracer gases either by mass or by volume. This method provides the greatest accuracy, reproducibility, and control of the three common release approaches. However, a flow controller can be costly depending on the desired features, such as accuracy, data storage, etc. For continuous tracer releases in the field, the manner in which these release methods are utilized can vary. Three main versions of the continuous release method are commonly employed. These versions are the constant injection method, the constant concentration method, and the tracer decay method (McWilliams 2002, Grot and Lagus 1991).

All versions of continuous releases, as the name implies, deploy tracer gases based on a continuous flow rate. The fundamental mathematical relationship between tracer gas, concentration, and ventilation flow rate for continuous releases is derived from instantaneous mass balances. For the constant injection method in a single contiguous zone, tracer gas is released into the test area at either a constant mass flow or a constant volumetric flow rate. The tracer is then allowed to equilibrate with the ventilation flow thus producing a mathematical

relationship between tracer concentration and single zone air flow rate. This relationship is represented in Equation (2.1). This equation assumes that the additional volumetric flow of the tracer as well as the loss of tracer flow due to leakage is negligible. The air flow is also assumed to be fully turbulent to ensure complete, homogeneous mixing of the tracer at the sampling point. The complete mixing of the tracer is essential for flow quantitation if an advanced ventilation model is not available for comparison. The concentration of the tracer gas by volume is represented in the following manner.

$$C_T = \frac{Q_T}{Q_A} = \frac{M_T}{\rho_T Q_A} \qquad (2.1)$$

C_T	Concentration of tracer gas downstream from release point as a fraction by volume
Q_T	Volumetric flow of tracer gas (m^3/s)
Q_A	Volumetric flow of air (m^3/s)
M_T	Mass flow of tracer gas (kg/s)
ρ_T	Density of tracer gas at ambient environmental conditions (kg/m^3)

Equation (2.1) can be rearranged as follows to determine the air flow quantity through the zone as a function of tracer gas release rate and concentration.

$$Q_A = \frac{Q_T}{C_T} = \frac{M_T}{\rho_T C_T} \qquad (2.2)$$

Equation (2.2) is valid only if the inflow air quantity to the zone is equal to the outflow air quantity at the sampling point. If the sampling area is located in a discontinuous branch that is not reconciled at the survey zone, then the ventilation characteristics of the individual branches must be known to conduct a proper quantitative analysis.

Without prior knowledge of the individual branch ventilation characteristics, flow quantitation is not possible using Equation (2.2). As a result, the study would be restricted to a qualitative characterization. Qualitative studies, nevertheless, are still useful in their ability to identify flow paths, leakage, and damage to ventilation controls. However, the extent of flows such as short-circuiting cannot be positively identified without quantitation.

The constant concentration method is the most complex option for the continuous release technique. This method releases tracer gas in a manner that maintains a constant tracer concentration in the target flow volume. In order to achieve this result, the tracer concentration in the zone is continuously monitored. The injection rate of the tracer is then adjusted electronically to maintain a continuous tracer concentration in the ventilation stream. Thus, a mathematical relationship between tracer injection rate and ventilation flow rate is produced. This relationship is given by the following equation.

$$Q_A(t) = \frac{Q_T(t)}{C_{target}} = \frac{M_T(t)}{\rho_T C_{target}} \qquad (2.3)$$

C_{target}	Target steady state concentration of tracer gas at the monitor point as a fraction by volume
$Q_T(t)$	Volumetric flow of tracer gas (m^3/s) over time
$Q_A(t)$	Volumetric flow of air (m^3/s) over time
$M_T(t)$	Mass flow of tracer gas (kg/s) over time
ρ_T	Density of tracer gas at ambient environmental conditions (kg/m^3)

The tracer decay method is the most widely implemented technique used in building ventilation studies due to its simplicity. Tracer gas is released into a target volume for a finite amount of time to achieve a desired tracer concentration. After the release period has elapsed, the ventilation flow is monitored over time to determine the decay of the tracer concentration. A relationship can thus be established between tracer decay and ventilation flow. This relationship is given in the following equation.

$$I = \frac{1}{t} \ln\left(\frac{C_{T_0}}{C_{T_1}}\right) \qquad (2.4)$$

I	Air change rate in zone (changes per second)
t	Monitor time (s)
C_{T_0}	Initial tracer concentration as a fraction by volume
C_{T_1}	Final tracer concentration as a fraction by volume

The air change rate is defined as the volume normalized ventilation rate, which is represented by the following equation.

$$I = \frac{Q_A}{V} \qquad (2.5)$$

I	Air change rate in zone (changes per second)
Q_A	Air flow rate in the zone (m^3/s)
V	Volume of the zone

The previous equation shows that the air change rate is the number of total air volume replacements per unit time that the zone undergoes. This technique is particularly useful in determining the time necessary to dilute a zone if a contaminant is released.

The previous overview of the continuous release technique demonstrates its one great advantage, an overall ease of execution. Planning and post-processing computations are straightforward and procedurally compact thus reducing occurrences of systematic errors. The non-reactive and gaseous nature of the three tracers allow a variety of both passive and active sampling techniques to be used. The most common passive sampling method is the capillary adsorption tubes (CAT). A CAT is a passive sampler used in tracer gas ventilation studies. The most common form of CAT sampler, or CATS, is composed of a glass tube filled with a measured amount of adsorbent, such as activated charcoal (Winberry et al. 1990). Once exposed to atmosphere, the adsorbent will sample the air at a constant rate thus producing self-integrating concentration over the exposure time period. The sensitivity of CATS can be improved if needed with the addition of air pumps and gas filters. Once adsorbed, the air sample will remain in the adsorbent until the CATS is thermally desorbed to a GC (Dietz et al. 1986, D'Ottavio, Goodrich, and Dietz 1986). The most common active sampling methods are gastight syringes, sampling bags, and evacuated containers. The tracer sampling process is further simplified due to the absence of a time dependent sampling interval. This simplification is a result of the fact that the continuous release technique is based on a consistent and homogeneous tracer concentration. Thus, as long as sufficient time is allotted for uniform mixing of the tracer in the ventilation stream, the actual instant and interval at which tracer samples are taken are inconsequential.

The primary disadvantage to the continuous release technique is the sheer amount of tracer that is needed for a large-scale ventilation study. Depending on the size of the ventilation system, such a study may become cost prohibitive. Additionally, the elevated size of a large-scale

continuous release dramatically increases the ambient background of the tracer. As a result, more time will be needed to reduce the tracer's background presence to an acceptable level if other surveys are desired. These issues are especially prevalent in tracer gas studies of underground mine ventilation systems. As a result, certain situations may warrant the use of an alternative method, such as the pulse release technique.

The pulse release technique discharges a known quantity of tracer gas as an "instantaneous" cloud that is allowed to travel through the ventilation system. Consider the analogy of a dye filled balloon submerged in a flowing stream. The balloon is popped at some point in time thus releasing the red dye as a cohesive plume in the stream. Given that the stream has sufficient turbulence, the cloud of dye will uniformly mix across the width of the stream thus producing homogeneous pulse of dye across the cross-section of the stream. This homogeneity across the cross-section of the flow volume is a representation of ideal pulse release tracer behavior. As can be inferred from the aforementioned example, a pulse release requires an integrated mass balance for quantitation. This mass balance is effectively demonstrated with a single zone pulse tracer study.

For a single zone pulse release, the downstream concentration of tracer gas must be computed over time. From the continuous release technique, the following relationships were established.

$$C = \frac{Q_g}{Q} \qquad (2.6)$$

$$Q_g = \frac{M_g}{\rho_g} \qquad (2.7)$$

C	Concentration of tracer gas downstream from release point as a fraction by volume
Q_g	Volumetric flow of tracer gas (m^3/s)
Q	Volumetric flow of air (m^3/s)
M_g	Mass flow of tracer gas (kg/s)
ρ_g	Density of tracer gas at ambient environmental conditions (kg/m^3)

Using the aforementioned relationships, the following figure of the flow-averaged tracer concentration can be generated by plotting concentration vs. time (C vs. t).

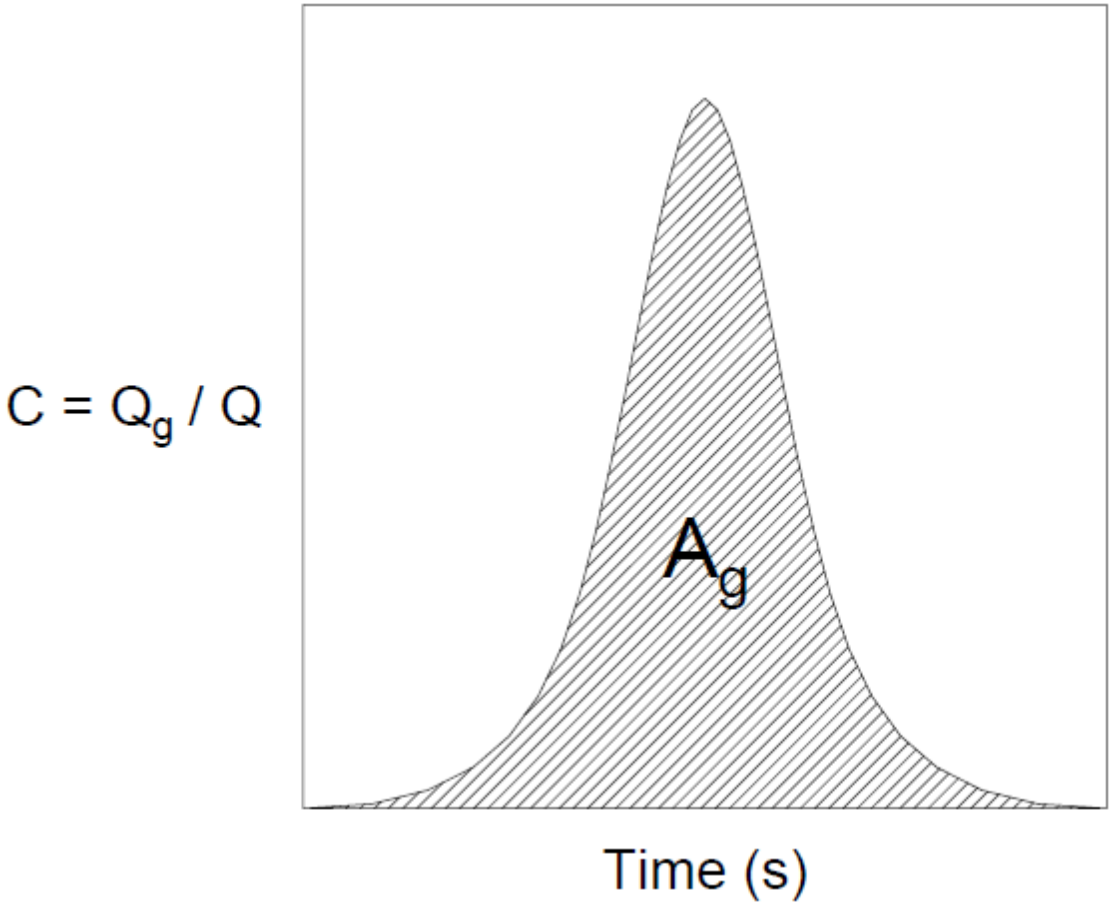

Figure 2.1. Plot of pulse tracer concentration over time.

Assuming that the tracer pulse concentration is well mixed across the cross-section of the flow and that the magnitude of the tracer pulse does not significantly impact the ventilation flow, the area under the curve, A_g, for **Figure 2.1** can be represented as follows.

$$A_g = \int_{t_0}^{t} C\ dt = \frac{1}{\rho_g Q} \int_{t_0}^{t} M_g\ dt \qquad (2.8)$$

A_g	Volume of tracer gas that passes the sampling point (m^3)
T	Total sampling time (s)

Additionally, the total released mass of tracer gas can be represented as follows assuming no losses in the system thus asserting that the mass of the tracer injected into to the zone is equal to the mass of the tracer exiting the zone.

$$M = \int_0^T M_g \, dt \qquad (2.9)$$

Equation (2.8) can be substituted into the relationship into Equation (2.9) give the following.

$$A_g = \frac{M}{\rho_g Q} \qquad (2.10)$$

Rearranging Equation (2.10), the following relationship can be established.

$$Q = \frac{M}{\rho_g \, A_g} \qquad (2.11)$$

Equation (2.11) can now be used to compute the airflow quantity in the target volume using the recorded concentration over time. Identically to the continuous concentration method, if the sampling locations are located in discontinuous branches, the volumetric flows of the individual branches must be known prior to post-processing so that the sampled concentration of the tracer can be used to establish unexpected ventilation conditions (Hartman et al. 1997, Grot and Lagus 1991, Persily and Axley 1990).

The data required to perform this integration is gathered from continuous air sampling of the zone. In order to acquire a sufficient amount of data points, unlike the continuous release technique, the sample must capture the mass change of the pulse over a period of time. As a result, traditional active sampling methods would require multiple individual samples to be taken for the duration of the pulse. Enough data points would need to be sampled to compute an integrated mass. Although the mediums in which the collection of air samples occur are identical to those used in continuous releases, pulse releases require a sampling time and sampling interval to be defined. This added complexity is necessary to capture the mass distribution of the plume

as it travels through the sampling area. This traditional real-time sampling technique is, however, very cumbersome and difficult to implement. The concentration integral can alternatively be determined using the average tracer gas concentration at the sampling point (Persily and Axley 1990).

The average concentration in this sense could be captured through a continuous extraction process. This process would require a container of appropriate size and a means to continually transfer air into the container at a constant rate. The sampling apparatus would be activated before the pulse release and sample until the tracer is completely purged from the flow volume. The concentration integral could then be determined by multiplying the average tracer concentration in the container by the total sampling time. A CATS could also be utilized for the same purpose. As can be seen by the aforementioned overview, the pulse tracer technique has some advantages and disadvantages over the continuous tracer technique. The main advantages are afforded by lower tracer gas quantity requirements and increased repeatability. The nature of the technique allows the deployment of multiple, consecutive pulses to occur over a short period of time thus allowing replication. As a result, an estimate of repeatability and reliability of the study can be calculated (Persily and Axley 1990, Dietz et al. 1986).

The summary of the continuous release technique and the pulse release technique given in the previous section presents analysis techniques for simple, single zone applications of a single tracer gas. Tracer gases can, however, be utilized for multi-zone, inter-zone, and multi-path studies by using multiple, simultaneous tracer gas releases, differential equation based flow models, or a combination of the two. Multiple, simultaneous tracer gas studies will be covered in a later section. An in-depth discussion of the associated flow models will not be provided as this subject matter is beyond the scope of this cursory introduction as well as beyond the scope of the study presented in this discussion.

2.2 Gas Chromatography

Gas chromatography (GC) is the primer technique in the trace analysis of volatile compounds. As such, GC is the primary means by which tracer gas samples are evaluated. The overwhelming implementation of this technique in tracer gas research is derived from the ability of GC to separate and analyze multiple volatile compounds in a single sample while simultaneously maintaining exceptional analytical precision. This three-part process occurs in a standalone device called the gas chromatograph (GC).

A GC is composed of three primary components, the injector, the column, and the detector. After an air sample is collected, it must be introduced to the GC for analysis. The injector is the portion of the GC where this occurs. This component is responsible for two principal tasks, volatilization and dilution of the sample. As the name implies, a GC can only process samples that are in either a gas or vapor state. In order to ensure that all components of the air sample are in the appropriate state, the injector is heated to a temperature sufficient to completely volatilize all compounds. Once vaporization is complete, the sample is then reduced to a level that allows rapid transfer to the column. The degree of reduction is tailored to the analytical method being utilized at the time. The GC method will change depending on the properties of the analytes. After the injector has processed the sample, the analytes are transferred to the column.

The GC column is the medium in which the various constituents of the sample are separated prior to entering the detector. Separation allows the individual analysis of the multiple tracer compounds that may be present in the sample while removing interference from undesired components. Without the column, the analytes would enter the detector as an overlapping collection of compounds thereby nullifying any possible analysis of the individual analytes. In tracer gas studies, a capillary type column is most commonly used. The outside wall of a capillary column is comprised of a cylindrical fused silica shell. The inside wall of the column is coated with a thin film called the stationary phase.

The stationary phase is composed of either a high boiling point liquid or a layer of solid adsorbent particles fused to the silica wall. The phase is applied to the interior of the column in a

manner that allows unobstructed passage of the mobile phase through the center, which essentially makes the column a long, thin hollow tube. The mobile phase in terms of GC is a gas, usually helium, hydrogen, or nitrogen, which carries the sample from the injector, through the column, and into the detector. As the analytes move through the column, they will partition in and out of the stationary phase depending on their individual affinities for the constituents of the phase. The varying rates of partitioning by each individual analyte causes the compounds to separate. Once the analytes have been adequately separated, the compounds then move into the detector (McNair and Miller 2009).

A multitude of detectors can be utilized by a GC. The two most popular detectors for tracer gas analysis are the ECD and the MS. The ECD utilizes a Ni^{63} radioactive source to create an electron cloud inside the detector. This electron cloud is generated when the beta particles emitted by the Ni^{63} impact a continuous stream of nitrogen gas. Once the electron cloud is produced, a steady electrical response is outputted when a current is applied to the detector. As an electronegative substance pass through the cloud, some of the electrons will be captured by these analytes thus causing a decrease in the electrical signal. The magnitude of the signal attenuation is proportional to the compound's concentration. The GC is able to quantify this reduction in signal with extreme accuracy (McNair and Miller 2009). The majority of common tracer gas compounds are electronegative in nature. As such, an ECD is one of the preferred detectors in tracer gas studies. Although not as popular, the MS is also utilized to a fair degree due to its ability to positively identify analytes.

Unlike an ECD, the MS is able to generate a mass spectrum of each analyte that enters the detector. The actual process by which the spectrum is produced is beyond the purpose of this overview and will not be discussed. The mass spectrum of a pure compound is unique to that analyte. Thus positive identification of fully separated analytes can be achieved, an ability that is generally not required in tracer studies due to the simplistic composition of the sample matrix. A MS also provides an electrical response proportional to the concentration of the analyte thus also allowing for quantitation. The MS additionally has the potential to achieve detection sensitivities beyond the ECD through the use of selected ion monitoring (SIM) and negative ion chemical ionization (NCI). Although more versatile from an analytical standpoint, the significantly higher

relative operating costs and overall operating difficulty of the MS compared to the ECD prevents the MS from being more significantly utilized.

2.3 Tracer Gases in Underground Mine Ventilation

The versatility of tracer gases as ventilation survey tools have resulted in their widespread utilization in a variety industries including underground mine ventilation. Tracer gases have the unique ability to probe areas of a mine that are either difficult to survey using conventional means or inaccessible to personnel. The overwhelming majority of these underground tracer gas studies have implemented SF_6 as the sole tracer compound.

SF_6 was originally produced in 1953 as an insulating gas for high voltage transformers and industrial circuit breakers (Turk et al. 1968). The physical properties that allowed SF_6 to serve as an ideal insulator naturally translated to the desired properties of an ideal tracer. SF_6 is a stable, inert, inorganic, colorless, odorless, and non-toxic gas with a boiling point of -64°C (-58°F) at 100 Pa (Lester and Greenberg 1950, Collins et al. 1965). SF_6 has a vapor pressure of 290 Pa at 21.1°C and a molecular weight of 146.055 g/mol. SF_6 is an anthropogenic compound and does not naturally exist in significant concentrations in the atmosphere. SF_6 is also readily available in multiple standardized gas cylinders, inexpensive, and readily deployable through various mediums. SF_6 also has a high ECD detection sensitivity resulting from its elevated electron absorption coefficient (Collins et al. 1965). This ECD sensitivity, near 1 PPB by moles, is granted by the high electronegativity of the six fluorine atoms surrounding the sulfur atom in the center (Turk et al. 1968). A graphical representation of SF_6 is displayed in **Figure 2.2**.

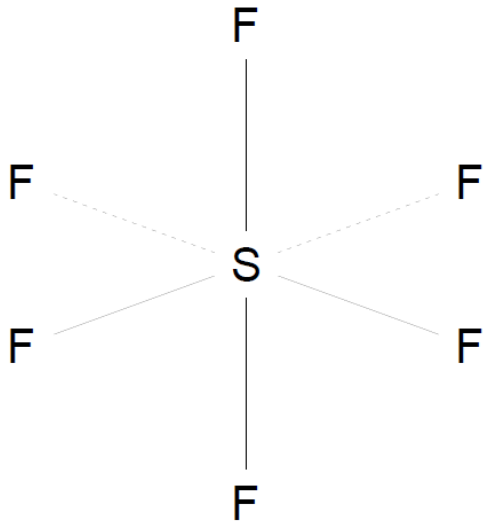

Figure 2.2. Sulfur hexafluoride molecule.

The detection sensitivity can be further enhanced using catalytic reaction or cold concentration GC techniques (Turk et al. 1968). Although the release of SF_6 is limited to a maximum of 100 PPM by volume, which is set by the American Conference of Governmental Industrial Hygienists (ACGIH), its detection sensitivity is sufficient to maintain its effectiveness as a tracer gas (Timko and Derick 1989). The main disadvantage of SF_6 can be attributed to its high molecular weight.

SF_6 is approximately five times heavier than air by molecular weight. This characteristic presents two challenges. These challenges are insufficient homogeneous mixing of SF_6 in non-turbulent conditions and longer background retention of SF_6 in complex geological areas. However, these challenges can be remediated with sufficient advance planning. Despite these issues, the physical properties of SF_6 classify this compound as an ideal tracer gas. As such, SF_6 has seen wide utilization in various disciplines.

Meteorological tracing and long-distance atmospheric pollutant transport studies have extensively used SF_6 as a tracer gas due to its high stability at altitudes below the mesosphere, the boundary of which is located about 50 km (30 mi) above the earth's surface (Clemons, Coleman, and Saltzman 1968). As an atmospheric tracer, SF_6 has been used in short-term studies to validate complex atmospheric transport circulation models and in long-term studies to

investigate atmospheric mixing between the stratosphere, hydrosphere, cryosphere, and troposphere (Maiss et al. 1996). In the field of pollutant transport, SF_6 has been used to track pollutant dispersion from an emission stack at the Keystone Power Plant in Shelocta, PA using a GC continuous analysis system configured for frontal chromatography. Frontal chromatography is a term used to describe a continuous tracer analysis technique that delays the passage of oxygen, nitrogen, and other such constituents to all the separation of SF_6 (Brown, Dietz, and Cote 1975). In related studies SF_6 was used to determine sulfur dioxide (SO_2) plume migration over the surrounding topography from various power plant stacks found at the Fawley Power station in Southern England. SO_2 plume migration for some of these studies was tracked using a GC-ECD built to apply nitric oxide to the molecular sieve column. This technique was shown to potentially track air mass movement for distances greater than 100 km (Dietz and Cote 1973, Emberlin 1981). In addition, SF_6 has been used to conduct tracer gas studies of various ventilation systems in buildings.

Building ventilation investigations have used SF_6 to determine the residence time of contaminants and the exhaust and post-exhaust reentry of contaminants in laboratories equipped with fume hoods (Drivas, Simmonds, and Shair 1972). SF_6 has also been used to evaluate the HVAC circulation profile of a seven-story federal office building (Grot et al. 1991) as well as to characterize ventilation flow rates in animal housing (Leonard, Feddes, and McQuitty 1984). The successful application of SF_6 to atmospheric, pollutant transport, and building ventilation studies demonstrates the flexibility of this substance as a multifaceted tracer gas. As such, this tracer has seen significant implementation in underground mine ventilation.

SF_6 has been used to determine the amount of return air recirculation from leakage between the intake and return (Kissell 1982), to quantify ventilation at coal faces (Timko and Thimons 1982), to evaluate auxiliary fans, to quantify low velocity flows, to measure flow rates in large entries, to determine the location of stopping leakage (Thimons, Bielicki, and Kissell 1974, Topuz, Bhamidipati, and Bartkoski 1982), to investigate shaft flows, to establish in-situ fan operating points, to evaluate auxiliary ventilation efficiency, to trace dust transportation paths, and to test escape route integrity with respect to fire contamination (Hardcastle et al. 1992). The unique ability of tracer gases to traverse areas that are either hazardous or inaccessible have simplified

the survey of gob, bleeder, collapsed areas, and the mine overall during an emergency situation. Studies of this type using SF_6 have included the determination of flow paths in longwall gobs to optimize methane drainage techniques (Diamond et al. 1999), the evaluation of longwall bleeder ventilation and gob gas vent-hole methane control systems (Mucho et al. 2000), the assessment of gob ventilation effectiveness and mine seal integrity (Timko, Kissell, and Thimons 1987), the determination of airflow paths and air velocities through gobs in room and pillar bleeder systems (Urosek and Watkins 1995), the quantification of gob porosity (Timko and Thimons 1982), as well as the identification of the neutral ventilation point in a collapsed tailgate gob (Young, Bonnell, and Genter 2001). The flexibility of SF_6 has also allowed its application to more novel underground tracer gas examinations.

Studies of this nature include using SF_6 to quantify the migration of radon from an East German uranium mine in Schlema, to determine the effect of fan-depressurization on radon levels in surface facilities (Raatschen, Grot, and Lobner 1995), as well as to simulate the progression of fire through intake and belt entries in a limited-entry mine (Timko and Derick 1989). SF_6 has also been applied to characterize airflow routes, identify leakage, and determine turbulent diffusion coefficients in the Pongkor cut and fill gold mine in Indonesia in an effort to verify a one dimensional Gaussian distribution ventilation model (Widodo et al. 2008).

As can be seen by the aforementioned summary, SF_6 has a variety of uses in surveying mine ventilation systems. However, the increasing complexity and scale of mines has caused a decrease in the capacity of SF_6 to function as a lone tracer. For example, although re-circulation and leakage have been analyzed using SF_6, the accuracy of such studies can be in question due to unknown discontinuities in flow paths. Along this lines, a single tracer can additionally not be used to fully determine interactions between multiple independent flow paths, a common facet of modern underground mines. The capacity of SF_6 as a tracer in terms of sensitivity is also beginning to diminish due to increasing atmospheric background levels.

Tracer gases rely on low background levels for their basic purpose, detectability against ambient background. In order for a tracer to be detectable, its released concentration must be higher than its background for an adequate signal to noise ratio. A higher tracer background presence

translates to a more concentrated deployment to achieve a detectable concentration. This effect is especially prevalent in high velocity flows or in flows through large openings. High tracer background may also prevent the detection of low quantity flows such as leakage. The problem of increasing background has especially affected SF_6 (Cooke et al. 2001).

Since the initial industrial production of SF_6 in 1953, its atmospheric concentration has increased by two orders of magnitude. This increase is a result of not only its popularity as a tracer gas but its widespread application in gas-insulated electrical systems and in molten reactive metal degassing, such as with magnesium and aluminum, as well (Maiss and Brenninkmeijer 1998, Levin et al. 2010). This problem is exacerbated by the fact that SF_6 is only destroyed in the mesosphere thus yielding an atmospheric lifetime of between 800 – 3,200 years depending on environmental conditions (Ravishankara et al. 1993, Geller et al. 1997). In order to increase the accuracy of multi-zone underground ventilation studies while simultaneously remediating the problem of increasing SF_6 background, an alternative tracer gas capable of both independent and concurrent usage with SF_6 can be implemented. One such alternative is presented by perfluoromethylcyclohexane (PMCH).

2.4 Properties of Perfluoromethylcyclohexane (PMCH)

PMCH, along with other similar perfluorochemical (PFC) compounds, was originally synthesized as a part of the Manhattan Project during World War II. The purpose of sub-project was to find a compound that was corrosion resistant to uranium hexafluoride, a substance used for uranium enrichment (Lowe 2002). The physical properties of PFC compounds has since allowed their application in other fields. PMCH, specifically, is comprised of seven carbon atoms and fourteen fluorine atoms (C_7F1_4). Due to its chemical structure, PMCH is classified as a cyclic perfluoroalkane. Perfluoroalkanes are molecules that have a hydrocarbon structure in which all the hydrogen atoms are replaced by fluorine atoms. The substitution of fluorine atoms for hydrogen atoms increases the molecular mass. Thus, PMCH is significantly heavier than comparable hydrocarbon oils with a specific gravity about 1.787. As a result, this highly fluorinated molecule has a high molecular mass of 350 g/mol.

The empirical formula of PMCH reflects the relationship C_nF_{2n+2}. Due to the fact that PMCH is a cyclic perfluoroalkane, two fluorine atoms are removed from the perfluorinated chain to form the cyclic structure. Therefore, cyclic perfluoroalkanes will have a slightly modified empirical formula of C_7F_{2n} (Sandford 2003). A graphical representation of PMCH and its cyclic structure can be seen in **Figure 2.3**.

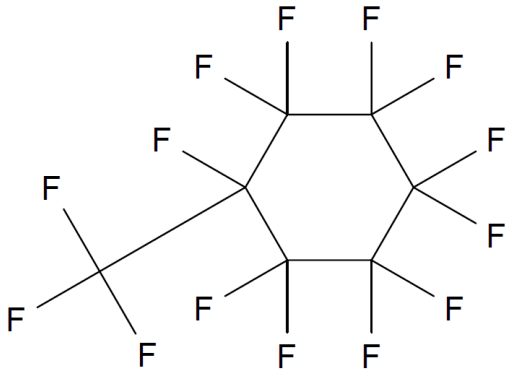

Figure 2.3. Perfluoromethylcyclohexane (PMCH) molecule.

As can be seen in the previous figure, PMCH is solely composed of carbon-fluorine single covalent bonds. Chemical bonds of this type are exceptionally strong by nature with typical bond disassociation energies of 452 kJ/mol to 531 kJ/mol. PMCH, as a result, is very stable with an estimated atmospheric lifetime of greater than 2,000 years. In contrast to its robust chemical bonds, PMCH exhibits very low intermolecular forces.

This weak attraction between PMCH molecules yields systems with high volatility coupled with low boiling points relative to other compounds with similar molecular weights. The volatility of PMCH, which is reflected by a vapor pressure of 14,100 Pa at 25°C, allows it to rapidly vaporize even at low temperatures (Sandford 2003, Lowe 2002). Once in a vapor state, PMCH will not condense even through cooler temperatures despite a critical temperature of 212.8°C. Although highly volatile, the 76°C (169°F) boiling point of PMCH causes this compound to exist as a liquid at room temperature and pressure (National Institute of Standards and Technology 2011, Cooke et al. 2001).

PMCH, similarly to other perfluoroalkanes, is inert, colorless, odorless, non-reactive, and non-toxic (Dietz 1986, Sandford 2003). The toxicity of perfluoroalkanes to humans is in fact so low that these compounds have been used in intravascular oxygenation of cells as well as to supply oxygen to the respiratory system through "liquid breathing" apparatuses to infants (Lowe 2002). The previously introduced characteristics of PMCH and of perfluoroalkanes in general have allowed these compounds to be successfully applied in numerous fields of study including biotechnology and medical research. The same properties also ideally suit PMCH for use in ventilation research as a tracer gas.

2.5 PMCH as a Tracer

PMCH is a member of the perfluorocarbon tracer (PFT) group of compounds. Other examples of PFT group compounds are, but not limited to, perfluorodimethylcyclobutane (PDCB or PMCB), perfluoromethylcyclopentane (PMCP), perfluorotrimethylcyclohexane (PTCH), and perfluorotrans 1,4 dimethylcyclohexane (ptPDCH). PFT group compounds are used as tracer gases due to their physical properties. PMCH is an effective tracer gas because it is biologically inert, chemically inert, and is exceptionally thermally as well as environmentally stable in vapor form. Additionally, PMCH does not exist naturally in the environment due to its anthropogenic production.

Using NCI-GCMS, the background presence of PMCH in the atmosphere was found to be 4.6 ± 0.8 femtoliters per liter (fL/L). This concentration falls in the sub parts per quadrillion (PPQ), 10^{-15}, range by volume. This level is approximately three orders of magnitude lower than SF_6 and easily classifies PMCH as having no significant natural background presence (Cooke et al. 2001, Dietz et al. 1998, Simmonds et al. 2002, Straume et al. 1998, Watson et al. 2007). As a result, a high signal to noise ratio can be achieved even at exceptionally low concentrations. The resulting low detectability threshold is the greatest advantage afforded by PMCH as a tracer gas.

PFC compounds react with free electrons, a property that increases ECD sensitivity. Free electron reactivity generally increases as the number of fluorine atoms in a molecule increases (Lovelock and Ferber 1982). The large grouping of fluorine atoms in PMCH creates molecular

electronegativity and thus a high affinity for reacting with electrons. As a result, PMCH, similar to other PFTs, have one of the highest detection sensitivities when using a GC-ECD (Dietz 1986, 1991). GC-ECDs, given that the correct analysis parameters have been applied, have the ability to achieve detection limits of 8 to 9 fg. Detection limits with PMCH have even been achieved in the 2 to 3 fg range with a heavily customized GCMS (Begley, Foulger, and Simmonds 1988). The aforementioned properties of PMCH and PFTs have resulted in their widespread utilization as tracer gases for a variety of disciplines.

As the sole tracer, PMCH has seen limited application. In this capacity, PMCH been used to identify the location of dielectric fluid leaks in high pressure fluid filled cables (Ghafurian et al. 1999) as well as to detect leaks in commercially buried electrical cables (Hassoun, McBride, and Russell 2000). Due to the extensive atmospheric stability of PMCH, it has been implemented in a variety of atmospheric tracer studies. Tracer gas studies of this nature include the investigation of atmospheric transport patterns of anthropogenic pollutants over the central Alps from the western Po valley in Northern Italy to and from the Swiss Plateau (Ambrosetti et al. 1998, Anfossi et al. 1998) as well as the determination of long-range flow characteristics in the Cross-Appalachian Tracer Experiment (CAPTEX ’83). The CAPTEX ’83 study used PMCH to simulate the dispersion of air pollutants over a 1,000 km area from the northeastern part of the United States to the southeastern part of Canada (Ferber et al. 1986). PMCH was also used as a tracer in the one year long Metropolitan Tracer Experiment (METREX) to study air flow patterns over the Washington D.C. area. The PMCH METREX simultaneously used PMCH to quantify error in meteorological air quality models. PMCH is more commonly combined with other PFTs in multiple tracer gas releases to facilitate complex studies.

The additional flexibility afforded by multiple tracer gas release enhances the analytical capabilities for ventilation systems and atmospheric transport projects. Multi-PFT releases have been used to analyze HVAC system performance in residential and commercial buildings, to develop models for contaminant infiltration in residences, and to evaluate the effective of residential weatherization systems (Leaderer, Schaap, and Dietz 1985). PMCH was one of several PFTs used to study the behavior of inert pollutants during nocturnal drainage flows over Brush Creek Valley located in the vicinity of Grand Junction, CO (Clements, Archuleta, and

Gudiksen 1989) and to improve the understanding of complex flow patterns over Salt Lake City, VT as a part of the Vertical Transport and Mixing (VTMX) field campaign (Fast et al. 2006). PMCH released in conjunction with other PFTs was also used to optimize the placement of wind stations, to determine the dispersion characteristics of airborne contaminants, and to validate atmospheric computer models for New York City, NY as a part of the four year New York City Urban Dispersion Program (UDP) research study (Watson et al. 2006). Due to their desirable tracer characteristic, multiple PFT deployments have also been utilized in research areas outside of air flows.

Studies of subsurface containment units have extensively used PFTs to evaluate barrier effectiveness and integrity. PFTs were used in a gas-phase partitioning test to determine the extent of non-aqueous phase liquid (NAPL), water, and air saturations in a chlorinated-solvent contaminated containment area in Tucson, AZ (Simon and Brusseau 2007). Direct subsurface barrier studies have included integrity verifications of a close-coupled polymer grout lined cement containment barrier at the Hanford Geotechnical Development Test Facility near Richland, WA, a closed-coupled containment barrier designed to hold laboratory waste, a colloidal silica grout barrier designed to contain contaminated glassware, and a cover system utilized in post-closure operations at various Department of Energy (DOE) facilities (Heiser and Sullivan 2002). PMCH with other PFTs has also been extensively modeled, evaluated, and deployed as an oil and gas reservoir tracer (Dugstad, Bjørnstad, and Hundere 1993) as well as a carbon capture and sequestration (CCS) tracers (Myers et al. 2013).

PMCH-PFT releases have already been used to evaluate water and gas production performance of the Gullfaks field petroleum reservoir in the North Sea as part of a pilot study (Ljosland et al. 1993). Similarly, PFTs are also well suited for short-term CCS studies such as integrity testing of new wells or seal verification of old wells (Watson and Sullivan 2012). Although CCS studies with PFTs are still in their infancy, PFTs have already successfully been used to track CO_2 breakthrough locations, subsurface plume migration patterns, and leakage rates (Myers et al. 2013). Examples of such PMCH-PFT combination studies include the monitoring of new surface leakage of sequestered CO_2 from a horizontal well in Bozeman, MO (Wells et al. 2010), and the

surveying of CO_2 leakage rates in a pilot study for the West Pearl Queen (WPQ) depleted oil formation in New Mexico (Wells et al. 2007).

The previous overview of PMCH tracer studies demonstrates the effectiveness and versatility of this substance in HVAC, atmospheric transport over complex terrain, oil and gas reservoirs, as well as subsurface studies (Dietz 1991). The inert, non-reactive, and non-toxic nature of PMCH makes it not only an ideal tracer gas choice but also a suitable alternative to SF_6. Despite substantial use in other fields, PMCH has not yet been implemented to study underground mine ventilation systems. This absence of use can be attributed to two primary issues, the lack of a suitable analytical method for simultaneous PMCH-SF_6 releases and the lack of a suitable mine-scale PMCH release system. Although recent research has yielded some PMCH-SF_6 analytical methods, this type of tracer gas release has seen far less application than the multi-PFT approach.

2.6 SF_6 and PMCH Simultaneous Tracer Gas Studies

The majority of tracer gas studies in commercial buildings and in dwellings before the 1990s were satisfied with the deployment of a single tracer in a single zone. This single zone treatment of ventilation systems is well tested, reliable, and accurate. However, as structures and their associated HVAC systems became more complex, the need for multi-zone tracer analysis techniques began to grow (Sherman 1989). This need is no longer merely isolated to commercial, industrial, and residential buildings, but has expanded to any ventilated space that can be divided into isolatable subsections, such as in underground mine ventilation systems. One of the fundamental principles of multi-zone treatments is the simultaneous release of multiple, independent tracer gases.

The use of multiple tracer gases is necessary in order to determine interactions between different zones. This issue can be seen with underground leakage studies. Leakage reduces the amount of air available for diluting contaminants to active areas of mines. In order to compensate for leakage, the air quantity delivered to the mine must be increased, which can result in a significant additional expense in fan power and increased stress on bulkheads. Leakage by nature is already difficult to locate using traditional ventilation survey techniques and even more so when

conducting a single zone tracer gas release. In order to accurately locate, characterize, and quantify leakage using a single zone tracer gas treatment, detailed knowledge regarding the ventilation flow around the suspected area must be known prior to the release. These details are necessary to correctly interpret the tracer gas concentration values. This difficulty is exacerbated when suspected leakage points are located in generally inaccessible areas such as the gob and the middle section of shafts (Hardcastle, Klinowski, and Mchaina 1993).

The use of multiple tracer gases allows not only for more accurate quantitative analyses of multi-zone interactions but can also give rapid qualitative feedback about flow paths. In order to implement a multi-zone analysis in an underground mine, SF_6, the industry standard tracer, would be released simultaneously with PMCH, the novel alternative tracer. Multiple studies have already utilized PMCH to supplement SF_6 in this manner to characterize complex atmospheric flow patterns over Salt Lake City, UT (Fast et al. 2006), to verify subsurface barrier integrity (Heiser and Sullivan 2002), and in CCS studies to track CO_2 breakthrough, subsurface plume migration patterns, and CO_2 leakage rates (Myers et al. 2013, Galdiga and Greibrokk 1997, Watson and Sullivan 2012). Despite these previous applications, an SF_6-PMCH simultaneous tracer gas release has not yet been used in an underground mine ventilation system. Before such a study can occur, a suitable mine scale release system must first be developed for PMCH.

2.7 Passive Release Sources

Underground mine ventilation tracer gas research has historically used SF_6 as its primary substance. The popularity of SF_6 stems not only because it exhibits all of the ideal tracer characteristic but also due to its ease of acquisition and release. As previously introduced, SF_6 exists as a gas in a wide range of environmental conditions. As such, a large variety of release options are available for both continuous and pulse studies. In contrast, PMCH exists as a volatile liquid. In order to be utilized as a tracer gas, PMCH must first be converted into a vapor and then released in a controlled manner. Several options for PMCH deployment are available.

PMCH can be purchased as a vapor in pressurized nitrogen (N_2) cylinders, be vaporized in heated N_2 streams, or be released from passive sources. PMCH-N_2 cylinders have been

successfully used to release PMCH in the previously introduced UDP study of atmospheric transport over New York City, NY. The turbulent N_2 stream system was used to release PMCH in the CAPTEX '83 study. This release system was not only designed to vaporize the tracer but also to simultaneously measure the exact concentration of the tracer. This system accomplished these tasks by mixing the volatile liquid with a pressurized stream of N_2 gas that was passed through a 105°C oven. Once completely vaporized, the concentration of the tracer stream was then determined with an electronic mass flow meter (Ferber et al. 1986). Both the pressurized cylinder and turbulent stream release systems have not been extensively utilized due to the inherent cost and difficulty associated with these methods. Passive release systems have been the preferred method for PMCH and PFT releases overall due to their cost effectiveness, ease, and reliability.

Passive release sources have been developed in two main forms, the permeation tube and the permeation plug. A permeation tube is a polymer tube, such as PTFE, that contains the volatile liquid tracer. The tube is plugged and sealed at both ends. Once sealed, the tube ends are airtight and impenetrable to the tracer. PMCH permeates through the walls of the tube at a constant rate in proportion to temperature and release as a vapor to atmosphere (Boyle 2010b, a). This particular version of the passive release source has seen limited use in tracer studies due to cost and narrow operating constraints. The permeation plug is considerably more common.

The property that allows the permeation plug to function is the natural permeability of silicone based rubbers (Van Amerongen 1947). This diffusion through a seemingly impermeable membrane can be achieved due to the chemical composition of silicone rubber. Silicone, also known as polysiloxane, is a name used to define any compound derived from polymerized siloxanes. Polymerized siloxanes are substances whose molecular structure is created by combining monomers into large chains of alternating silicon and oxygen atoms (Encyclopædia Britannica 2012). A siloxane can be further defined as any compound that has alternate silicon (Si) and oxygen (O) atoms (e.g. Si-O) where organic groups or hydrogen atoms are bonded to the Si atom (Merriam-Webster 2012, Polmanteer and Falender 1984). An example of a structural formula for a common type of silicone is displayed in figure that follows.

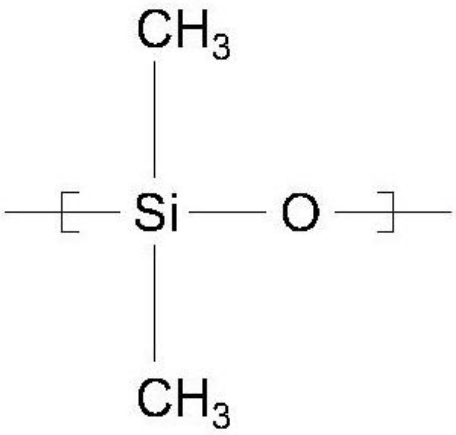

Figure 2.4. Chemical structure of polydimethylsiloxane (PDMS), the most common form of silicone rubber.

As can be seen in **Figure 2.4**, the siloxane molecules can rotate freely around the Si-O bond, which allows silicone compounds to be highly flexible (Encyclopædia Britannica 2012). This inherent flexibility afforded by the Si-O bond also permits the existence of free volumes within the compound thus allowing for gas permeability. Incidentally, silicone also has the highest permeability of any polymer, which ideally suits this compound for use in the PMCH permeation plug (Zhang and Cloud 2006).

One of the first iterations of the permeation plug was manufactured by impregnating the center of a fluoroelastomer with liquid PMCH using a syringe. The impregnated plug would then be crimped into a cylindrical aluminum shell so that only one end of the plug would be open to atmosphere. The PMCH would then diffuse through the fluoroelastomer and release to atmosphere at a constant rate once equilibrium was reached. This form of the passive release source has been deployed in conjunction with a CATS to measure air infiltration into a home (Dietz and Cote 1982) and to tag illicit drugs and paper currency (Balestrieri and Kaish 1995), as well as to tag pre-detonation blasting caps to facilitate the detection of clandestine bombs at security checkpoints (Senum et al. 1980). This design was followed by the permeation plug release cylinder (PPRC) design.

The version of the permeation plug was originally composed of a 32 mm long aluminum cylinder filled with 0.4 mL of PMCH. Both ends of the cylinder were slightly flared at both ends

to allow the press-fit of two slightly oversized silicone plugs. Once sealed, PMCH would achieve diffusion equilibrium with the plug in approximately two hours (Winberry et al. 1990). The PPRC design was then refined slightly so that one end of the aluminum cylinder was sealed and the other end was left open to atmosphere. The shell was first filled with liquid PMCH and then immediately sealed with an oversized silicone plug pressed flush to the end of the cylinder. Once sealed, the operating principle remained the same. PMCH would diffuse through the plug and release to atmosphere at a constant rate proportional to atmosphere. This final design, for the purposes of this discussion, will be referred to the permeation plug release vessel (PPRV).

The PPRV has been utilized in a variety of tracer gas application such as the analysis of air infiltration and air exfiltration in buildings (Dietz et al. 1986, D'Ottavio, Senum, and Dietz 1988), the quantification of air exchange rates (Winberry et al. 1990), and the determination of ventilation rates in Swedish dwellings as a part of a nationwide energy and indoor climate survey (Stymne, Bowman, and Kronvall 1994). The PPRV has also been applied to more unique studies including subsurface barrier integrity studies at Brookhaven National Laboratory's (BNL) Waldo test site (Heiser and Sullivan 2002), large-scale, continuous CCS integrity verification studies (Watson and Sullivan 2012), and laboratory based research on gas reservoirs located in the North Sea (Galdiga and Greibrokk 1997). Despite the significant use of the PPRV, information regarding how certain design aspects, such as plug thickness, affect the release of PMCH is practically non-existent. This lack of information most likely results from the confined use of the PPRV to HVAC studies thus removing the need for more universal design specification. The PPRV has also not yet been used in tracer gas studies of underground mine ventilation systems. The purpose of the discussion that follows is to develop a PPRV design that is suitable for mine-scale tracer gas studies and well as to present laboratory and field verification studies of the final PPRV design.

2.8 Bibliography

Ambrosetti, P., D. Anfossi, S. Cieslik, G. Graziani, R. Lamprecht, A. Marzorati, K. Nodop, S. Sandroni, A. Stingele, and H. Zimmermann. 1998. "Mesoscale transport of atmospheric trace constituents across the central Alps: transalp tracer experiments." *Atmospheric Environment* no. 32 (7):1257-1272. doi: 10.1016/S1352-2310(97)00185-4.

Anfossi, D., F. Desiato, G. Tinarelli, G. Brusasca, E. Ferrero, and D. Sacchetti. 1998. "TRANSALP 1989 experimental campaign - Part II: Simulation of a tracer experiment with Lagrangian particle models." *Atmospheric Environment* no. 32 (7):1157-1166. doi: 10.1016/S1352-2310(97)00191-X.

Balestrieri, G., and N. Kaish. 1995. Method of tagging and detecting drugs, crops, chemical compounds and currency with perfluorocarbon tracers (PFT's). United States: International Electronic Technology Corp.

Begley, P., B. Foulger, and P. G. Simmonds. 1988. "Femtogram detection of perfluorocarbon tracers using capillary gas chromatography electron capture negative-ion chemical ionization mass spectrometry." *Journal of Chromatography* no. 1988 (445):119-128.

Boyle, B. 2010a. The complete guide to testing chemical sensors. edited by Owlstone Nanotech Inc.

Boyle, B. 2010b. Guide to building your own permeation tubes. edited by Owlstone Nanotech Inc.

Brown, R. M., R. N. Dietz, and E. A. Cote. 1975. "Use of sulfur hexafluoride in atmospheric transport and diffusion studies." *Journal of Geophysical Research-Oceans and Atmospheres* no. 80 (24):3393-3398.

Clements, W. E., J. A. Archuleta, and P. H. Gudiksen. 1989. "Experimental design of the 1984 ASCOT field study." *Journal of Applied Meteorology* no. 28 (6):405-413. doi: 10.1175/1520-0450(1989)028<0405:EDOTAF>2.0.CO;2.

Clemons, C. A., A. I. Coleman, and B. E. Saltzman. 1968. "Concentration and ultrasensitive chromatographic determination of sulfur hexafluoride for application to meteorological tracing." *Environmental Science and Technology* no. 2 (7):551-556. doi: 10.1021/es60019a005.

Collins, G. F., F. E. Bartlett, A. Turk, S. M. Edmonds, and H. L. Mark. 1965. "A preliminary evaluation of gas air tracers." *Journal of the Air Pollution Control Association* no. 15 (3):109-112.

Cooke, K. M., P. G. Simmonds, G. Nickless, and A. P. Makepeace. 2001. "Use of capillary gas chromatography with negative ion-chemical ionization mass spectrometry for the determination of perfluorocarbon tracers in the atmosphere." *Analytical Chemistry* no. 73 (17):4295-4300. doi: 10.1021/ac001253d.

D'Ottavio, T. W., R. W. Goodrich, and R. N. Dietz. 1986. "Perfluorocarbon measurement using an automated dual-trap analyzer." *Environmental Science and Technology* no. 20 (1):100-104.

D'Ottavio, T. W., G. I. Senum, and R. N. Dietz. 1988. "Error analysis techniques for perfluorocarbon tracer derived multizone ventilation rates." *Building and Environment* no. 23 (3):187-194.

Diamond, W. P., S. J. Schatzel, F. Garcia, J. C. LaScola, F. E. McCall, P. W. Jeran, and T. P. Mucho. 1999. Characterization of gas flow in longwall gobs: Pittsburgh Coalbed, PA.

Dietz, R. N. 1986. Perfluorocarbon tracer technology. Paper read at Regional and Long-range Transport of Air Pollution, 15-19 SEP, at Ispra, Italy.

Dietz, R. N. 1991. Commercial applications of perfluorocarbon tracer (PFT) technology. In *The Department of Commerce Environmental Conference, "Protecting the Environment: New Technologies - New Markets"*. Reston, VA.

Dietz, R. N., and E. A. Cote. 1973. "Tracing atmospheric pollutants by gas chromatographic determination of sulfur hexafluoride." *Environmental Science and Technology* no. 7 (4):338-342.

Dietz, R. N., and E. A. Cote. 1982. "Air infiltration measurements in a home using a convenient perfluorocarbon tracer technique." *Environmental International* no. 8:419-433.

Dietz, R. N., R. W. Goodrich, E. A. Cote, and R. F. Wieser. 1986. "Detailed description and performance of a passive perfluorocarbon tracer system for building ventilation and air exchange measurements." In *Measured Air Leakage of Buildings*, edited by H. R. Trechsel and P. L. Lagus, 203-264. Philadelphia, PA: American Society for Testing and Materials.

Dietz, R. N., G. I. Senum, R. W. Fajer, R. F. Wieser, and T. J. Rappolt. 1998. New detectability in atmospheric perfluorocarbon tracing. In *216th American Chemical Society Meeting*. Boston, MA.

Drivas, P. J., P. G. Simmonds, and F. H. Shair. 1972. "Experimental characterization of ventilation systems in buildings." *Environmental Science and Technology* no. 6 (7):609-614. doi: 10.1021/es60066a005.

Dugstad, Ø., T. Bjørnstad, and I. Hundere. 1993. "Measurements of gas tracer retention under simulated reservoir conditions." *Journal of Petroleum Science and Engineering* no. 1993 (10):17-25.

Emberlin, J. C. 1981. "A sulphur hexafluoride tracer experiment from a tall stack over complex topography in a coastal area of Southern England." *Atmospheric Environment* no. 15 (9):1523-1530.

Encyclopædia Britannica. 2012. silicone. In *Encyclopædia Britannica Online*: Encyclopædia Britannica Inc.

Fast, J. D., K. J. Allwine, R. N. Dietz, K. L. Clawson, and J. C. Torcolini. 2006. "Dispersion of perfluorocarbon tracers within the Salt Lake Valley during VTMX 2000." *Journal of Applied Meteorology and Climatology* no. 45 (6):793-812.

Ferber, G. J., J. L. Heffter, R. R. Draxler, R. J. Lagomarsino, F. L. Thomas, R. N. Dietz, and C. M. Benkovitz. 1986. Cross-apalachian tracer experiment (CPATEX '83) final report. Silver Spring, MD: National Oceanic and Atmospheric Administration.

Galdiga, C. U., and T. Greibrokk. 1997. "Simultaneous determination of trace amounts of sulphur hexafluoride and cyclic perfluorocarbons in reservoir samples by gas chromatography." *Chromatographia* no. 46 (7/8):440-443.

Geller, L. S., J. W. Elkins, J. M. Lobert, A. D. Clarke, D. F. Hurst, J. H. Butler, and R. C. Myers. 1997. "Tropospheric SF_6: Observed latitudinal distribution and trends, derived emissions and interhemispheric exchange time." *Geophysical Research Letters* no. 24 (6):675-678.

Ghafurian, R., R. N. Dietz, T. Rodenbaugh, J. Dominguez, and N. Tai. 1999. "Leak location in fluid filled cables using the PFT method." *IEEE Transactions on Power Delivery* no. 14 (1):18-22.

Grot, R. A., A. T. Hodgson, J. M. Daisey, and A. Persily. 1991. "Indoor air quality evaluation of a new office building." *American Society of Heating, Refrigerating, and Air Conditioning* no. 33 (9):16.

Grot, R. A., and P. L. Lagus. 1991. "Application of tracer gas analysis to industrial hygiene investigations." *Industrial Hygiene News*, MAY.

Grot, R. A., P. L. Lagus, R. Hyle, R. Ledsky, M. Evans, and E. Sutton. 1995. Protocol for measuring the air change rate in non-residential buildings. Lagus Applied Technology, Inc.

Hardcastle, S. G., G. Klinowski, and D. Mchaina. 1993. Remedial mine ventilation planning - tracer gas definition of leakage routes. Paper read at Innovative Mine Design for the 21st Century, AUG, at Kingston, ON, Canada.

Hartman, H. L., J. M. Mutmansky, R. V. Ramani, and Y. J. Wang. 1997. *Mine ventilation and air conditioning*. 3rd ed. New York: John Wiley & Sons, Inc.

Hassoun, S., T. McBride, and D. A. Russell. 2000. "Development of perfluorocarbon tracer technology for underground leak location." *Journal of Environmental Monitoring* no. 2000 (2):432-435. doi: 10.1039/B005190J.

Heiser, J., and T. Sullivan. 2002. The Brookhaven National Laboratory perfluorocarbon tracer technology: a proven and cost-effective method to verify integrity and monitor long-term performance of walls, floors, caps, and cover systems. Long Island, NY: Brookhaven National Laboratory.

Kissell, F. N. 1982. "New developments in mine ventilation." In *Underground Mining Methods Handbook*, 1674-1679.

Leaderer, B. P., L. Schaap, and R. N. Dietz. 1985. "Evaluation of the perfluorocarbon tracer technique for determining infiltration rates in residences." *Environmental Science and Technology* no. 19 (12):1225-1232.

Leonard, J. J., J. J. R. Feddes, and J. B. McQuitty. 1984. "Measurement of ventilation rates using a tracer gas." *Canadian Agricultural Engineering* no. 26 (1):49-51.

Lester, D., and L. A. Greenberg. 1950. "The toxicity of sulfur hexafluoride." *Archives of Industrial Hygiene and Occupational Medicine* no. 2 (3):348-349.

Levin, I., T. Naegler, R. Heinz, D. Osusko, E. Cuevas, A. Engel, J. Ilmberger, R. L. Langenfelds, B. Neininger, C. v. Rohden, L. P. Steele, R. Weller, D. E. Worthy, and S. A. Zimov.

2010. "The global SF_6 source inferred from long-term high precision atmospheric measurements and its comparison with emission inventories." *Atmospheric Chemistry and Physics* no. 10 (6):2655-2662. doi: 10.5194/acp-10-2655-2010.

Ljosland, E., T. Bjørnstad, Ø. Dugstad, and I. Hundere. 1993. "Perfluorocarbon tracer studies at the Gullfaks field in the North Sea." *Journal of Petroleum Science and Engineering* no. 10 (1):27-38. doi: 10.1016/0920-4105(93)90048-J.

Lovelock, J. E., and G. J. Ferber. 1982. "Exotic tracers for atmospheric studies." *Atmospheric Environment* no. 16 (6):1467-1471. doi: 10.1016/0004-6981(82)90069-5.

Lowe, K. C. 2002. "Perfluorochemical respiratory gas carriers: benefits to cell culture systems." *Journal of Fluorine Chemistry* no. 118 (1-2):19-26. doi: 10.1016/S0022-1139(02)00200-2.

Maiss, M., and C. A. M. Brenninkmeijer. 1998. "Atmospheric SF_6: Trends, sources, and prospects." *Environmental Science and Technology* no. 32 (20):3077-3086.

Maiss, M., L. P. Steele, R. J. Francey, P. J. Fraser, R. L. Langenfelds, N. B. A. Trivett, and I. Levin. 1996. "Sulfur hexafluoride - a powerful new atmospheric tracer." *Atmospheric Environment* no. 30 (10):1621-1629.

McNair, H. M., and J. M. Miller. 2009. *Basic gas chromatography*. 2nd ed. New Jersey: John Wiley & Sons, Inc.

McWilliams, J. 2002. Review of airflow measurement techniques. Lawrence Berkeley National Laboratory.

Merriam-Webster. 2012. siloxane. In *Merriam-Webster.com*: Merriam-Webster.

Mucho, T. P., W. P. Diamond, F. Garcia, J. D. Byars, and S. L. Cario. 2000. Implications of recent NIOSH tracer gas studies on bleeder and gob gas ventilation design. In *SME Annual Meeting and Exhibit*. Salt Lake City, UT.

Myers, M., L. Stalker, B. Pejcic, and A. Ross. 2013. "Tracers - Past, present and future applications in CO_2 geosquestration." *Applied Geochemistry* no. 2013 (30):125-135. doi: 10.1016/j.apgeochem.2012.06.001.

National Institute of Standards and Technology. 2011. Perfluoro(methylcyclohexane). U.S. Secretary of Commerce.

Persily, A. K., and J. W. Axley. 1990. Measuring airflow rates with pulse tracer techniques. Paper read at Air Change Rate and Airtightness in Buildings, at Philadelphia, PA.

Polmanteer, K. E., and J. R. Falender. 1984. "Silicone and fluorosilicone elastomers: structure and properties." In *Polymers for fibers and elastomers*, edited by J. C. Arthur, R. J. Diefendorf, T. F. Yen, H. L. Needles, J. R. Schaefgen, M. Jaffe and A. L. Logothetis, 117-141. American Chemical Society.

Raatschen, W., R. A. Grot, and W. Lobner. 1995. Quantification of randon migration from a uranium mine through the soil into buildings by the use of tracer techniques. In *16th Air Infiltration and Centilation Center Conference*. Palm Springs, CA.

Ravishankara, A. R., S. Solomon, A. A. Turnipseed, and R. F. Warren. 1993. "Atmospheric lifetimes of long-lived halogenated species." *Science* no. 259 (5092):194-199.

Sandford, G. 2003. "Perfluoroalkanes." *Tetrahedron* no. 59 (4):437-454. doi: 10.1016/S0040-4020(02)01568-5.

Senum, G. I., R. P. Gergley, E. M. Ferreri, M. W. Greene, and R. N. Dietz. 1980. Final report of the evaluation of vapor taggants and substrates for the tagging of blasting caps. Brookhaven National Laboratory.

Sherman, M. H. 1989. "On the estimation of multizone ventilation rates from tracer gas measurements." *Building and Environment* no. 24 (4):355-362.

Simmonds, P. G., B. R. Greally, S. Olivier, G. Nickless, K. M. Cooke, and R. N. Dietz. 2002. "The background atmospheric concentrations of cyclic perfluorocarbon tracers determined by negative ion-chemical ionization mass spectrometry." *Atmospheric Environment* no. 36 (13):2147-2156.

Simon, M. A., and M. L. Brusseau. 2007. "Analysis of a gas-phase partitioning tracer test conducted in an unsaturated fractured-clay formation." *Journal of Contaminant Hydrology* no. 90:146-158. doi: 10.1016/j.jconhyd.2006.09.010.

Straume, A. G., R. N. Dietz, E. N. Koffi, and K. Nodop. 1998. "Perfluorocarbon background concentrations in Europe." *Atmospheric Environment* no. 32 (24):4109-4122.

Stymne, H., C. A. Bowman, and J. Kronvall. 1994. "Measuring ventilation rates in the Swedish housing stock." *Building and Environment* no. 29 (3):373-379.

Thimons, E. D., R. J. Bielicki, and F. N. Kissell. 1974. Using sulfur hexafluoride as a gaseous tracer to study ventilation systems in mines. In *Bureau of Mines Report of Investigations*: United States Department of the Interior.

Timko, R. J., and R. L. Derick. 1989. Determining the integrity of escapeways during a simulated fire in an underground coal mine. In *4th U.S. Mine Ventilation Symposium*. Berkeley, CA.

Timko, R. J., F. N. Kissell, and E. D. Thimons. 1987. Evaluating ventilation parameters of three coal mine gobs. In *3rd U.S. Mine Ventilation Symposium*. State College, PA.

Timko, R. J., and E. D. Thimons. 1982. Sulfur hexafluoride as a mine ventilation research tool - recent field applications. United States Department of the Interior.

Topuz, E., S. Bhamidipati, and M. Bartkoski. 1982. Improvement of ventilation system efficiency through the analysis of air leakage. In *1st U.S. Mine Ventilation Symposium*. Tuscaloosa, AL.

Turk, A., S. M. Edmonds, H. L. Mark, and G. F. Collins. 1968. "Sulfur hexafluoride as a gas-air tracer." *Environmental Science and Technology* no. 2 (1):44-48. doi: 10.1021/es60013a001.

Urosek, J. E., and T. R. Watkins. 1995. Gob ventilation and bleeder systems in U.S. coal mines. In *7th U.S. Mine Ventilation Symposium*. Lexington, KY.

Van Amerongen, G. J. 1947. "The permeability of different rubbers to gases and its relation to diffusivity and solubility." *Rubber Chemistry and Technology* no. 20 (2):494-514.

Watson, T. B., J. Heiser, P. Kalb, R. N. Dietz, R. Wilke, R. F. Weiss, and G. Vignato. 2006. The New York City urban dispersion program March 2005 field study: tracer methods and results. Upton, NY: Brookhaven National Laboratory.

Watson, T. B., and T. Sullivan. 2012. "Feasibility of a perfluorocarbon tracer based network to support monitoring, verification, and accounting of sequestered CO_2." *Environmental Science and Technology* no. 46 (3):1692-1699. doi: 10.1021/es2034284.

Watson, T. B., R. Wilke, R. N. Dietz, J. Heiser, and P. Kalb. 2007. "The atmospheric background of perfluorocarbon compounds used as tracers." *Environmental Science and Technology* no. 41 (20):6909-6913.

Wells, A. W., J. R. Diehl, G. Bromhal, B. R. Strazisar, T. H. Wilson, and C. M. White. 2007. "The use of tracers to assess leakage from the sequestration of CO_2 in a depleted oil reservoir, New Mexico, USA." *Applied Geochemistry* no. 2007 (22):996-1016.

Wells, A. W., B. R. Strazisar, J. R. Diehl, and G. Veloski. 2010. "Atmospheric tracer monitoring and surface plume development at the ZERT pilot test in Bozeman, Montana, USA." *Environmental Earth Science* no. 2010 (60):299-305.

Widodo, N. P., K. Sasaki, R. S. Gautama, and Risono. 2008. "Mine ventilation measurements with tracer gas method and evaluations of turbulent diffusion coefficient." *International Journal of Mining, Reclamation and Environment* no. 22 (1):60-69.

Winberry, W. T., Jr., L. Forehand, N. T. Murphy, A. Ceroli, B. Phinney, and A. Evans. 1990. Compendium of methods for the determination of air pollutants in indoor air. Triangle Park, NC: Atmospheric Research and Exposure Assessment Laboratory.

Young, D. A., G. W. Bonnell, and D. G. Genter. 2001. Tracer gas techniques for mapping air and methane migration through a longwall waste in an underground coal mine using tube bundle systems. In *SME Annual Meeting*. Denver, CO.

Zhang, H., and A. Cloud. 2006. The permeability characteristics of silicone rubber. In *38th SAMPE Fall Technical Conference: Global Advances in Materials and Process Engineering*. Dallas, TX: Society for the Advancement of Material and Process Engineering.

Chapter 3: A technique for creating perfluorocarbon tracer (PFT) calibration curves for tracer gas studies

ABSTRACT: The use of sulfur hexafluoride (SF_6) as a tracer gas for analyzing underground mine ventilation systems has been practiced for many years. As a result, the methods used to release, sample, and analyze SF_6 are well accepted. Although improvements are still being made to enhance the analysis of this tracer gas, the technique remains largely the same. However, as the complexity and size of underground mine ventilation networks increase, the ability of a single gas to function as a convenient and rapid means of analysis diminishes. This problem arises from the need to allow SF_6 to be completely cleared from a ventilation system before another test can be started. The utilization of multiple tracer gases can mitigate this problem by allowing for simultaneous releases in multiple underground locations thus facilitating a more comprehensive evaluation. Additionally, tracer gas tests can be executed in a consecutive manner without the risk of cross-contamination. Although multiple tracer gases have already been extensively used in the fields of heating, ventilation, and air conditioning (HVAC) and large-scale atmospheric monitoring, this technique has not been widely implemented in underground mine ventilation. This lack of use is partially due to the difficulty of releasing additional tracer gases. A well-documented alternative in HVAC studies to SF_6 as tracer gas are perfluorocarbon tracers (PFT). However, many PFTs exist as volatile liquids at room temperature and pressure. This characteristic provides a challenge for quantification using gas chromatography (GC). This paper introduces a method for creating a GC calibration curve for gaseous perfluoromethylcyclohexane (PMCH) from its liquid form and details the experimental parameters used in the evaluation.

3.1 Introduction

The use of sulfur hexafluoride (SF_6) as a tracer gas for modeling underground mine ventilation systems has been practiced for many years. As a result, the methods used to release, sample, and analyze SF_6 are well defined and accepted. Although improvements are still being made to enhance the analysis of this tracer gas, the applied techniques remain largely the same across the mining industry. The basic method is initiated by releasing SF_6 and then sampling the mine air at pre-selected locations either on a one-time, instantaneous basis or on a continuous, automated basis. The air sample is then examined to determine the concentration of the tracer gas at the sampling points (Hartman et al. 1997). This data can then be used to model the ventilation flow within the mine. Although this method of SF_6 deployment and analysis is proven, its application may be limited.

This difficulty largely stems from the increasing complexity of underground mines. The advancement of mining technologies and techniques has allowed for larger and more intricate mine geometry. The ability of a single gas to function as a convenient, rapid means of ventilation network analysis is diminished by the continual expansion of underground mines. A standard tracer gas examination requires that SF_6 be released either as a constant stream until its concentration is uniform at the release point and the outlet (i.e. conservation of mass) or as a large pulse. Either method requires a significant amount of tracer gas to achieve detectable levels at the sampling points. The background presence of SF_6 caused by such large releases presents some problems.

In order to conduct a consecutive release tracer gas studies, sufficient time must be allowed between tests to reduce the background presence of the gas. The reduction of background presence is essential so that subsequent tests of the ventilation system are not affected by the residual concentration of the previous release. At the concentration levels generally captured at sampling locations, which can range from parts per million (PPM) to parts per trillion (PPT), even minute amounts of additional tracer gas can drastically affect the final analysis. Unfortunately, this problem is especially present with SF_6 due to its natural tendency to adhere to surfaces. Additionally, SF_6 is approximately five times heavier than air, which causes the gas to

linger in areas of low ventilation flow. As a result, a substantial amount of time must be allowed to ventilate the excess tracer gas prior to subsequent ventilation surveys (Thimons, Bielicki, and Kissell 1974). The utilization of additional tracer gases has the potential to mitigate these problems in underground mine ventilation.

The ability to deploy multiple tracer gases not only allows for consecutive releases with minimal delay and without concern of contamination, but can also facilitate simultaneous, multi-location releases. These added capabilities may allow for a more rapid, comprehensive evaluation of ventilation systems. Multiple tracer gases have already been extensively used in the fields of heating, ventilation, and air conditioning (HVAC), as well as large-scale atmospheric monitoring. For example, a well-documented alternative in HVAC studies to SF_6 as tracer gas are perfluorocarbon tracers (PFT). This classification of tracer gas, more specifically the gas perfluoromethylcyclohexane (PMCH), will be the main topic of discussion in this paper.

Despite the use of PFTs in HVAC, there is no evidence in the literature that these tracers have been implemented in underground mines. The lack of use in underground mines is partially due to the difficulty of concurrently analyzing alternative tracer gases with SF_6. Previous work by the authors has shown that both gases can be detected with similar sensitivity on a single column via gas chromatography. However, before field tests can be conducted, an additional complication still exists with PFTs that must be resolved. Many PFTs exist as volatile liquids at room temperature and pressure. This characteristic adds a level of difficulty when quantifying the tracer from air samples. This paper introduces a method for creating a GC calibration curve for gaseous PMCH from its liquid form and details the experimental parameters used in the evaluation.

3.2 Background

PMCH is a volatile liquid that is part of the PFT compound group. These compounds are composed of perfluoroalkanes (e.g. PMCH, perfluoromethylcyclobutane (PMCB), perfluoromethylcyclopentane (PMCP), etc.), which are biologically inert, chemically inert, and thermally stable. The inert, non-reactive, and non-toxic nature of PFT compounds makes them

ideal choices as alternative tracer gases. Although PMCH can potentially be complimented by other PFTs, these other tracers have not yet been successfully deployed in conjunction with SF_6.

The chemical formula of PMCH is C_7F_{14} and has a molecular weight of 350 g/mol with a boiling point of 76°C. This compound, as previously stated, exists as a volatile liquid at room temperature. The volatile nature of PMCH allows it to vaporize at relatively low temperatures. Once in a vapor state, PMCH will remain a vapor even through cooler temperatures (National Institute of Standards and Technology 2011).

PMCH, similar to other tracer gases, can be used as a tracer gas because it does not adversely affect people or the environment at trace levels. Additionally, the low ambient background of PMCH in the atmosphere, in the parts per quadrillion (PPQ) range, classifies this compound as having no significant natural presence (Watson et al. 2007). Thus, this trace background presence will not significantly impact the concentration of the data collected in tracer gas studies. Perhaps the greatest advantage afforded by PMCH is its ability to be used in concurrent deployments of tracers due to its ability to be separated from SF_6, the standard tracer gas employed in the mining industry, as well as oxygen. Despite these tracer characteristics, PMCH has not yet been implemented as a tool in underground mine ventilation analysis. However, this tracer along with other PFT group compounds has been deployed extensively in other fields.

Building ventilation is an area of study that has seen significant implementation of PFTs. This utilization of PFTs is a result of the inherent limitations present in more conventional ventilation analysis techniques. These limitations impede accurate measurements of low air flows and low leakages, such as those found in HVAC systems. PFTs have been used in extensive studies to investigate air infiltration into single family homes using passive liquid PFT permeation sources coupled with passive adsorption tube samplers (Dietz and Cote 1982, Leaderer, Schaap, and Dietz 1985) as well as to evaluate the performance of multi-zone deployment of passive PFT sources for categorizing air infiltration, air exfiltration, and air exchanges (Dietz et al. 1986). PFTs have also been used to evaluate ventilation rates in the housing stock of Sweden as a nation-wide effort to determine the adequacy of the ventilation systems (Stymne, Bowman, and Kronvall 1994) as well as to characterize down-valley flow, canyon outflow, and interacting

circulations at the lower slopes of the Wasatch Front (Fast et al. 2006). The versatility of PFTs as a tracer has found some novel deployments in fields outside of ventilation as well.

PFTs have been used in the area of explosives for the pre-detonation tagging of electric blasting caps to allow the detection of clandestine bombs in high security areas (Senum et al. 1980). The tracing ability of PFTs has also been used to characterize the complex flow found in the Gullfaks oil fields in the North Sea (Ljosland et al. 1993), to locate dielectric fluid leaks on pipe-type/self-contained cables on the Con Edison transmission system (Ghafurian et al. 1999), and to determine the integrity of subsurface barriers used for the confinement of waste sites (Sullivan et al. 1999).

The previously introduced examples of PFT applications demonstrate the versatility of this compound as a tracer. Presently, only PMCH, a PFT group compound, has been successfully separated from SF_6 in preliminary laboratory based mine ventilation research by the authors. This tracer has not yet been deployed in underground field studies due to its initial existence as a volatile liquid at normal temperature and pressure (NTP). Thus, no techniques exist for creating a calibration curve for PMCH in the field of underground mine ventilation.

The generation of a calibration curve is a necessary aspect of quantitative GC investigations due to the nature of this technology. Although GCs are manufactured using nearly identical specifications, each device is unique depending on installation parameters (e.g. length of column, composition of the stationary phase, composition of the mobile phase, etc.) and device configurations (e.g. linear velocity of the mobile phase, temperature of the column, etc.). Thus, a calibration curve using known standards must be created for each analysis to serve as a reference for samples with unknown concentrations (McNair and Miller 2009). This paper introduces a method for creating a GC calibration curve for gaseous PMCH from its liquid form to facilitate the quantification of tracer concentration following a tracer release.

3.3 Experimental Design

In order to develop a method for creating a GC calibration curve for gaseous PMCH, three primary tasks were identified: creating the master standard, creating the liquid standards, and creating the gaseous standards. The following sections detail the experimental parameters from preparing the PMCH master standard to final generation of the calibration curve. A section is also provided that discusses the PMCH release sources that can be potentially quantified by the calibration curve.

3.3.1 Equipment

The analysis of PMCH was completed using a gas chromatograph (GC) equipped with an electron capture detector (ECD). The ECD was chosen due to its high sensitivity to trace amounts of electronegative compounds (McNair and Miller 2009). The GC was fitted with a 30 m long, 0.25 mm ID porous layer open tube (PLOT) alumina oxide capillary column deactivated with sodium sulfate. The column has a film thickness of 5 µm. In order to minimize error in the sample introduction process, an auto-injector equipped with a 2.5 mL headspace syringe, syringe heater, sample heater, and sample agitator was used. The details of how the auto-sampler was used in conjunction with the GC as well as their analysis settings will be discussed later in this section.

3.3.2 Concentration Range

Tracer gas standards are created to calibrate a GC for measuring concentrations of a target substance in gas and liquid samples. Tracer analyses are generally conducted to find volumetric ratios of tracer gas to total volume of gas (i.e. PPM, PPB, and PPT based on volume). Thus standards are created using the same scale. Standards can be generated using a variety of techniques. A simple but popular method is to use a container of known volume that is filled with an inert gas such as nitrogen. A known volume of tracer is then injected into the nitrogen-filled container thus producing a known volumetric ratio of tracer gas to total volume of gas.

However, this method must be modified for this experiment due to the chemical properties of PMCH.

PMCH exists as a volatile liquid at normal temperature and pressure (NTP) but must be deployed as a gas when used as a tracer. As a result, the calibration standards should be made using gaseous PMCH. Although a GC can accept liquid samples, the volume increases as liquid transitions into gas. This expansion causes the concentration to change. As a result, gaseous PMCH must be used in lieu of liquid PMCH to create a suitable calibration curve. The process of creating gaseous PMCH standards from a pure liquid is challenging because errors can be easily propagated through each step of the process. These errors can be minimized by acquiring commercially prepared gaseous PMCH standards.

These commercial standards can be further diluted very accurately as a gas to generate calibration standards using various means. However, commercial standards can be expensive, especially if a wide range of concentrations is required. Thus, a technique was developed to produce the calibration standards using readily available equipment. The procedure for creating gaseous standards from pure liquid PMCH for this experiment will now be discussed.

The range of concentrations required for the calibration curve was dictated by the expected concentration two PMCH release sources that will be used in a subsequent experiment. These sources are discussed in Section 5. The expected sampling concentrations from the two release sources were computed with the following steps. The sources will be deployed in a straight section of 5.08 cm (2 in) diameter pipe with a constant air flow of 5 m/s (980 fpm). This linear velocity was estimated prior to the experiment to provide a means for predicting PMCH concentrations in the pipe. The cross-sectional area of the pipe was first computed to be 0.00203 m^2. The area was then used in Equation (3.1) to determine the volumetric flow rate in the pipe.

$$Q = VA \quad \left(\frac{m^3}{s}\right) \qquad (3.1)$$

Where:
Q = volumetric flow (m^3/s)
V = linear velocity (m/s)
A = cross-sectional area (m^2)

Substituting known values into Equation (3.1) and converting the resulting units, the following calculation can be made.

$$Q = 5 \cdot 0.00203 = 0.01 \frac{m^3}{s} = 0.61 \frac{m^3}{min}$$

The volumetric flow was then used in conjunction to the mass flow rate of the release source to compute the expected concentration of PMCH at the sampling point. Due to the similarity of the computation, only the expected concentration calculation for one of the PMCH release sources will be provided. This source is expected to provide a flow rate of 26.4 $\frac{\eta L}{min}$. The computations were completed assuming a constant temperature of 21.5°C, a straight pipe, and a constant linear velocity. A liquid density of 1,787 $\frac{g}{L}$ is also used for PMCH (National Institute of Standards and Technology 2011). The mass flow of PMCH from the release source was calculated as follows.

$$\frac{26.4\ \eta L}{min} \cdot \frac{L}{10^9\ \eta L} \cdot \frac{1787\ g}{L} = 4.75 \cdot 10^{-5}\ \frac{g}{min}$$

Using the volumetric flow rate from Equation (3.1) and the mass flow rate of the release source, the expected concentration of PMCH can determined as follows.

$$\frac{4.75 \cdot 10^{-5}\ \frac{g_{PMCH}}{min}}{0.61\ \frac{m^3{}_{air}}{min}} \cdot \frac{kg}{1000g} = 7.76 \cdot 10^{-8}\ \frac{kg_{PMCH}}{m^3{}_{air}}$$

This concentration can also be represented in PPB by molarity by converting the volumetric flow of air and the mass flow of PMCH to molar flow, which is a more convenient means of

representation in certain data collection scenarios. The molar flow of air is calculated first by determining the mass flow assuming a dry air density of 1.205 $\frac{g}{L}$.

$$\frac{0.61\ m^3}{min} \cdot \frac{1000\ L}{m^3} \cdot \frac{1.205\ g}{L} = 733\ \frac{g}{min}$$

The mass flow can then be converted to a molar flow using a molecular weight of 28.97 $\frac{g}{mol}$ for dry air.

$$\frac{733\ g}{min} \cdot \frac{mol}{28.97\ g} = 25.29\ \frac{mol}{min}$$

Please note that the previous calculations for the molar flow of air was completed using the density and molecular weight of dry air. This molar flow does not represent the exact flow in the future quantification experiment due to varying atmospheric conditions, such as humidity and barometric pressure. The chemical properties of dry air were chosen as an initial point or reference from which the tracer concentration could be approximated. The molar flow of PMCH from the release source can now be computed as follows using the previously determined mass flow of $4.75 \cdot 10^{-5}\ \frac{g}{min}$ and a given molecular weight of 350.05 $\frac{g}{mol}$ (National Institute of Standards and Technology 2011).

$$\frac{4.75 * 10^{-5}\ g}{min} \cdot \frac{mol}{350.05\ g} = 1.35 \cdot 10^{-7}\ \frac{mol}{min}$$

The previously derived values can now be used to find the ratio of the molar flow of PMCH to the total molar flow of PMCH and air.

$$\frac{1.35 \cdot 10^{-7}\ \frac{mol}{min}}{1.35 \cdot 10^{-7}\ \frac{mol}{min} + 25.29\ \frac{mol}{min}} = 5.33 \cdot 10^{-9}$$

This ratio represents the molar percent of PMCH in the total flow. The molar percent can then be multiplied by 10^9 to convert the ratio into molar PPB.

$$5.33 \cdot 10^{-9} \cdot 10^{9} = 5.33\ PPB$$

The sampling concentration of the other release source was approximated to be $2.23 \cdot 10^{-9}\ \frac{kg}{m^3}$ (0.15 PPB by moles). Thus, the calibration curve must at least contain these two points for adequate interpolation. A target concentration range of $1.34 \cdot 10^{-9}\ \frac{kg}{m^3}$ to $1.39 \cdot 10^{-7}\ \frac{kg}{m^3}$ (0.09 PPB to 9.58. PPB by moles) was selected for the calibration curve to both encompass the two approximated sampling concentrations and allow for any fluctuations in PMCH concentrations. The process by which the standards were created will now be discussed.

3.3.3 Standard Preparation

The creation of gaseous PMCH standards from a pure liquid was completed by the three-step process described below.

1. A master liquid standard of diluted PMCH was prepared.
2. Varying volumes of the master standard depending on the desired final concentration were transferred to four separate containers for further dilution.
3. A small, constant volume of each liquid standard was individually transferred to four headspace containers and allowed to vaporize thus creating the gaseous standards.

For step one, the master standard was prepared in a 20 mL screw top, airtight, septum-capped vial. Using a volumetric flask, 20 mL of hexanes were added to the sample vial. The vial was then immediately sealed to prevent any significant loss of the solvent. Five µL of pure liquid PMCH was then injected into the hexanes through the septum using a liquid syringe. The 5 µL volume of PMCH was chosen because this amount was the lowest that could be reliably injected with reasonable precision and readily available equipment. The PMCH was injected through the septum to eliminate sample loss from the high volatility of PMCH, which was not a concern for the hexanes. The master standard was then agitated to ensure homogeneous distribution of the solute. The concentration of the master standard was determined using the mass of PMCH per unit volume of hexanes relationship shown below.

$$\frac{5\ \mu L_{PMCH} \cdot \frac{L}{10^6\ \mu L} \cdot \frac{1787\ g_{PMCH}}{L} \cdot \frac{kg}{1000\ g}}{20\ mL_{Hexanes} \cdot \frac{L}{1000\ mL} \cdot \frac{m^3}{1000\ L}}$$

$$= 0.45\ \frac{kg_{PMCH}}{m^3{}_{Hexanes}}$$

The second step was to prepare the individual liquid standards from which the final gaseous standards would be made. A total of four liquid standards were created with varying concentrations from the master standard. This step was accomplished by injecting varying volumes of the master standard to four separate screw-top, septum-capped vials each filled with 20 mL of hexanes. As a result, the four liquid standards contained varying dilutions of PMCH. The injection volumes from the master standard to each of the sample vials were determined based on how the dilution would affect the final gaseous concentration after the final transfer-vaporization phase in step three.

In order to determine the transfer volume in this manner, a computational sheet was created where different transfer volumes could be entered. The resulting gaseous concentration would then be displayed thus allowing for the transfer volumes to be found through a trial-and-error process. A sample calculation showing the computation of the final gaseous concentration will now be explained. The concentration of the master standard was first converted to a molarity, which is defined as moles of solute per liter of solution, to simplify the dilution calculation of the individual dilutions.

$$\frac{0.45\ kg_{PMCH}}{m^3{}_{Hexanes}} \cdot \frac{1000\ g}{kg} \cdot \frac{m^3}{1000\ L} \cdot \frac{mol_{PMCH}}{350.05\ g_{PMCH}}$$

$$= 0.0013\ \frac{mol_{PMCH}}{L_{Hexanes}}$$

The molarity of the standard can now be calculated based on the transfer volume based on the following equation.

$$M_1V_1 = M_2V_2 \qquad (3.2)$$

Where:
M = molarity $(mol_{Solute}/L_{Solution})$
V = volume of solution (L)

A value of 7 μL will be used in this demonstration for the volume transferred from the master standard to the separate sample vial filled with 20 mL of hexanes. This transfer volume was used to create the 2.68 PPB by moles calibration point. The following equation is created by rearranging Equation (3.2).

$$M_2 = \frac{M_1V_1}{V_2} \quad \left(\frac{mol}{L}\right) \qquad (3.3)$$

Substituting known values into Equation yields the following result for molarity.

$$M_2 = \frac{0.0013 \cdot (7 \cdot 10^{-6})}{[0.02 + (7 \cdot 10^{-6})]} = 4.5 \cdot 10^{-7}\ \frac{mol}{L}$$

During the final step, 5 μL of each liquid standard was injected into separate 20 mL screw-top, septum-sealed headspace vials. Using the molarity of the liquid standard, the mass of PMCH in each of the headspace vials can be calculated by converting molarity to density in units of grams per microliter $\left(\frac{g}{\mu L}\right)$. The density of the standard is $1.6 \cdot 10^{-10}\ \frac{g}{\mu L}$ for the standard in the calculation previously shown using Equation (3.3). The final transfer volume of 5 μL can then be used to determine the mass of PMCH in the final injection.

$$5\ \mu L \cdot \frac{1.6 \cdot 10^{-10}\ g}{\mu L} = 7.8 \cdot 10^{-10}\ g$$

Using the mass of PMCH, the gaseous density of PMCH in the final standard can be computed by dividing the mass of PMCH by the volume of the container. This calculation is reasonable because the small amount of liquid PMCH was allowed to vaporize completely inside the sealed headspace vial. Once vaporized, the gaseous PMCH is assumed to be well diffused inside the vial, thus creating a standard with a known mass per unit volume concentration. For this sample

calculation, a mass of $7.8 \cdot 10^{-10}\ g$ was injected into a 20 mL container giving a gaseous density of $3.9 \cdot 10^{-8}\ \frac{kg}{m^3}$. For convenience, this concentration can be converted to a PPB by moles using the previously introduced process for estimating PMCH concentration of the release sources. The concentration of the gaseous standard in PPB by moles was 2.68 PPB.

Using the aforementioned process, four gaseous standards were created for the calibration curve by transferring 0.24 µL, 7 µL, 15 µL, and 25 µL of the 0.0013 molar master standard to four separate vials filled with 20 mL of hexanes. 5 µL from each of the four liquid standards were then injected into their own respective headspace vials to create four gaseous standards thereby defining the calibration curve. The four point quantity was chosen because this is the minimum number of points required to confidently interpolate a linear relationship. The parameters, or method, used by the GC to analyze the PMCH standards will now be discussed.

3.3.4 Gas Chromatograph Method

The calibration standards were all injected into the GC using an auto-sampler. Prior to the injection, both the sample vial and the needle were heated to 50°C to encourage vaporization of the PMCH into the headspace and to prevent condensation on the needle, respectively. In addition, the sample vials were agitated at 500 RPM for one minute to ensure even distribution of the gaseous PMCH in the sample vial prior to injection. Once injected, the GC method was initiated.

The GC method used for this experiment required 16 min to analyze each injection and consisted of the following static parameters.

Table 3.1. GC method static parameters

Parameter	**Description**
Carrier Gas	He
Make-Up Gas	N_2
Injector Temperature	150°C
Split Ratio	30:1
Linear Velocity	30 cm/s
Detector Temperature	200°C

The only dynamic parameter in the method was the temperature of the column. The temperature program used for the column is displayed in the following table.

Table 3.2. GC Column Temperature Program

Parameter	**Description**
Initial Column Temperature	67°C
Hold Initial Temperature	2.75 min
Temperature Increase	120°C/min at 2.75 min
Final Column Temperature	Hold 180°C until end
Total Program Runtime	15.99 min

In order to prevent any contamination from residual compounds present in the GC, the column temperature was raised to 175°C and held for 30 min to thermally dissociate, or bake-off, these compounds. After the baking process, the PMCH analysis method described above was executed without an injection to verify the cleanliness of the column (i.e. column blank). A sample of the laboratory atmosphere was then injected into the GC using the auto-sampler syringe to ensure that PMCH was neither present in the air (i.e. air blank) nor in the syringe (i.e. syringe blank). Once this process was completed, the calibration standards could then be injected.
A total of three consecutive injections per calibration standard were made into the GC to quantify relative standard deviations (RSD) between the injections. The column was baked at 175°C for 15 min between injections of different calibration standards to remove any residual contaminants prior to the next set of injections. Another syringe blank was also completed prior to injecting the next calibration standard to re-verify the cleanliness of the syringe. The resulting calibration curve data are presented in the following section.

3.4 Experimental Results

The GC analysis of the gaseous PMCH standards produced a chromatogram for each injection. Only select chromatograms that best represent each calibration point will be displayed due to the fact that the inclusion of every chromatogram in this paper would be cumbersome. The overlaid chromatograms for the 0.09 PPB PMCH, 2.68 PPB PMCH, 5.75 PPB PMCH, and 9.78 PPB

PMCH calibration points are displayed in **Figure 3.1**, **Figure 3.2**, **Figure 3.3**, and **Figure 3.4** respectively.

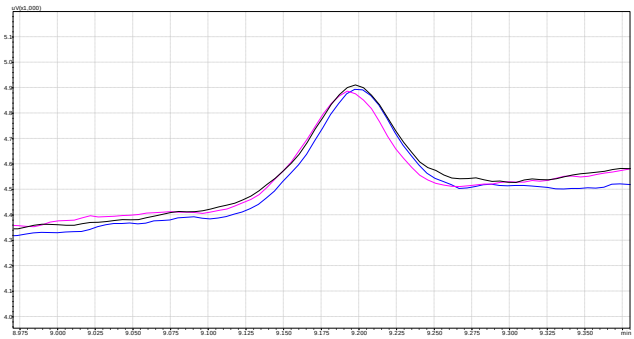

Figure 3.1. Overlaid chromatograms for 0.09 PPB of PMCH

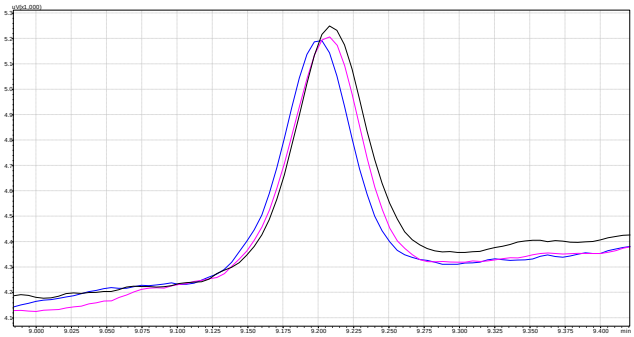

Figure 3.2. Overlaid chromatograms for 2.68 PPB of PMCH

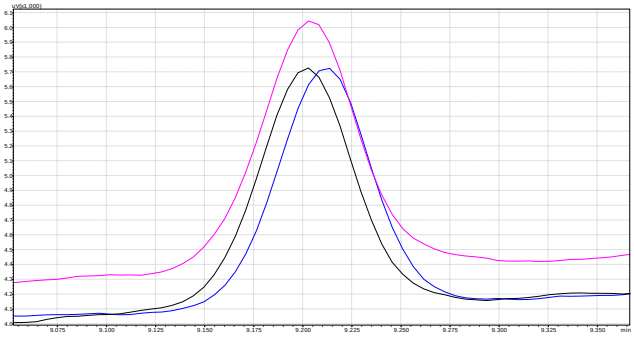

Figure 3.3. Chromatograms for 5.75 PPB of PMCH

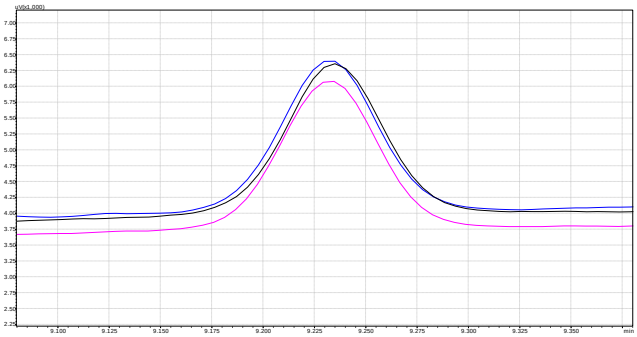

Figure 3.4. Overlaid chromatograms for 9.58 PPB of PMCH

A single chromatogram peak for each concentration was then overlaid in a single graph in **Figure 3.5** to demonstrate the consistency of the method.

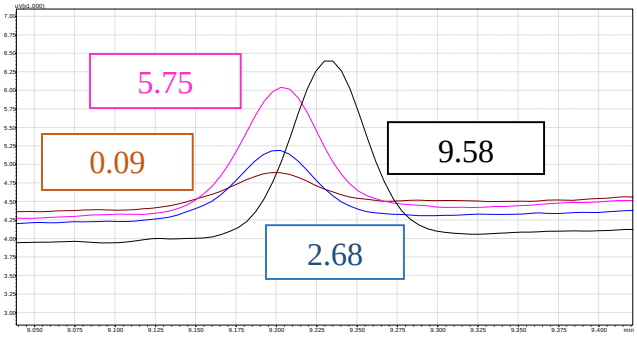

Figure 3.5. Overlaid chromatograms for the 0.09 PPB, 2.68 PPB, 5.75 PPB, and 9.58 PPB PMCH calibration points

The calibration curve results are summarized in **Table 3.3**.

Table 3.3. Calibration Curve Results for PMCH

Concentration (PPB)	Retention Time (min)	Peak Area (µV·min)	Average Peak Area (µV·min)	Standard Deviation (µV·min)	% RSD
0.09	9.198 9.193 9.199	2020.50 1666.40 1754.70	1813.87	184.32	10.16
2.68	9.209 9.207 9.200	3759.60 3816.80 3594.30	3723.57	115.54	3.10
5.75	9.202 9.204 9.212	5996.40 6277.00 5749.10	6007.50	264.12	4.40
9.58	9.235 9.232 9.232	8427.20 8224.10 8426.40	8359.23	117.03	1.40

A graphical representation of the calibration curve can be seen in **Figure 3.6**.

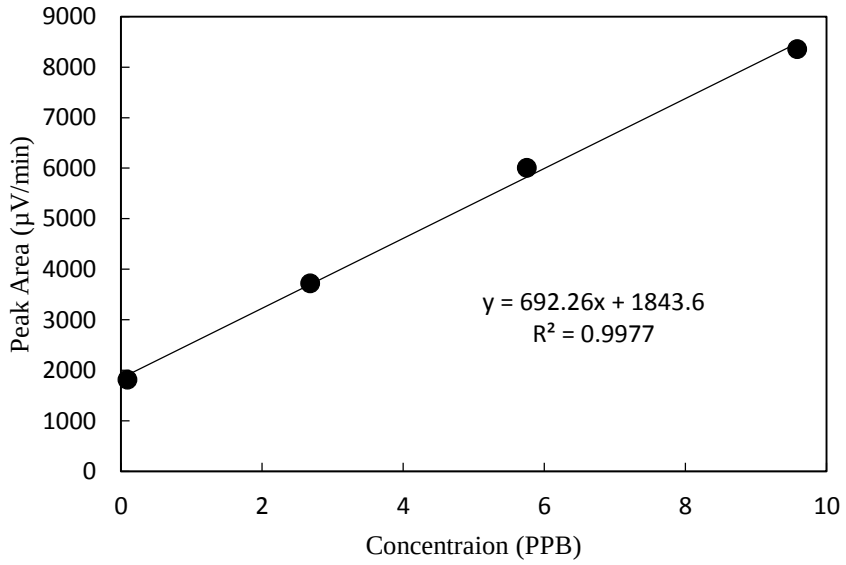

Figure 3.6. PMCH Calibration Curve

The 0.998 regression value displayed in **Figure 3.6** and the low relative standard deviations for the injections displayed in Table 3 show that the methodology used to create the curve is robust. The completed calibration curve can now be used to evaluate the concentrations of two PMCH release sources. These two sources are discussed in detail in the following section.

3.5 Potential PMCH Release Sources

The first release method was developed by Brookhaven National Laboratory (BNL) and consists of a hollow aluminum cylinder that is 32 mm (1.25 in) long with an inside diameter of 6.6 mm (0.25 in). One end of the cylinder is open to atmosphere while the other end is closed. Precisely 0.4 mL of liquid PMCH is injected into the aluminum vessel and sealed with an oversized silicone plug pressed flush to the end. The plug is 12.7 mm (0.5 in) long with an outside diameter of 7 mm (0.275 in). Once the vessel is sealed, the PMCH is slowly absorbed by the silicone plug until equilibrium is reached. Once the PMCH equilibrates, vapor PMCH will begin desorbing to atmosphere from the plug at a predictable rate directly proportional to temperature. At equilibrium, the source acquired from BNL will release PMCH at 26.4 ηL/min at 21.5°C (Dietz et al. 1986). This release source is reliable and relatively inexpensive either purchased or manufactured. The main disadvantage of this release source is the exceptionally small release rate thereby requiring the use of many sources in parallel to produce an acceptable concentration on a mine scale. The second release method functions using the same basic principle, but its construction and release rate differs slightly.

The second release method is a commercially available permeation tube. The permeation device is a small, inert tube that contains pure PMCH in a two-phase equilibrium, gas and liquid. At a constant temperature, the device releases PMCH by permeation through the walls of a Teflon tube for the entire length between the two impermeable plugs located at the ends. The range of release rates can be modified by varying the length and thickness of the tube. Permeation tubes are available that can release PMCH at rates ranging from 5 ηg/min to 50,000 ηg/min (Valco Instruments Co. Inc. 2011). For the future release experiment, a 2.1 cm permeation tube rated to release PMCH at 645 ηg/min/cm at 40°C was selected. Permeation tubes are readily available and can be produced with exceptionally accurate release rates. However, unlike the aluminum

vessel, the permeation tube may need to be heated to release any PMCH. This aspect may present a challenge, especially for release in permissible areas of underground coal mines. Additionally, its manufacturing complexity also yields a higher acquisition cost relative to the aluminum vessel.

3.6 Conclusions

The study presented in this paper presents a viable method for creating a GC calibration curve for gaseous PMCH from its volatile liquid state. The procedure used to generate the curve can be found in Section 4.3. The final calibration curve is displayed in Section 4.4. The technique introduced in this paper only represents one of many that can be used to achieve the same end. The specific method detailed in Section 4.3 was selected based on the available tools in the laboratory. The 0.998 regression value displayed in **Figure 3.6** and the low relative standard deviations for the injections displayed in **Table 3.3** show that the methodology used to create the curve is in fact robust, which demonstrates its reproducibility. However, the purpose of this experiment was not only to discover a viable procedure for creating a gaseous PMCH calibration curve but to ultimately quantify the PMCH concentration produced by two potential tracer release sources in future studies.

In order to accurately measure the PMCH release, the range of concentrations of the calibration curve was dictated by the expected concentration of PMCH produced by the two potential tracer release media. The first considered release method is manufactured by Brookhaven National Laboratory (BNL) and consists of a hollow aluminum cylinder with one end open to atmosphere and with the other end sealed closed. The second considered release method is a commercially available permeation device. The permeation device is a small, inert tube that contains pure PMCH in a two-phase equilibrium, gas and liquid. At a constant temperature, the tube releases PMCH by permeation through the walls of the Teflon tube for the entire length between the two impermeable plugs located at the ends. The evaluation of these two release sources in the laboratory in preparation for large-scale underground deployment will be the next phase of this research project.

The aforementioned details presented about the PMCH calibration curve's characteristics and ultimate purpose show that this technique used for its can be customized to fit many concentration ranges. Only the master standard concentration and injection volumes need to be changed to achieve this end. Thus, the techniques introduced in this paper are universally applicable to similar application of PMCH. Additionally, as more PFTs are identified as viable tracers, this technique may be potentially used to prepare calibration curves for these added volatile liquids.

3.7 Acknowledgements

The authors wish to thank Dr. Russell Dietz, Brookhaven National Laboratory, who has been generous with his time and knowledge of perfluorocarbon tracers. This publication was developed under Contract No. 200-2009-31933, awarded by the National Institute for Occupational Safety and Health (NIOSH). The findings and conclusions in this report are those of the authors and do not reflect the official policies of the Department of Health and Human Services; nor does mention of trade names, commercial practices, or organizations imply endorsement by the U.S. Government.

3.8 Bibliography

Dietz, R. N., and E. A. Cote. 1982. "Air infiltration measurements in a home using a convenient perfluorocarbon tracer technique." *Environmental International* no. 8:419-433.

Dietz, R. N., R. W. Goodrich, E. A. Cote, and R. F. Wieser. 1986. "Detailed description and performance of a passive perfluorocarbon tracer system for building ventilation and air exchange measurements." In *Measured Air Leakage of Buildings*, edited by H. R. Trechsel and P. L. Lagus, 203-264. Philadelphia, PA: American Society for Testing and Materials.

Fast, J. D., K. J. Allwine, R. N. Dietz, K. L. Clawson, and J. C. Torcolini. 2006. "Dispersion of perfluorocarbon tracers within the Salt Lake Valley during VTMX 2000." *Journal of Applied Meteorology and Climatology* no. 45 (6):793-812.

Ghafurian, R., R. N. Dietz, T. Rodenbaugh, J. Dominguez, and N. Tai. 1999. "Leak location in fluid filled cables using the PFT method." *IEEE Transactions on Power Delivery* no. 14 (1):18-22.

Hartman, H. L., J. M. Mutmansky, R. V. Ramani, and Y. J. Wang. 1997. *Mine ventilation and air conditioning*. 3rd ed. New York: John Wiley & Sons, Inc.

Leaderer, B. P., L. Schaap, and R. N. Dietz. 1985. "Evaluation of the perfluorocarbon tracer technique for determining infiltration rates in residences." *Environmental Science and Technology* no. 19 (12):1225-1232.

Ljosland, E., T. Bjørnstad, Ø. Dugstad, and I. Hundere. 1993. "Perfluorocarbon tracer studies at the Gullfaks field in the North Sea." *Journal of Petroleum Science and Engineering* no. 10 (1):27-38. doi: 10.1016/0920-4105(93)90048-J.

McNair, H. M., and J. M. Miller. 2009. *Basic gas chromatography*. 2nd ed. New Jersey: John Wiley & Sons, Inc.

National Institute of Standards and Technology. 2011. Perfluoro(methylcyclohexane). U.S. Secretary of Commerce.

Senum, G. I., R. P. Gergley, E. M. Ferreri, M. W. Greene, and R. N. Dietz. 1980. Final report of the evaluation of vapor taggants and substrates for the tagging of blasting caps. Brookhaven National Laboratory.

Stymne, H., C. A. Bowman, and J. Kronvall. 1994. "Measuring ventilation rates in the Swedish housing stock." *Building and Environment* no. 29 (3):373-379.

Sullivan, T., J. Heiser, G. I. Senum, and L. Millian. 1999. Use of perfluorocarbon tracer (PFT) technology for subsurface barrier integrity verification at the Waldo Test Site. Long Island, NY: Brookhaven National Laboratory.

Thimons, E. D., R. J. Bielicki, and F. N. Kissell. 1974. Using sulfur hexafluoride as a gaseous tracer to study ventilation systems in mines. In *Bureau of Mines Report of Investigations*: United States Department of the Interior.

Valco Instruments Co. Inc. 2011. *Dynacal permeation tubes and devices from VICI Metronics* 2011 [cited 10 NOV 2011]. Available from http://www.vici.com/calib/perm_dyna.php.

Watson, T. B., R. Wilke, R. N. Dietz, J. Heiser, and P. Kalb. 2007. "The atmospheric background of perfluorocarbon compounds used as tracers." *Environmental Science and Technology* no. 41 (20):6909-6913.

Chapter 4: A preliminary evaluation of potential perfluoromethylcyclohexane (PMCH) release vessel designs for tracer gas studies in underground mines

ABSTRACT: Perfluoromethylcyclohexane (PMCH) is a member of the perfluorocarbon tracer (PFT) group of compounds. PMCH has shown to be a viable alternative to the widely used tracer gas sulfur hexafluoride (SF_6). This viability stems from the fact that PMCH can be used concurrently with SF_6 while maintaining adequate chromatographic separation and comparable sensitivity during analysis. However, the release of PMCH in an underground mine ventilation system is challenging due to its physical characteristics. SF_6 exists as a gas at room temperature and pressure and can be accurately released using a variety of means. In contrast, PMCH exists as a volatile liquid at room temperature and pressure, a characteristic that prevents PMCH from being released using traditional means. One of the methods that can be used to release PMCH is the permeation plug release vessel (PPRV). The PPRV allows for a controlled, passive deployment of PMCH as a vapor. This paper evaluates several designs that incorporate varying manufacturing techniques, plug thicknesses, and plug materials for the PPRV so that a source appropriate for the mine scale may be developed in the future.

4.1 Introduction

Sulfur hexafluoride (SF_6) has been the predominant compound used in underground mine ventilation tracer gas studies for over 30 years (Thimons, Bielicki, and Kissell 1974). However, the ability of SF_6 to function individually as a tracer is being hindered by the advancement of mines. In order to support such growth, a subsequent increase in the complexity and the size of the ventilation systems must also occur. The sheer quantity of air that is pulled through underground mines and the area that the ventilation system must now service has diminished the effectiveness of SF_6 as a mine ventilation analysis tool. In order to mitigate this issue, recent studies have identified the compound perfluoromethylcyclohexane (PMCH) as a viable supplement for SF_6.

PMCH is classified as a perfluorinated cyclic hydrocarbon. Other compounds in this group classification include perfluoromethylcyclobutane (PMCB) and perfluoromethylcyclopentane (PMCP) (Galdiga and Greibrokk 1997). These compounds are also known as perfluorocarbon tracers (PFT) due to their chemical inertness, low toxicity, and trace level background presence in the environment thus uniquely suiting them to be used as tracer gases (Dietz 1991, Watson et al. 2007). Compounds of this type have already been widely implemented in heating, ventilation, and air conditioning (HVAC) as well as atmospheric monitoring studies (Dietz 1991) but not yet in the field of underground mine ventilation due to deployment complications. In contrast to SF_6, PFTs generally exist as volatile liquids at room temperature and pressure (National Institute of Standards and Technology 2011). This physical property of PFTs removes one of the great advantages afforded by SF_6, its existence as a gas. As a gas, SF_6 can be purchased in convenient, standardized gas cylinders and released in a controlled manner using a variety of options (Thimons, Bielicki, and Kissell 1974). Two examples of release options are the flow meter method and the flow controller method.

The flow meter method utilizes an analog or a digital flow meter attached to the gas cylinder. SF_6 is then deployed at a pre-determined volumetric flow rate over time, which can be computed to a mass flow rate over time if necessary. This method offers a significant amount of control and flexibility. The flow controller method utilizes a sophisticated electronic regulator that allows for

precise deployment of SF_6 either by mass or by volume depending on the controller. This method provides perhaps the greatest accuracy, reproducibility, and control of any readily available release approach. However, the established release systems for SF_6 are applicable to volatile liquids like PMCH. This paper evaluates several PMCH PPRV designs that have varying preparation techniques, plug thicknesses, and plug materials, so that a source appropriate for the mine scale may be developed.

4.2 Background

PMCH is a perfluorinated cyclic hydrocarbon whose chemical structure is composed of perfluoroalkanes (Watson et al. 2007). Compounds of this type are biologically inert, chemically inert, and thermally stable (F2 Chemicals Ltd. 2011). The inert, non-reactive, and non-toxic nature of PMCH makes it an ideal choice as a tracer gases. PMCH is comprised of seven carbon atoms and fourteen fluorine atoms, which gives it a chemical formula of C_7F_{14}. This highly fluorinated molecule has a molecular weight of 350 g/mol and a boiling point of 76°C (169°F). Although highly volatile, its molecular weight causes PMCH to exist as a liquid at room temperature and pressure. Simultaneously, the volatile nature of PMCH allows it to vaporize even at low temperatures. Once in a vapor state, PMCH, will remain a vapor even through cooler temperatures (National Institute of Standards and Technology 2011). Another advantage of PMCH is its detectability by GC even at low concentrations. This ability stems from PMCH's low ambient background in the atmosphere with concentrations in the parts per quadrillion (PPQ) (Cooke et al. 2001, Simmonds et al. 2002, Watson et al. 2007) and high detection sensitivity when using an electron capture detector (ECD) (Simmonds et al. 2002). Perhaps the greatest advantage afforded by PMCH is its ability to be simultaneously analyzed with SF_6, which is the standard tracer gas employed in the mining industry. Despite these tracer characteristics, PMCH has not yet been implemented in underground mine ventilation. PMCH has, however, seen widespread use in other fields of study in conjunction with other PFT group compounds.

Building ventilation is one area that has implemented PFTs. PFTs have been used to investigate air infiltration into single family homes using passive PFT permeation sources coupled with passive capillary adsorption tube samplers (CATS) (Leaderer, Schaap, and Dietz 1985, Dietz and Cote 1982) as well as to evaluate the performance of multi-zone deployments of passive PFT sources for categorizing air infiltration, air exfiltration, and air exchanges (Dietz et al. 1986). PFTs have also been used to evaluate ventilation rates in Swedish housing stock to determine the adequacy of agricultural ventilation systems (Stymne, Bowman, and Kronvall 1994).

In the field of atmospheric tracing, PFTs have been used to characterize down-valley flow, canyon outflow, and interacting circulations on the lower slopes of the Wasatch Front (Fast et al. 2006). They have also been deployed to evaluate air flow patterns in New York City to improve wind station placements, to supplement knowledge of contaminant flow patterns, and to update atmospheric flow models (Watson et al. 2006). PFTs have additionally been used in long-term, large-scale investigations of the transport and diffusion of gases over the Alpine topography in Switzerland (Ambrosetti et al. 1998) as well as to evaluate the accuracy of meteorological air quality models in Washington, D.C. (Draxler 1967).

The aforementioned examples of PMCH applications demonstrate the versatility of this compound as a tracer. Despite PMCH's use in numerous ventilation studies, its physical properties at room temperature and pressure do present a challenge for translating this technique to a mine environment. In a traditional SF_6 tracer study, a combination of pressure and flow regulators would be used to perform a controlled release. These tools can no longer be used due to the fact that PMCH is a liquid. The PPRV may serve as a viable alternative.

The basic concept of the PPRV detailed in this study has been heavily used by Brookhaven National Laboratory (BNL). In order to provide a cursory understanding of how the BNL source operates some background regarding the gas diffusion mechanism must be presented. The controlled release of PMCH is facilitated by the permeability characteristics of silicone rubber. The passage of a gas through rubber-type mediums such as silicone is a well-documented phenomenon that has undergone intensive study for over 50 years (Barbier 1955, Hammon, Ernst, and Newton 1977, Jordan and Koros 1990, Stern, Onorato, and Libove 1977, van Amerongen 1946, Zhang and Cloud 2006). In silicone rubber, similarly to other rubber-type polymers, gas diffusion occurs in three distinct steps: solution of the gas molecules on one side of the silicone membrane, diffusion of the gas molecule through the silicone, and evaporation of the gas from the other side (Barbier 1955, Zhang and Cloud 2006). This diffusion through a seemingly impermeable medium can be achieved due to the chemical composition of silicone rubber.

Silicone, also known as polysiloxane, is a name used to define any compound derived from polymerized siloxanes. Polymerized siloxanes are substances whose molecular structure is created by combining monomers into large chains of alternating silicon and oxygen atoms (Encyclopædia Britannica 2012). A siloxane can be further defined as any compound that has alternate silicon (Si) and oxygen (O) atoms (e.g. Si-O) where organic groups or hydrogen atoms are bonded to the Si atom (Merriam-Webster 2012). An example of a structural formula for a common type of silicone is displayed in figure that follows.

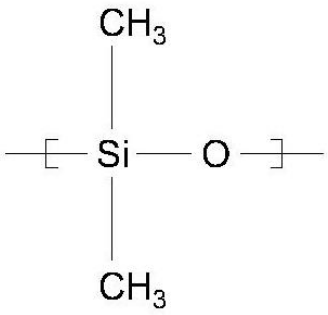

Figure 4.1. Chemical structure of polydimethylsiloxane (PDMS), the most common form of silicone rubber.

As can be seen in **Figure 4.1**, the siloxane molecules can rotate freely around the Si-O bond, which allows silicone compounds to be highly flexible. The flexibility afforded by the Si-O bond permits the existence of free volumes within the compound thus allowing for gas permeability. Incidentally, silicone also has the highest permeability of any polymer, which ideally suits this compound for use in the PMCH release source (Zhang and Cloud 2006). The BNL release source will now be discussed.

The original BNL design consists of a hollow aluminum cylinder that is 32 mm (1.25 in) in length with an inside diameter of 6.6 mm (0.25 in). One end of the cylinder is open to atmosphere while the other end is closed. Precisely 0.4 mL of liquid PMCH is injected into the aluminum vessel and sealed with an oversized silicone plug pressed flush to the end. The plug is 12.7 mm (0.5 in) long with an outside diameter of 7 mm (0.275 in). The source deploys PMCH by allowing the state change to occur inside the source. This conversion immediately begins once the vessel is sealed after which vapor PMCH slowly diffuses through the plug (Dietz et al. 1986).

Once the PMCH equilibrates within the plug (approximately 12 days after the vessel is sealed), vapor PMCH begins desorbing to atmosphere from the plug at a predictable rate directly proportional to temperature. The source releases PMCH at a rate of $4.14 \cdot 10^{-7}$ g/min at 21.9°C (71.5°F) (Dietz et al. 1986). The release rate changes in direct proportion to temperature. The release source design presented in this paper is based on the overall concept of the BNL source but changes some of the design parameters. A detailed description of the experimental source is presented in Section 3.

4.3 Experimental Design

The study presented in this paper will examine several PMCH release source designs. This assessment was completed in two main parts: assembling the PMCH release sources and determining the mass flow rate of each release source design. The following section details the experimental parameters from preparing the PMCH release vessel to final analysis of the flow rate. The PMCH release source components and designs will first be discussed.

The main body of the release vessel is comprised of an aluminum cylinder that is 6.35 cm (2.50 in) in length with an outside diameter (OD) of 0.747 cm (0.294 in). The cylinder itself is comprised of a hollow shell with one end sealed and the other end open to atmosphere. The shell has a wall thickness of 0.0356 cm (0.0140 in) that is consistent throughout the body of the cylinder, which gives an inside length of 6.31 cm (2.49 in) and an inside diameter (ID) of 0.711 cm (0.280 in). A schematic of the aluminum shell is displayed in **Figure 4.2**.

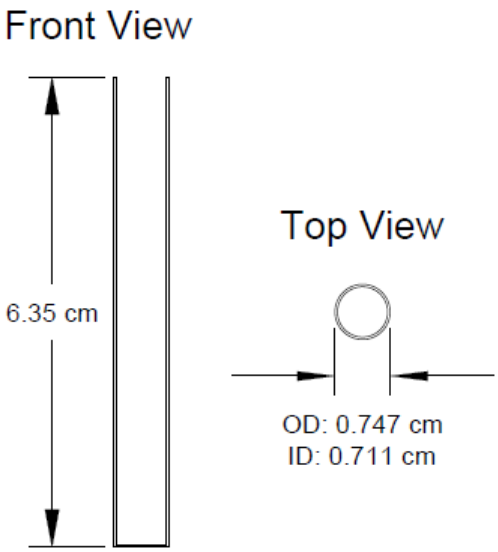

Figure 4.2. Schematic of an aluminum shell used for the PMCH release source.

As such, the shell can contain up to 2.5 mL (0.15 in^3) of liquid PMCH. A slightly oversized silicone plug with a diameter of 0.699 cm (0.275 in) was inserted into the open end of the aluminum cylinder and pressed flush to the end. Silicone grease was used as a lubricant to facilitate the press-fitting of the plug. The silicone plug serves as the diffusion membrane for PMCH after the liquid volatizes inside the vessel. A cutaway diagram of a completed PMCH source can be seen in **Figure 4.3**.

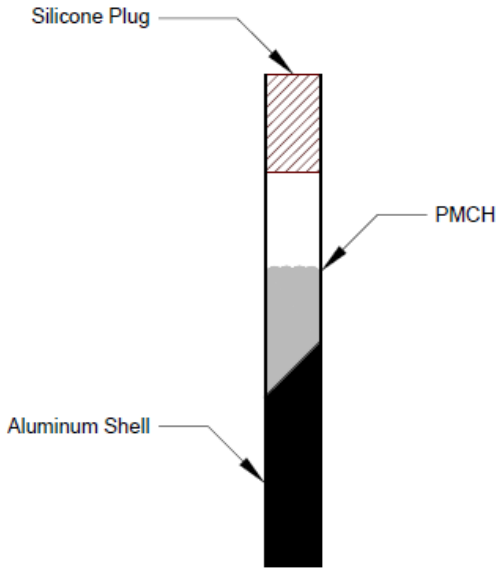

Figure 4.3. Cutaway diagram of a fully assembled PMCH release source.

Two different types of silicone rubber will be used for this experiment to determine the impact of these materials on the release rate of the source. A third material, a silicone coated bromobutyl/chlorobutyl rubber, was also considered in a precursor feasibility study but was immediately eliminated as an option due its highly impermeable nature. The first type of silicone rubber has a temperature rating from -55°C (-67°F) to 204°C (400°F). The second type of silicone rubber is black in color and is significantly softer with a durometer hardness of A50. The black silicone rubber has a maximum rated temperature of 200°C (392°F) with no rated minimum temperature from the manufacturer. The various designs evaluated in this paper will now be discussed.

The main modifications of the release vessel's design were applied to the plug due to the fact that the silicone membrane serves as the means by which PMCH is deployed. Different plug thicknesses (i.e. plug length) and materials were examined in this experiment for their effect on the release rate. Additionally, two in-vessel liquid PMCH filling techniques, pre-filling and post-filling, were compared. The pre-filling technique was completed by injecting liquid PMCH into the vessel prior to capping while the post-filling technique was accomplished by injecting liquid PMCH with a syringe through the plug after capping. The release vessels were all filled with precisely 0.5 mL of liquid PMCH regardless of the design. The size of the aluminum shell itself remained constant throughout the experiment as lengthening the vessel only serves to increase its PMCH storage capacity. The shell manufacturer used for this experiment did not produce shells of varying diameters so the effect of modifying this variable was not examined. A detailed listing of the different designs can be found in **Table 4.1** to **Table 4.3**.

Table 4.1. PMCH post-filling release source designs.

Design	Plug Material	Plug Thickness (cm)	PMCH Fill Technique
G1	Silicone	1.270	Post
G2	Silicone	1.270	Post
G3	Silicone	1.270	Post
SP1	Silicone	1.270	Post
SP2	Silicone	1.270	Post
SP3	Silicone	1.270	Post
SS1	Soft Silicone	1.270	Post
SS2	Soft Silicone	1.270	Post
SS3	Soft Silicone	1.270	Post

Table 4.2. PMCH silicone pre-filling release source designs.

Design	Plug Material	Plug Thickness (cm)	PMCH Fill Technique
S1	Silicone	1.270	Pre
S2	Silicone	1.270	Pre
S3	Silicone	1.270	Pre
S4	Silicone	0.635	Pre
S5	Silicone	0.635	Pre
S6	Silicone	0.635	Pre
S7	Silicone	1.905	Pre
S8	Silicone	1.905	Pre
S9	Silicone	1.905	Pre

Table 4.3. PMCH soft silicone pre-filling release source designs.

Design	Plug Material	Plug Thickness (cm)	PMCH Fill Technique
SS4	Soft Silicone	1.270	Pre
SS5	Soft Silicone	1.270	Pre
SS6	Soft Silicone	1.270	Pre
SS7	Soft Silicone	0.635	Pre
SS8	Soft Silicone	0.635	Pre
SS9	Soft Silicone	0.635	Pre
SS10	Soft Silicone	1.905	Pre
SS11	Soft Silicone	1.905	Pre
SS12	Soft Silicone	1.905	Pre

The sources were created in triplicate for each design to determine its reproducibility and reliability. In addition, triplicate sources served to identify any errors that may have occurred during assembly. Once the sources were completed, their initial masses were recorded. The mass of the sources was then monitored over time at an average temperature of 22.1°C (71.8°F) to determine the mass flow rate. Once a sufficient number of data points were collected, the data was processed to determine how the release sources were affected. The fully compiled and processed results are presented in Section 4.4.

4.4 Results

A full summary of the experimental results including a relative standard deviation (RSD) value for each triplicate can be found in **Table 4.4** to **Table 4.6**.

Table 4.4. PMCH post-filling release sources.

Source	Change in Mass (g)	Release Time (Days)	Release Rate (g/Day)	R^2	% RSD
G1	0.0504	95	$5.44 \cdot 10^{-4}$	1.00	
G2	0.0409	95	$4.76 \cdot 10^{-4}$	1.00	8.56
G3	0.0529	95	$5.88 \cdot 10^{-4}$	1.00	
SP1	0.0447	87	$5.26 \cdot 10^{-4}$	1.00	
SP2	0.0432	87	$5.22 \cdot 10^{-4}$	1.00	6.36
SP3	0.0517	87	$5.98 \cdot 10^{-4}$	1.00	
SS1	0.0476	87	$5.86 \cdot 10^{-4}$	1.00	
SS2	0.0464	87	$5.75 \cdot 10^{-4}$	1.00	1.42
SS3	0.0455	87	$5.66 \cdot 10^{-4}$	1.00	

Table 4.5. PMCH silicone plug pre-filling release sources.

Source	Change in Mass (g)	Release Time (Days)	Release Rate (g/Day)	R^2	% RSD
S4	0.0715	87	$8.44 \cdot 10^{-4}$	1.00	
S5	0.0722	87	$8.56 \cdot 10^{-4}$	1.00	0.92
S6	0.0728	87	$8.63 \cdot 10^{-4}$	1.00	
S1	0.0385	87	$4.76 \cdot 10^{-4}$	1.00	
S2	0.0386	87	$4.80 \cdot 10^{-4}$	1.00	2.50
S3	0.0411	87	$5.03 \cdot 10^{-4}$	1.00	
S7	0.0223	87	$3.01 \cdot 10^{-4}$	1.00	
S8	0.0154	60	$3.32 \cdot 10^{-4}$	0.99	4.98
S9	0.0168	60	$3.33 \cdot 10^{-4}$	0.99	

Table 4.6. PMCH soft silicone plug pre-filling release sources.

Source	Change in Mass (g)	Release Time (Days)	Release Rate (g/Day)	R^2	% RSD
SS7	0.0461	49	$9.78 \cdot 10^{-4}$	1.00	
SS8	0.0496	49	$1.05 \cdot 10^{-3}$	1.00	3.23
SS9	0.0462	49	$9.76 \cdot 10^{-4}$	1.00	
SS4	0.0465	87	$5.80 \cdot 10^{-4}$	1.00	
SS5	0.0456	87	$5.71 \cdot 10^{-4}$	1.00	2.28
SS6	0.0439	87	$5.49 \cdot 10^{-4}$	1.00	
SS10	0.0134	49	$3.87 \cdot 10^{-4}$	1.00	
SS11	0.0134	49	$3.86 \cdot 10^{-4}$	0.99	0.17
SS12	0.0132	49	$3.85 \cdot 10^{-4}$	0.99	

The previous table shows that the techniques used to construct each release vessel design is both robust and repeatable. Additionally, these exceptionally low RSD values demonstrate that the construction of each design triplicate were free of any major errors. The following tables display a summary of how the release rate was affected by the various changes. **Table 4.7** shows the percent difference between the average silicone plug and soft silicone plug release rates.

Table 4.7. Percent difference between release rates of silicone and soft silicone by thickness

Plug Thickness (cm)	Silicone (g/Day)	Soft Silicone (g/Day)	% Difference
0.635	$8.54 \cdot 10^{-4}$	$1.00 \cdot 10^{-3}$	7.87
1.270	$4.86 \cdot 10^{-4}$	$5.67 \cdot 10^{-4}$	7.65
1.905	$3.23 \cdot 10^{-4}$	$3.86 \cdot 10^{-4}$	8.82

Table 4.8. Percent change in the release rate with increasing plug thickness.

Plug Thickness (cm)	Silicone	Soft Silicone
0.635 to 1.270	-43.07%	-43.31%
1.270 to 1.905	-33.51%	-31.93%

Table 4.9. Estimated time to depletion (ETD) of each PMCH release design

Plug Material	Plug Thickness (cm)	Filling Method	ETD (yrs)
Silicone	1.270	Post	4.4
Soft Silicone	1.270	Post	4.1
Silicone	0.635	Pre	2.8
Silicone	1.270	Pre	4.9
Silicone	1.905	Pre	7.4
Soft Silicone	0.635	Pre	2.4
Soft Silicone	1.270	Pre	4.2
Soft Silicone	1.905	Pre	6.2

The following figures visually displays the recorded change of mass over time from the various release vessels. A graphical summary of the post-filling vessel mass change over time is presented in **Figure 4.4**.

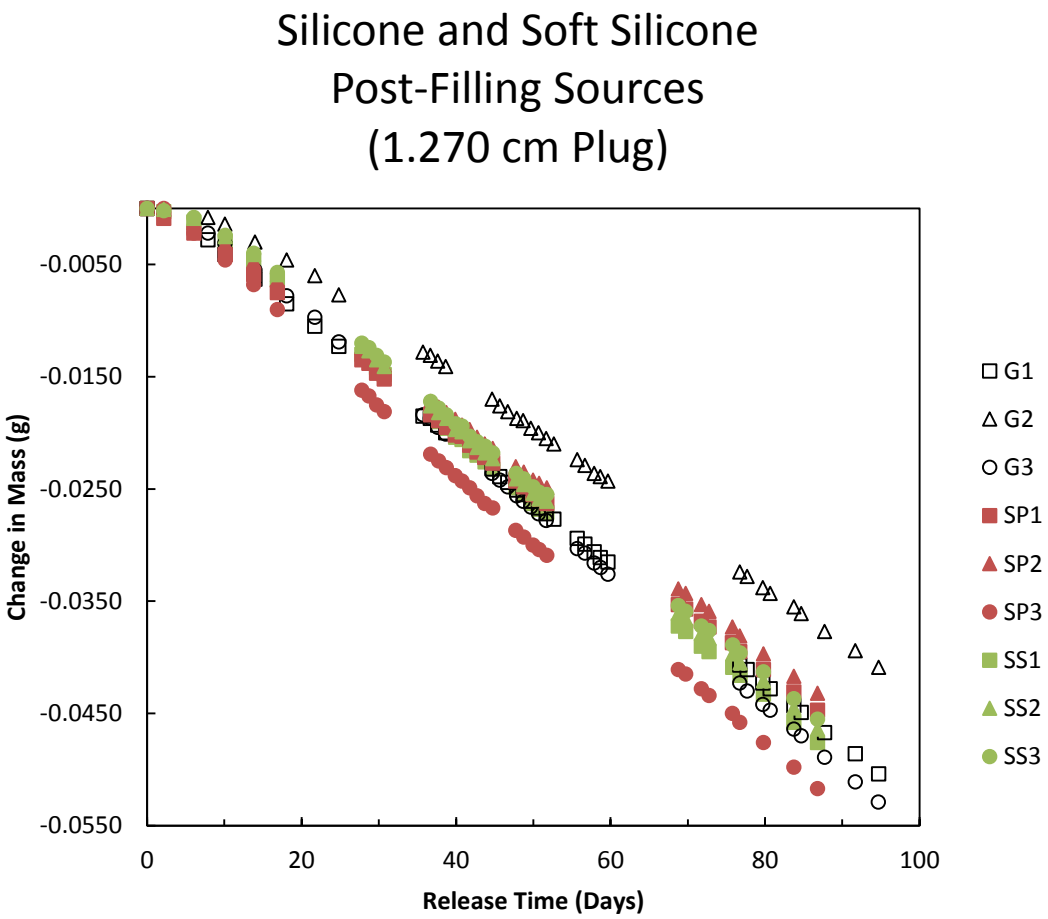

Figure 4.4. Post-filling release vessels prepared with a 1.270 cm silicone plug.

A graphical summary of the silicone plug pre-filling vessel mass change over time is presented in **Figure 4.5**.

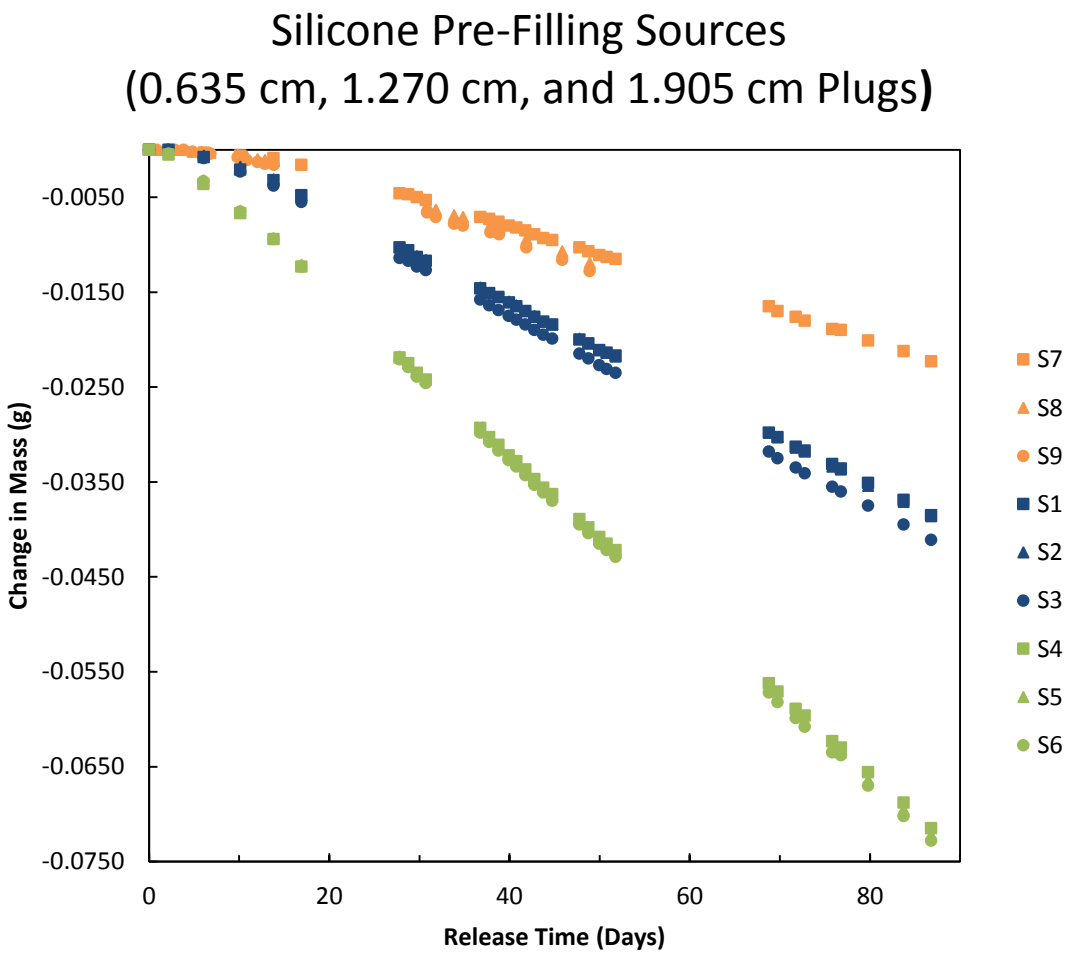

Figure 4.5. Pre-filling release sources prepared with the 0.635 cm, 1.270 cm, and 1.905 cm silicone plugs.

A graphical summary of the soft silicone plug pre-filling vessel mass change over time is presented in **Figure 4.6**.

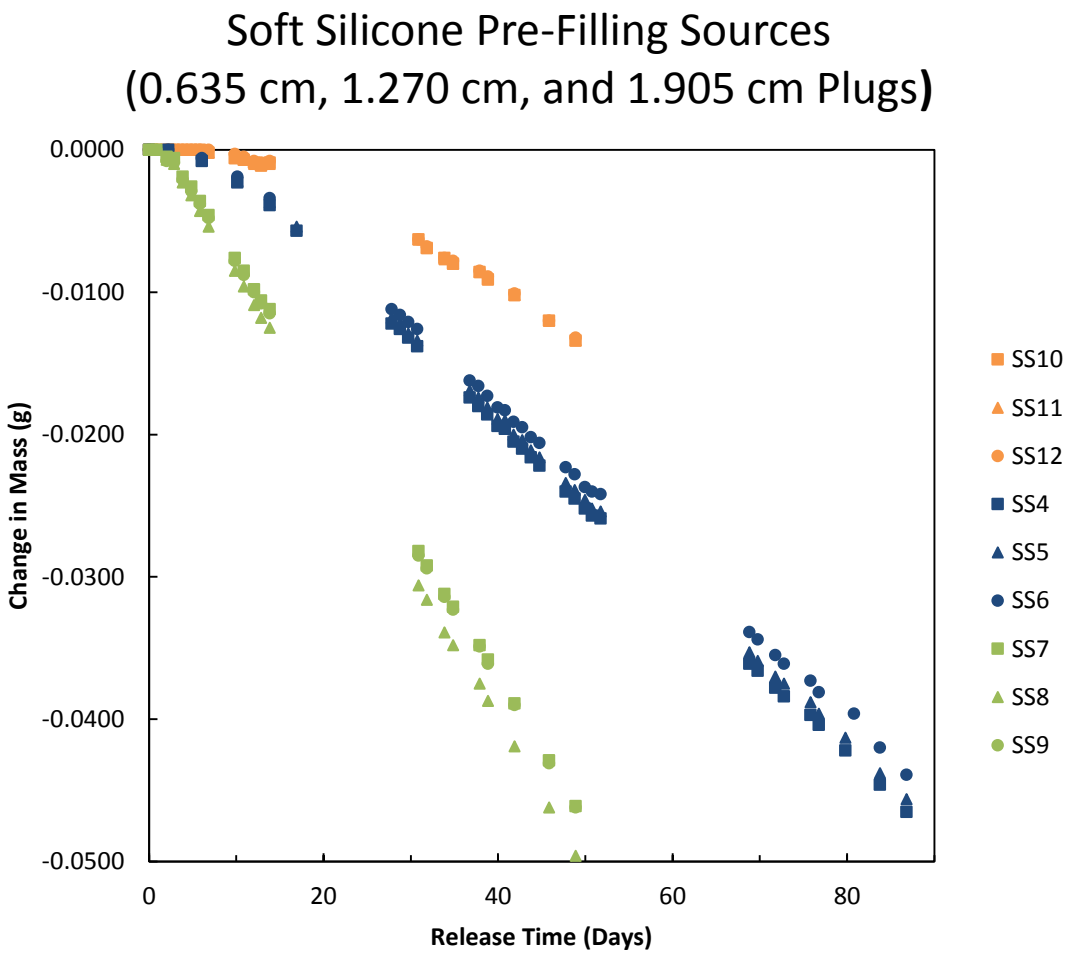

Figure 4.6. Pre-filling release sources prepared with the 0.635 cm, 1.270 cm, and 1.905 cm soft silicone plugs.

A detailed discussion of the previously presented experimental results is provided in Section 4.5.

4.5 Discussion and Conclusions

The preliminary study presented in this paper successfully produced multiple PMCH release source designs. The low RSD values between each triplicate set of designs show that the fabrication technique used to create the sources was robust, repeatable, and free of major defects. The experimental results provided in Section 4.4 of this paper clearly present how the various design variables affected the performance of the vessels. The post-filling, silicone plug release vessels will be discussed first.

The post-filling vessels were the simplest to construct amongst the other designs. However, the simplicity afforded by being able to inject PMCH through the silicone plug also gave the highest release rate variability. The larger RSD values for the post-filling sources presented in **Table 4.1** are immediately apparent in **Figure 4.4**. The relatively larger separation between the release rates of the post-filling sources is likely the result of damage to the plug caused by the needle during injection. Although the soft silicone material resulted in the lowest RSD values for the post-filling sources, these sources were still subject to injection damage thus placing its long-term reliability in question. Due to the manual nature of the PMCH injection, the plugs were damaged both unpredictably and inconsistently thus causing the higher release rate variability. However, despite the higher RSD values, the individual release rates from the post-filling sources have proven to be exceptionally reliable over the time of this experiment given linear regression values of near one.

The pre-filling release vessels were the most difficult to construct but proved to have the least release rate variability. The lower relative RSD values comparatively to the post-filling sources is likely due to the uncompromised integrity of the plug. As a result, the pre-filling technique is preferred over the post-filling technique. Two different materials and three different plug thicknesses were also studied using the pre-filling technique to determine the effect of these variables on the release rate. These variables were not modified in the post-filling sources to a significant degree because the post-filling technique had already been shown to contain the highest possibility for error.

The relationship between the two plug materials, traditional silicone and soft silicone, is apparent in **Table 4.5**, **Table 4.6**, and **Table 4.7**. The release rates for the soft silicone plugs are consistently higher than the silicone plugs for each plug thickness. The release rates differ consistently across plug materials by plug thickness by about 8%. This result is logical due to the higher flexibility of the soft silicone, which produces a higher permeability according to the physical properties of PDMS materials. Both materials produce PMCH release rates that are equally reliable and reproducible based on the parameters of this preliminary study. A slight advantage is provided by the increased temperature resistance and overall resilience of the traditional silicone over the soft silicone.

Figure 4.5 and **Figure 4.6** clearly show that the plug thickness has an inverse relationship to the release rate. As the plug thickness increased, the release rate decreased. The amount by which the release rates changed between the different thicknesses by plug material, displayed in **Table 4.8**, proved to be intriguing. The lengthening of the plug from 0.635 cm (0.25 in) to 1.270 cm (0.50 in) caused an approximate 40% reduction in release rate for both materials. However, the lengthening of the plug from 1.270 cm (0.50 in) to 1.905 cm (0.75 in) caused an approximate 30% reduction in release rate for both materials. This result suggests that the relationship between plug thickness and release rate may not be linear. A full statistical verification of this prospect was beyond the scope of this preliminary study and was not examined. The plug thickness was also found to have a direct relationship with PMCH equilibrium time. Equilibrium time for this study is defined as the time required for PMCH to completely absorb into the plug and achieve a stable release rate to atmosphere. As the plug thickness increased, the equilibrium time, as seen in **Figure 4.5** and **Figure 4.6**, also increased. Thus, the plug thicknesses were found to only have an effect on the PMCH release rate and vessel equilibration time but not on the overall reliability of the sources.

This preliminary study successfully determined the relationship between modifying several design variable on the PMCH release sources based on the experimental parameters. The post-filling technique was found to be less robust than the pre-filling technique. Although the pre-filling technique is more difficult to execute, this method is preferred for its increased reliability. The type of material and plug thickness were found to both affect the magnitude of the release

rate but not the overall reliability of the source. The plug thickness was also found to have an effect on the PMCH equilibration time of each vessel. As can be seen by the aforementioned discussion, the study successfully produced and evaluated several PMCH release source designs. The results of this study will be used to develop a more intricate study to derive an equation for the release rate of the PPRV as a function of environmental conditions and significant design variables.

4.6 Acknowledgements

The authors wish to thank Dr. Russell Dietz, Brookhaven National Laboratory, who has been generous with his time and knowledge of perfluorocarbon tracers and Rudy Maurer Jr., Dyno Nobel, who has been instrumental in supplying the aluminum shells used in this experiment.

This publication was developed under Contract No. 200-2009-31933, awarded by the National Institute for Occupational Safety and Health (NIOSH). The findings and conclusions in this report are those of the authors and do not reflect the official policies of the Department of Health and Human Services; nor does mention of trade names, commercial practices, or organizations imply endorsement by the U.S. Government.

4.7 Bibliography

Ambrosetti, P., D. Anfossi, S. Cieslik, G. Graziani, R. Lamprecht, A. Marzorati, K. Nodop, S. Sandroni, A. Stingele, and H. Zimmermann. 1998. "Mesoscale transport of atmospheric trace constituents across the central Alps: transalp tracer experiments." *Atmospheric Environment* no. 32 (7):1257-1272. doi: 10.1016/S1352-2310(97)00185-4.

Barbier, J. 1955. "A study of permeability to gases. Mixtures of natural rubber and other elastomers." *Rubber Chemistry and Technology* no. 28 (3):814-820.

Cooke, K. M., P. G. Simmonds, G. Nickless, and A. P. Makepeace. 2001. "Use of capillary gas chromatography with negative ion-chemical ionization mass spectrometry for the determination of perfluorocarbon tracers in the atmosphere." *Analytical Chemistry* no. 73 (17):4295-4300. doi: 10.1021/ac001253d.

Dietz, R. N. 1991. Commercial applications of perfluorocarbon tracer (PFT) technology. In *The Department of Commerce Environmental Conference, "Protecting the Environment: New Technologies - New Markets"*. Reston, VA.

Dietz, R. N., and E. A. Cote. 1982. "Air infiltration measurements in a home using a convenient perfluorocarbon tracer technique." *Environmental International* no. 8:419-433.

Dietz, R. N., R. W. Goodrich, E. A. Cote, and R. F. Wieser. 1986. "Detailed description and performance of a passive perfluorocarbon tracer system for building ventilation and air exchange measurements." In *Measured Air Leakage of Buildings*, edited by H. R. Trechsel and P. L. Lagus, 203-264. Philadelphia, PA: American Society for Testing and Materials.

Draxler, R. R. 1967. "One year of tracer dispersion measurements over Washington, D.C." *Atmospheric Environment* no. 21 (1):69-77. doi: 10.1016/0004-6981(87)90272-1.

Encyclopædia Britannica. 2012. silicone. In *Encyclopædia Britannica Online*: Encyclopædia Britannica Inc.

F2 Chemicals Ltd. 2011. Perfluoromethylcyclohexane. Lancashire, United Kingdom.

Fast, J. D., K. J. Allwine, R. N. Dietz, K. L. Clawson, and J. C. Torcolini. 2006. "Dispersion of perfluorocarbon tracers within the Salt Lake Valley during VTMX 2000." *Journal of Applied Meteorology and Climatology* no. 45 (6):793-812.

Galdiga, C. U., and T. Greibrokk. 1997. "Simultaneous determination of trace amounts of sulphur hexafluoride and cyclic perfluorocarbons in reservoir samples by gas chromatography." *Chromatographia* no. 46 (7/8):440-443.

Hammon, H. G., K. Ernst, and J. C. Newton. 1977. "Noble gas permeability of polymer films and coatings." *Journal of Applied Polymer Science* no. 21 (7):1989-1997. doi: 10.1002/app.1977.07021072.

Jordan, S. M., and W. J. Koros. 1990. "Permeability of pure and mixed gases in silicone rubber at elevated pressures." *Journal of Polymer Science Part B: Polymer Physics* no. 28 (6):795-809. doi: 10.1002/polb.1990.090280602.

Leaderer, B. P., L. Schaap, and R. N. Dietz. 1985. "Evaluation of the perfluorocarbon tracer technique for determining infiltration rates in residences." *Environmental Science and Technology* no. 19 (12):1225-1232.

Merriam-Webster. 2012. siloxane. In *Merriam-Webster.com*: Merriam-Webster.

National Institute of Standards and Technology. 2011. Perfluoro(methylcyclohexane). U.S. Secretary of Commerce.

Simmonds, P. G., B. R. Greally, S. Olivier, G. Nickless, K. M. Cooke, and R. N. Dietz. 2002. "The background atmospheric concentrations of cyclic perfluorocarbon tracers determined by negative ion-chemical ionization mass spectrometry." *Atmospheric Environment* no. 36 (13):2147-2156.

Stern, S. A., F. J. Onorato, and C. Libove. 1977. "The permeation of gases through hollow silicone rubber fibers: effect of fiber elasticity on gas permeability." *American Society of Chemical Engineers* no. 23 (4):567-578.

Stymne, H., C. A. Bowman, and J. Kronvall. 1994. "Measuring ventilation rates in the Swedish housing stock." *Building and Environment* no. 29 (3):373-379.

Thimons, E. D., R. J. Bielicki, and F. N. Kissell. 1974. Using sulfur hexafluoride as a gaseous tracer to study ventilation systems in mines. In *Bureau of Mines Report of Investigations*: United States Department of the Interior.

van Amerongen, G. J. 1946. "The permeability of different rubbers to gases and its relation to diffusivity and solubility." *Journal of Applied Physics* no. 17:972-985. doi: 10.1063/1.1707667.

Watson, T. B., J. Heiser, P. Kalb, R. N. Dietz, R. Wilke, R. F. Weiss, and G. Vignato. 2006. The New York City urban dispersion program March 2005 field study: tracer methods and results. Upton, NY: Brookhaven National Laboratory.

Watson, T. B., R. Wilke, R. N. Dietz, J. Heiser, and P. Kalb. 2007. "The atmospheric background of perfluorocarbon compounds used as tracers." *Environmental Science and Technology* no. 41 (20):6909-6913.

Zhang, H., and A. Cloud. 2006. The permeability characteristics of silicone rubber. In *38th SAMPE Fall Technical Conference: Global Advances in Materials and Process Engineering*. Dallas, TX: Society for the Advancement of Material and Process Engineering.

Chapter 5: An evaluation of a perfluoromethyl-cyclohexane (PMCH) permeation plug release vessel (PPRV) in a controlled turbulent environment

ABSTRACT: The use of sulfur hexafluoride (SF_6) as a tracer gas for analyzing underground mine ventilation systems has been practiced for over 30 years. As a result, the methods used to release, sample, and analyze SF_6 are well accepted. Although improvements are still being made to enhance the analysis of this tracer, the overall technique remains largely the same. However, as the complexity and size of underground mine ventilation networks increase, coupled with steadily rising SF_6 background levels, the ability of a single gas to function as a convenient, rapid means of analysis diminishes. The utilization of multiple tracer gases can mitigate these problems by allowing for a more comprehensive evaluation using multi-zone techniques. Although multiple tracer gases have already been extensively used in the fields of heating, ventilation, and air conditioning (HVAC) and large-scale atmospheric monitoring, this technique has not been widely implemented in underground mine ventilation. This lack of use is partially due to the difficulty of releasing the other available tracer. A well-documented alternative in HVAC studies to SF_6 as a tracer are perfluorocarbon tracers (PFT). Many PFTs exist as volatile liquids at room temperature and pressure. This characteristic prevents a PFT from being released using the same technique as SF_6, which exists as a gas under the same conditions. This paper evaluates a permeation plug release vessel (PPRV) under controlled turbulent conditions. The PPRV used in this study is designed to deploy PMCH. The details of the experimental parameters used in this evaluation are also presented in this paper.

5.1 Introduction

The use of sulfur hexafluoride (SF_6) as a tracer gas for modeling underground mine ventilation systems has been practiced for over three decades (Thimons, Bielicki et al. 1974). As a result, the methods used to release, sample, and analyze SF_6 are well defined and accepted. Although improvements are still being made to enhance the analytical tools for detecting this tracer, the overall technique remains largely the same across the mining industry. The basic method consists of the following steps: SF_6 is first released either continuously or in a single pulse depending on the requirements of the study. Mine air is then sampled at pre-selected locations either on an individual, manual basis or on a continuous, automated basis. The air samples are then examined to determine the concentration of the tracer gas at the sampling points (Hartman, Mutmansky et al. 1997). These data can then be used to characterize the ventilation flow within the target area. Although the use of SF_6 is a time proven technique, it is becoming increasingly difficult to implement it in the modern day.

This difficulty largely stems from the increasing complexity of underground mines. The advancement of mining technologies and techniques has allowed for larger and more intricate mine designs. As mines grow in this manner, so must the ventilation networks that support them. This escalation has caused the design, maintenance, and evaluation of underground ventilation networks to become increasingly cumbersome. As a result, many traditional ventilation engineering evaluation practices are becoming either inefficient or obsolete.

The ability of SF_6 to function as a convenient, rapid means of ventilation network analysis is diminished by the continual expansion of underground mines. This problem arises from a combination of multi-zone analysis difficulties, increasing natural background of SF_6, and the sheer amount of SF_6 needed to complete a full ventilation investigation. A standard tracer gas examination requires that SF_6 be released either as a constant stream until its concentration is uniform at the release point and the outlet (i.e. conservation of mass) or as a large pulse. This single tracer method is very effective at characterizing a single flow volume but cannot be used to show interaction between independent ventilation branches, which constrains the scope of a tracer gas study. The natural background presence of SF_6 has also been steadily increasing since

1953. High background equates to lower single to noise ratios and thus lower detection sensitivity (Ravishankara, Solomon et al. 1993, Maiss and Brenninkmeijer 1998, Levin, Naegler et al. 2010). In addition, both release methods require a significant amount of tracer to achieve detectable levels in large-scale investigations. The artificially increased background presence of SF_6 resulting from these large releases creates some additional challenges.

In order to conduct multiple consecutive release tracer gas studies, sufficient time must be allowed between tests to reduce the background presence of the gas. The reduction of background presence is essential so that subsequent tests of the ventilation system are not affected by the residual concentration of the previous release. As the concentrations generally captured at sampling locations, ranging from parts per million (PPM) to parts per trillion (PPT), even minute amounts of additional tracer gas can drastically affect the final analysis. Unfortunately, this problem is more pronounced with SF_6 due to its natural tendency to adhere to surfaces. SF_6 is also approximately five times heavier than air and causes the gas to linger in areas of low ventilation flow. As a result, a significant amount of time must be allowed to ventilate the excess tracer gas prior to subsequent releases (Thimons, Bielicki et al. 1974). The utilization of additional tracer gases has the potential to mitigate these problems in underground mine ventilation surveys.

The ability to deploy multiple tracer gases not only allows for consecutive releases that are free of cross-contamination, but can also facilitate simultaneous, multi-location releases. These added benefits will facilitate a more rapid, comprehensive evaluation of ventilation systems as well as provide insightful information regarding the interaction of independent ventilation streams. Multiple tracer gases have already been extensively used in the fields of heating, ventilation, and air conditioning (HVAC) as well as in large-scale atmospheric monitoring. For example, a well-documented alternative in HVAC studies to SF_6 are perfluorocarbon tracers (PFT) (Dietz and Cote 1982, Dietz 1991, Grot, Lagus et al. 1995, Heiser and Sullivan 2002). This classification of tracer gas, more specifically the gas perfluoromethylcyclohexane (PMCH), will be the main topic of discussion in this paper.

Despite the use of PFTs in HVAC, these additional tracers have not been implemented in underground mine ventilation. The lack of use in underground mines is partially due to the difficulty of concurrently analyzing alternative tracer gases with SF_6 using a single gas chromatograph (GC). This problem has recently been mitigated in recent tracer gas research on PMCH and SF_6. However, before field tests can be conducted, an additional challenge arises with PMCH that must first be resolved. PMCH exists as a volatile liquid at room temperature and pressure. This characteristic prevents PMCH from being released using the same technique as SF_6, which exists as a gas under the same conditions. This paper evaluates a permeation plug release vessel (PPRV) for PMCH, a PFT previously identified as a suitable tracer when used in combination with SF_6, and details the experimental parameters used in the evaluation.

5.2 Background

Perfluoromethylcyclohexane (PMCH) is a volatile liquid that is part of the perfluorocarbon tracer (PFT) compound group. These compounds are composed of perfluoroalkanes which are group of substances that are biologically inert, chemically inert, and thermally stability. The inert, non-reactive, and non-toxic nature of PFT compounds makes them ideal choices as alternative tracer gases to SF_6. Although PMCH can potentially be complimented by other PFTs, these other tracers have not yet been successfully deployed in conjunction with SF_6 in underground mines (Sandford 2003).

The chemical formula of PMCH is C_7F_{14} and has a molecular weight of 350 g/mol with a boiling point of 76°C. This compound, as previously stated, exists as a volatile liquid at room temperature. The volatile nature of PMCH allows it to vaporize even at relatively low temperatures. Once in a vapor state, PMCH will remain a vapor even through cooler temperatures (Dietz 1986, National Institute of Standards and Technology 2011). PMCH, similar to other tracer gases, can be used as a tracer because it does not adversely affect people or the environment. Additionally, the low ambient background of PMCH in the atmosphere, with concentrations in the parts per quadrillion (PPQ), classifies this compound as having no significant natural presence (Watson, Wilke et al. 2007). Thus, PMCH's background presence is effectively zero. Perhaps the greatest advantage afforded by PMCH is its ability to be separated from SF_6 on a single column. Despite these advantages, PMCH has not yet been implemented in underground mine ventilation. However, this tracer, along with other PFT group compounds, has been extensively deployed in other fields.

Building ventilation is an area of study that has significantly implemented PFTs. This heavy utilization of PFTs is a result of the inherent limitations present in more conventional ventilation analysis techniques when measuring low air flows and leakages. PFTs have been used in extensive studies to investigate air infiltration into single family homes using passive liquid PFT permeation sources coupled with passive adsorption tube samplers (Dietz and Cote 1982, Leaderer, Schaap et al. 1985) as well as to evaluate the performance of multi-zone deployments of passive PFT sources for categorizing air infiltration, air exfiltration, and air exchanges (Dietz,

Goodrich et al. 1986). PFTs have also been used to evaluate ventilation rates in Swedish housing stock to determine the adequacy of the ventilation systems (Stymne, Bowman et al. 1994) and to characterize down-valley flow, canyon outflow, and interacting circulations at the lower slopes of the Wasatch Front (Fast, Allwine et al. 2006).

The previously introduced examples of PFT applications demonstrate the versatility of this compound as a tracer. Presently, only PMCH, a PFT group compound, has been successfully separated from SF_6 in preliminary mine ventilation research. This tracer has not yet been deployed in underground field studies. This paper seeks to evaluate the predictability and reproducibility of two potential deployment methods designed to release liquid PMCH as a vapor from its liquid state under controlled conditions.

5.3 Experimental Design

The study presented in this paper will evaluate the deployment of a PPRV developed in a previous experiment. This experiment was completed in three main parts: sample PMCH released by the PPRV from a controlled turbulent environment, generate the calibration curve, and perform GC analysis. The following sections detail the experimental parameters of this study.

5.3.1 Release Sources

The main body of the release vessel is comprised of an aluminum cylinder that is 6.35 cm (2.50 in) in length with an outside diameter (OD) of 0.747 cm (0.294 in). The cylinder itself is a hollow shell with one end sealed and the other end opened to atmosphere. The shell has a wall thickness of 0.0356 cm (0.0140 in) that is consistent throughout the body of the cylinder, which gives an inside length of 6.31 cm (2.49 in) and an inside diameter (ID) of 0.711 cm (0.280 in). A schematic of the aluminum shell is displayed in **Figure 5.1**.

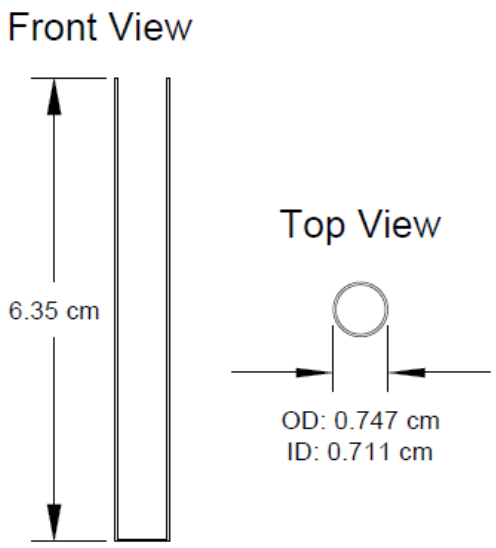

Figure 5.1. Schematic of an aluminum shell used for the PMCH PPRV.

As such, the shell can contain up to 2.5 mL (0.15 in^3) of liquid PMCH. A slightly oversized silicone plug with a diameter of 0.699 cm (0.275 in) was inserted into the open end of the aluminum cylinder and pressed flush to the end. Silicone grease was used as a lubricant to facilitate the press-fitting of the plug. The silicone plug serves as the diffusion membrane for PMCH after the liquid volatizes inside the vessel. A cutaway diagram of a completed PMCH source can be seen in **Figure 5.2**.

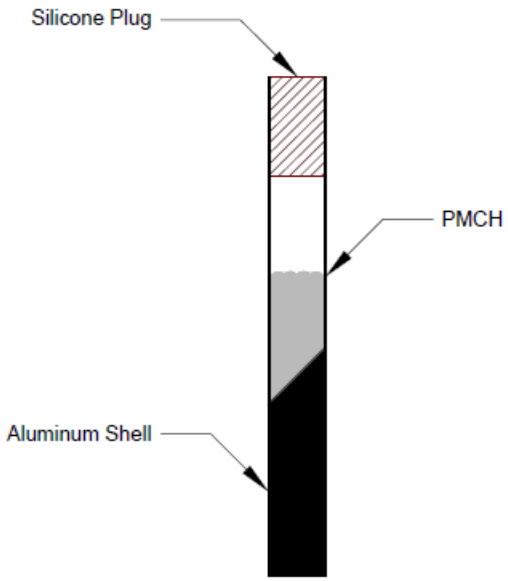

Figure 5.2. Cutaway diagram of a fully assembled PPRV.

Three PPRVs with a total PMCH release rate of $2.97 \cdot 10^{-8}$ g/s were placed in parallel inside a container designed to create a turbulent, blowing-type airflow environment from which the PMCH will be sampled.

5.3.2 Turbulent Flow Container

The vessel consisted of three main parts: the inlet, the PMCH release area, and the outlet. The inlet was built using a nylon 1.27 cm (0.5 in) male NPT to 0.635 cm (0.25 in) female NPT reducing bushing and a 0.635 cm (0.25 in) hose barb. The hose barb accepted airflow through a flexible plastic hose from two air pumps connected in parallel. The combined pumping system was capable of creating flow quantities greater than 100 LPM. The flow from the pump was controlled by an adjustable flow controller placed in-line between the air pump and the turbulence container. The inlet directed airflow to the PMCH release area. A schematic diagram and of the flow induction system can be seen in **Figure 5.3** and **Figure 5.4**.

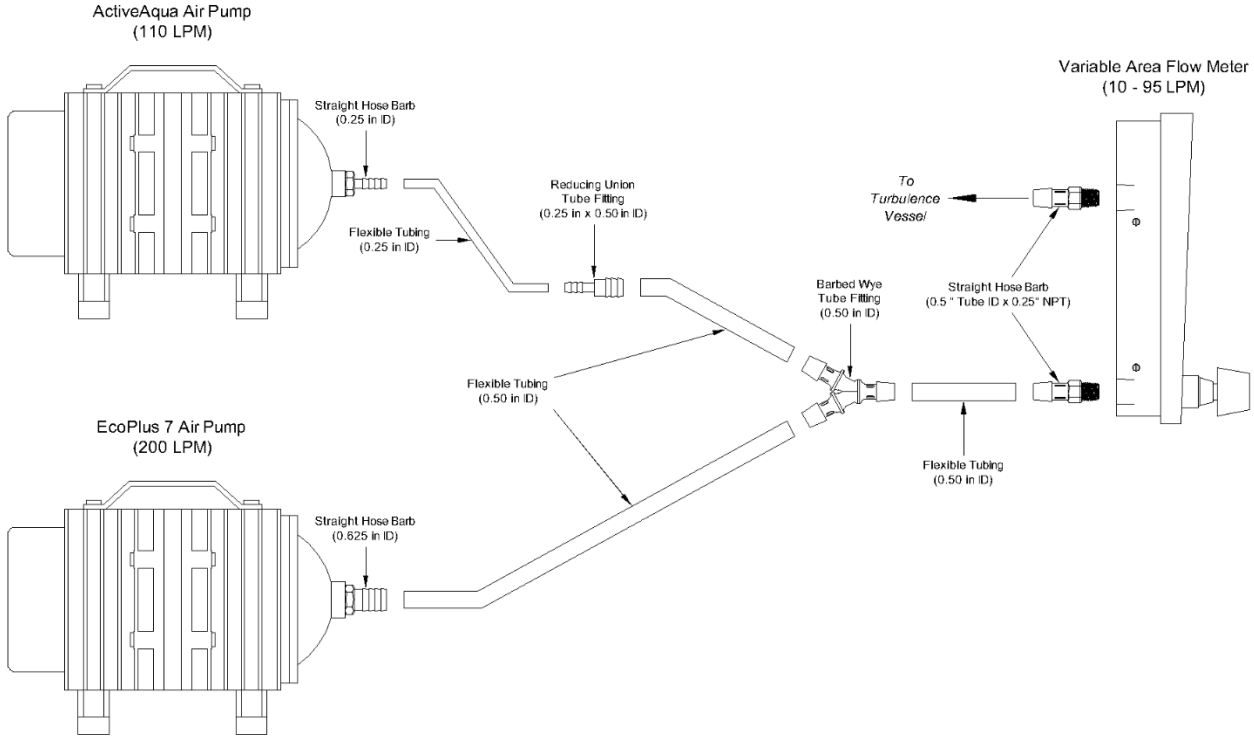

Figure 5.3. Schematic diagram of turbulent flow generation system.

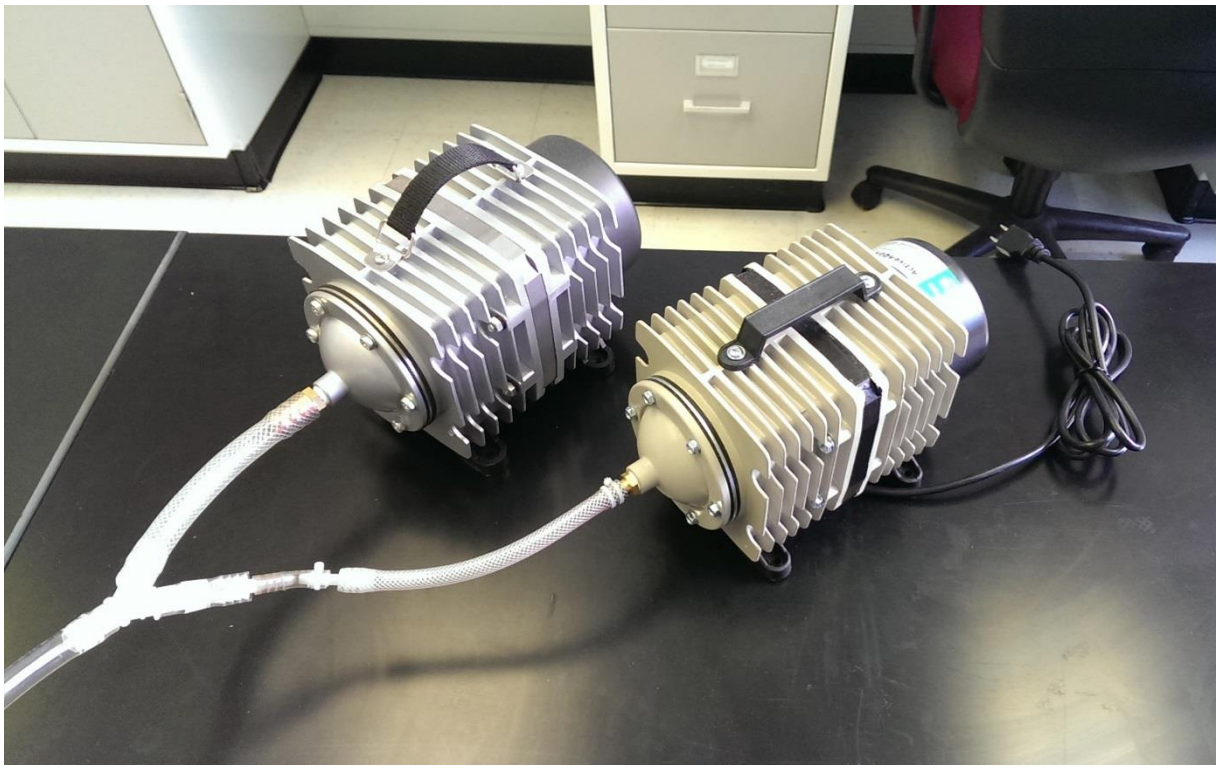

Figure 5.4. Picture of actual flow generation system used in this study.

The release area was constructed using a plastic cylinder with a diameter of 14.60 cm (5.749 in) and a height of 30.27 cm (11.918 in). The bottom of the cylinder was sealed while the top was left opened to accept a removable, airtight cover. The removable cover allowed for the placement and removal of the PPRVs. The outlet was connected to the PMCH release area and opened to the atmosphere. The air stream exhausted into a fume hood to eliminate any contamination resulting from recirculation. The outlet consisted of a plastic pipe with an internal diameter (ID) of 1.58 cm (0.622 in) and a length of 15.54 cm (6.118 in). A sample port was connected perpendicular to the outlet using a T-interface. The sample port, which was 3.782 cm (1.489 in) in length, was attached using the same pipe as the outlet. The port was designed to accept a rubber septum to allow sampling of the exhaust stream using either an evacuated sample vial or a syringe. The entire vessel was designed to be airtight between the inlet and the outlet so that the PMCH stream was neither lost nor contaminated from external sources during sampling. Detailed schematics and a picture of the container can be seen in **Figure 5.5** through **Figure 5.8**.

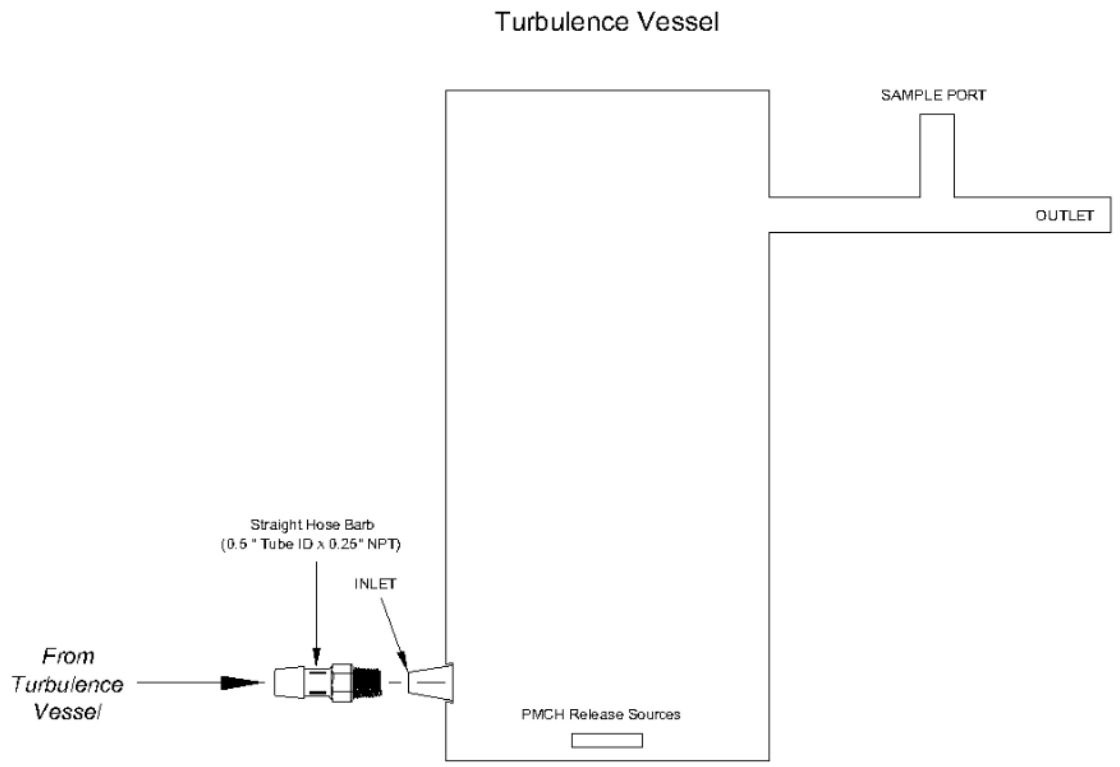

Figure 5.5. Front view of the turbulence container with detailed schematic of inlet connector.

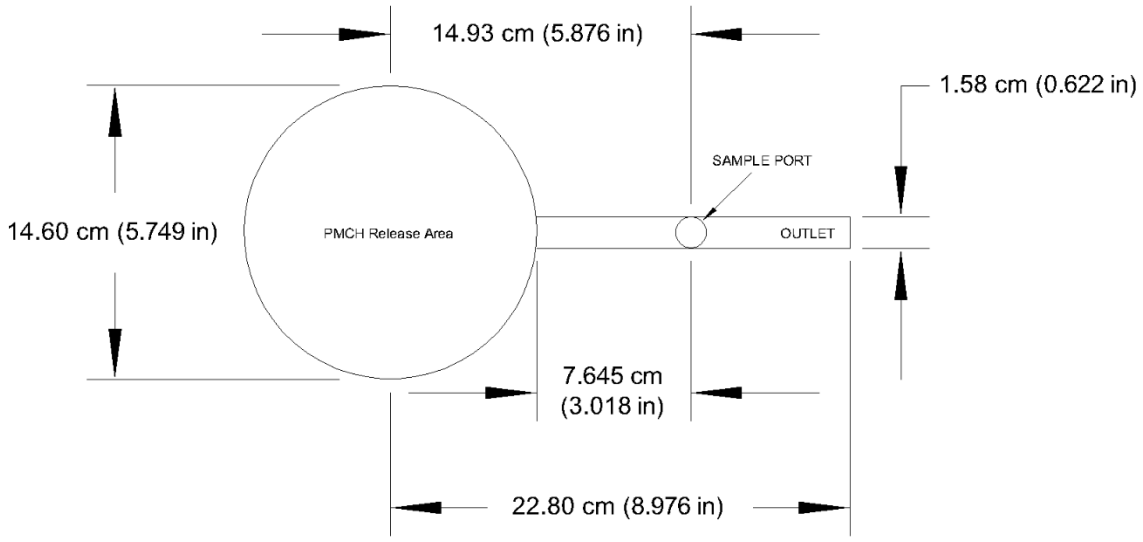

Figure 5.6. Top view of the turbulent flow container.

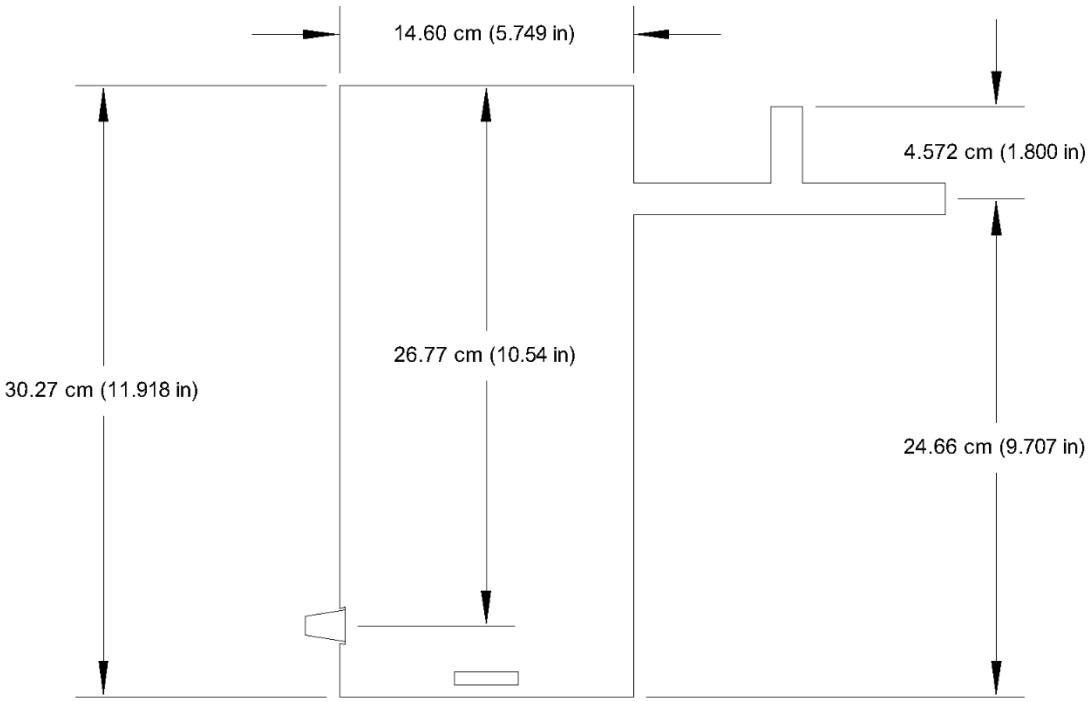

Figure 5.7. Front view of the turbulent flow container.

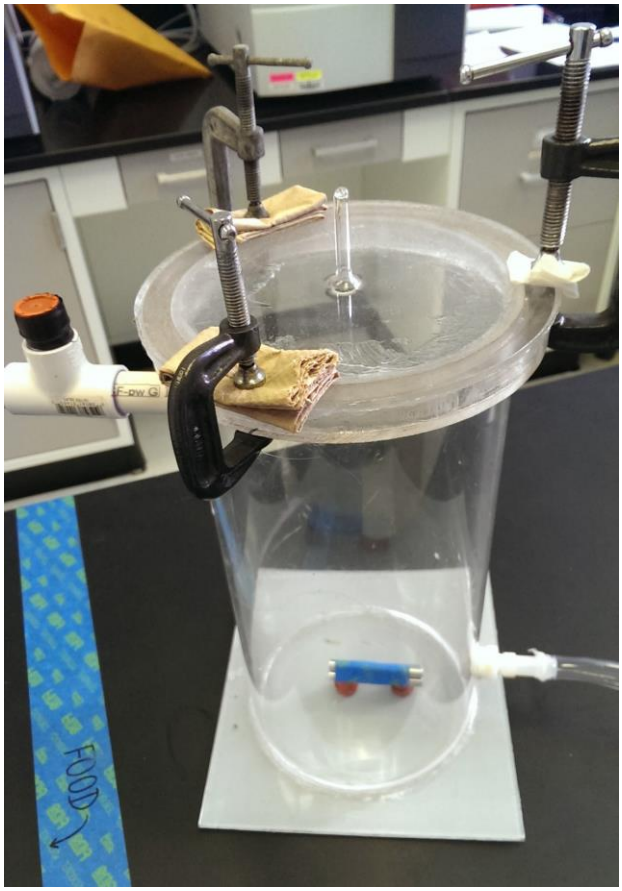

Figure 5.8. Picture of the actual turbulence flow container used in this study.

The PPRVs were exposed to five different flow quantities representing transitional and turbulent flows. The five flow quantities were 30 LPM, 40, LPM, 50 LPM, 60 LPM, and 70 LPM. **Table 5.1** displays each flow quantity paired with their respective Reynold's number. The Reynold's numbers were determined at each quantity using a dynamic viscosity of $1.983 \cdot 10^{-5}$ N·s/m^2, a hydraulic diameter of 0.0158 m based on the outlet, and a dry air density of 1.225 kg/m^3.

Table 5.1. Flow quantities with associated Reynold's numbers.

Flow Quantity (LPM)	Reynold's Number	Flow Type
30	2,759	Transitional
40	3,678	Transitional
50	4,598	Turbulent
60	5,517	Turbulent
70	6,437	Turbulent

Each flow quantity was applied to the PPRVs in a random time order and replicated four times to determine release rate variability. Two lab technicians were used to apply the different flow quantities as well as take tracer samples from the turbulence container. In order to account for any variance caused by the technicians, a generalized randomized complete blocking design (GRCBD) was implemented in this study. Each lab assistant was randomly assigned two replicates of each flow quantity. A summary of the GRCBD is provided in **Table 5.2** and **Table 5.3**.

Table 5.2. Treatment randomization by investigator.

Flow Quantity	Investigator 1	Investigator 2
30	6	10
30	9	5
40	3	8
40	10	6
50	4	2
50	5	1
60	7	3
60	1	4
70	8	7
70	2	9

Table 5.3. Treatment randomization by flow quantity (LPM).

Order	Investigator 1	Investigator 2
1	60	50
2	70	50
3	40	60
4	50	60
5	50	30
6	30	40
7	60	70
8	70	40
9	30	70
10	40	30

5.4 Gas Chromatography

5.4.1 Equipment

The analysis of PMCH was completed using a GC equipped with an electron capture detector (ECD). The ECD was chosen due to its high detection sensitivity to electronegative compounds (McNair and Miller 2009). The GC was fitted with a 30 m long, 0.25 mm ID porous layer open tube (PLOT) alumina chloride capillary column (HP-AL/S). The HP-AL/S column was deactivated with sodium sulfate and had a film thickness of 5 µm. This column was selected based on its ability to separate perfluorinated compounds.

5.4.2 Calibration Curve

The generation of a calibration curve is a necessary aspect of quantitative GC investigations due to the equipment-specific nature of GC technology. Although GCs are manufactured using identical principles, each device's detector response is unique and varies with installation parameters (e.g. length of column, composition of the stationary phase, composition of the mobile phase, etc.) and device configurations (e.g. linear velocity of the mobile phase, temperature of the column, etc.). Thus, a calibration curve using known standards must be created for each analysis to serve as a reference for known sample types with unknown concentrations (McNair and Miller 2009).

The concentration range of the PMCH calibration curve was defined by the expected concentration of PMCH at the sampling point. As previously stated, the sources were exposed to a range of air quantities from 30 LPM to 70 LPM in 10 LPM increments. The expected range of sampling concentrations can be determined using the low bound and high bound quantities of 30 LPM and 70 LPM respectively. These two points represent the highest and lowest possible concentrations of PMCH at the sampling point thus defining the extremes of the calibration curve. The expected concentration was determined using the following assumption: the turbulence vessel is airtight between the inlet and the outlet thus establishing $Q_{in} = Q_{out}$. As a result, the volumetric flow rate at the inlet, which was set by a flow controller, is the same as the volumetric flow rate at the sampling point within the outlet.

The minimum and maximum volumetric flow rates were then used in conjunction with the mass flow rate of the release sources to compute the expected concentration range of PMCH at the sampling point. The additional volumetric flow produced by the three PPRVs in parallel was assumed to have an insignificant impact on the overall volumetric flow of air. The mass flow of PMCH, as previously introduced, was expected to be $1.78 \cdot 10^{-6}$ g/min. The expected PMCH concentration using an upper bound volumetric flow rate of 70 LPM and a lower bound volumetric flow rate of 30 LPM was determined as follows.

$$PMCH_{min} = \frac{1.78 \cdot 10^{-6} \ \frac{g_{PMCH}}{min} \cdot \frac{kg}{1000 \ g}}{70 \ \frac{L_{air}}{min} \cdot \frac{m^3}{1000 \ L}} = 2.54 \cdot 10^{-8} \ \frac{kg_{PMCH}}{m^3{}_{air}}$$

$$PMCH_{max} = \frac{1.78 \cdot 10^{-6} \ \frac{g_{PMCH}}{min} \cdot \frac{kg}{1000 \ g}}{30 \ \frac{L_{air}}{min} \cdot \frac{m^3}{1000 \ L}} = 5.93 \cdot 10^{-8} \ \frac{kg_{PMCH}}{m^3{}_{air}}$$

The boundaries of the concentration curve must contain a concentration range of at least these calculated values. The PMCH concentrations can also be represented in PPB by moles (PPBM). This conversion can be accomplished by translating the volumetric flow of air and the mass flow

of PMCH to molar flows. The molar flow of air is determined assuming a dry air density of 1.205 g/L.

$$\frac{70\ L}{min} \cdot \frac{1.205\ g}{L} = 84 \frac{g}{min}$$

$$\frac{30\ L}{min} \cdot \frac{1.205\ g}{L} = 36 \frac{g}{min}$$

The mass flow can then be converted to a molar flow using a molecular weight of 28.97 g/mol for dry air.

$$\frac{84\ g}{min} \cdot \frac{mol}{28.97\ g} = 2.9 \frac{mol}{min}$$

$$\frac{36\ g}{min} \cdot \frac{mol}{28.97\ g} = 1.2 \frac{mol}{min}$$

The previous calculations for the molar flow of air was completed using the density and molecular weight of dry air. This molar flow does not represent the exact flow in the experiment due to the possibility of varying atmospheric conditions in the laboratory, such as humidity, temperature, and barometric pressure. A more accurate representation of the expected concentrations can be completed using psychometric properties and the idea gas law. However, the purpose of the previous calculation was to provide an initial point or reference from which a calibration curve could be generated. If the calculated boundaries did not provide an adequate range for interpolation, the calibration standards would simply need to be adjusted relative to the existing points.

The molar flow of PMCH was computed as follows using the previously determined mass flow of $1.78 \cdot 10^{-6}$ g/min and a molecular weight of 350.05 g/mol.

$$\frac{1.78 \cdot 10^{-6}\ g}{min} \cdot \frac{mol}{350.05\ g} = 5.08 \cdot 10^{-9}\ \frac{mol}{min}$$

The previously derived values can now be used to find the ratio of the molar flow of PMCH to the total molar flow, M, of PMCH and air. This ratio represents the molar fraction of PMCH in the total flow. The molar fraction can then be multiplied by 10^9 to convert the ratio into a PPBM.

$$PPBM_{min} = \frac{5.08 \cdot 10^{-9}\ \frac{mol}{min}}{5.08 \cdot 10^{-9}\ \frac{mol}{min} + 2.9\ \frac{mol}{min}} \cdot 10^9 = 1.8\ PPBM$$

$$PPBM_{max} = \frac{5.08 \cdot 10^{-9}\ \frac{mol}{min}}{5.08 \cdot 10^{-9}\ \frac{mol}{min} + 1.2\ \frac{mol}{min}} \cdot 10^9 = 4.1\ PPBM$$

Based on the previous computations, a target concentration range of 0.15 PPBM to 23 PPBM was selected to encompass the range of sampling concentrations as well as to allow for any fluctuations in PMCH release due to changing temperatures in the laboratory.

5.4.3 Standard Preparation

The creation of gaseous PMCH standards from a pure liquid was completed by following the three step process described below.

1. A master liquid standard was prepared by diluting 90% technical grade PMCH with a solvent.
2. A defined aliquot of the master standard was transferred to another vial for further solvent dilution.
3. A defined volume of the diluted master standard was then transferred to a headspace container and allowed to vaporize to create a gaseous standard.

Table 5.4 displays the dilution scheme for the five calibration standards.

Table 5.4. Dilution scheme for PMCH calibration curve standards.

	Master Standard (MS)		Intermediate Standard (IS)		Final Standard	
Standard Number	PMCH Volume (µL)	Solvent Volume (mL)	MS Transfer Volume (µL)	Solvent Volume (mL)	IS Transfer Volume (µL)	Headspace Volume (mL)
1	5	20	5	20	5	275
2	5	20	5	20	20	275
3	10	20	10	20	10	275
4	20	20	20	20	20	275
5	20	20	20	20	50	275

The calibration standards were all manually injected into the GC using a 100 µL gastight syringe. A total of three consecutive injections per calibration standard were made into the GC to detect any major relative standard deviations (RSD) between the injections. The resulting calibration curve data is presented in **Table 3.3**.

Table 5.5. GC calibration curve results.

	PMCH Peak			
Concentration (PPBV)	Retention Time (min)	Peak Area	Average Peak Area	% RSD
0.14	5.273	176.4	165.5	2.23
	5.284	168.7		
	5.279	151.3		
0.27	5.290	242.0	256.5	11.05
	5.282	275.7		
	5.279	251.7		
1.07	5.173	1300.3	1355.4	6.80
	5.174	1407.9		
	5.177	1205.6		
	5.179	1395.0		
	5.177	1468.2		
8.66	5.418	2553.9	2509.3	1.75
	5.413	2449.5		
	5.404	2524.4		
21.65	5.390	6613.5	6827.8	6.86
	5.380	6391.9		
	5.373	7477.9		

A graphical representation of the calibration curve can be seen in **Figure 5.9**.

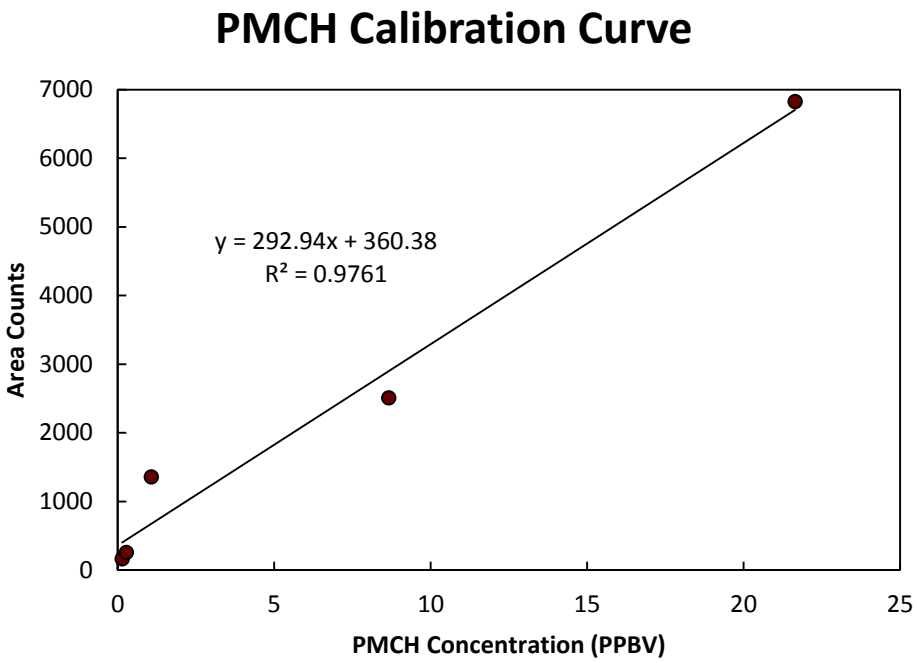

Figure 5.9. PMCH calibration curve.

All of the calibration standards were produced with an acceptable linear trend and processed with an adequate level of precision.

5.5 PPRV Evaluation

In order to complete the evaluation of the PPRV, the sources were deployed in controlled turbulent conditions. A detailed description of the release sources and the turbulence container can be found in previous sections. Air samples from the flow stream were then collected and analyzed using a GC to determine the concentration of PMCH at different volumetric flow rates.

5.5.1 Deployment

The PMCH PPRVs were first placed in the release area of the turbulence container. The container was then capped as quickly as possible and sealed with silicone grease to prevent contamination. The PPRVs were allowed to release PMCH into the flow stream for five minutes at the first assigned flow rate. The temperature of the laboratory was monitored to ensure that no significant fluctuations occurred during sampling. After the five minutes had elapsed, a 100 μL gas tight syringe was used to extract 30 μL of air from the sampling port. The 30 μL sample was then immediately injected into the GC for analysis.

Two additional consecutive samples were taken and injected in the same manner. All of the replicates for each flow quantity were taken in triplicate (i.e. a total of 60 individual samples). Two minutes were allotted between replicates to allow the PPRVs to equilibrate with each new flow setting. In order to accurately determine the expected concentration of PMCH in the flow stream, the environmental conditions were also recorded. Over the course of the experiment, the turbulence container experienced an average temperature of 295 K and an average absolute barometric pressure (i.e. station pressure) of 94,000 Pa. Using these values and assuming ideal gas behavior, the expected concentration in parts per billion by volume (PPBV) is presented in **Table 5.6**.

Table 5.6. Expected PMCH concentrations at each flow quantity.

Air Quantity (LPM)	**PMCH (PPBV)**
30	4.40
40	3.30
50	2.64
60	2.20
70	1.88

5.6 Experimental Results

The GC method used to quantify the samples and to generate the calibration curve is outlined in **Table 5.7**.

Table 5.7. GC analytical method.

Parameter	**Description**
Carrier Gas	He
Injector Temperature	150°C
Split Ratio	20:1
Linear Velocity	25 cm/s
Detector Temperature	200°C
Initial Column Temperature	180°C
Hold Initial Temperature	5.50 min
Temperature Increase	3.0°C/min to 190°C
Final Column Temperature	Hold 190°C for 0.75 min
Total Program Runtime	6.58 min

The raw data from the GC analysis performed by the two lab technicians are presented in **Table 5.8** and **Table 5.9**.

Table 5.8. PMCH data from Technician #1.

Run Number	Flow Quantity (LPM)	Retention Time (min)	Peak Area	Average Peak Area	Std. Dev.	% RSD
1		5.374	1025.1			
2	60	5.452	1084.3	1092.1	58.19	5.33
3		5.457	1167.0			
4		5.455	1044.2			
5	70	5.450	1035.7	1028.0	17.25	1.68
6		5.449	1004.1			
7		5.478	1002.1			
8	40	5.475	891.4	1037.5	136.06	13.11
9		5.465	1219.0			
10		5.465	958.8			
11	50	5.458	1369.1	1247.5	204.99	16.43
12		5.435	1414.6			
13		5.458	1397.5			
14	50	5.457	1354.6	1382.1	19.49	1.41
15		5.459	1394.2			
16		5.461	2101.9			
17	30	5.463	2141.5	2134.7	24.45	1.15
18		5.467	2160.6			
19		5.461	1147.9			
20	60	5.464	1230.8	1214.4	48.96	4.03
21		5.465	1264.4			
22		5.466	1064.7			
23	70	5.470	1083.9	1066.1	14.00	1.31
24		5.473	1049.7			
25		5.469	2134.5			
26	30	5.471	2075.3	2078.7	44.28	2.13
27		5.477	2026.2			
28		5.473	1507.2			
29	40	5.477	1572.8	1592.4	78.75	4.95
30		5.479	1697.1			

Table 5.9. PMCH data from Technician #2.

Run Number	Flow Quantity (LPM)	Retention Time (min)	Peak Area	Average Peak Area	Std. Dev.	% RSD
1	60	5.484	1333.5	1315.5	12.98	0.99
2		5.481	1303.4			
3		5.484	1309.6			
4	70	5.485	1320.7	1305.2	11.52	0.88
5		5.486	1293.1			
6		5.483	1301.8			
7	40	5.470	1157.9	1157.1	7.61	0.66
8		5.466	1166.0			
9		5.469	1147.4			
10	50	5.467	1142.0	1139.5	4.41	0.39
11		5.471	1143.2			
12		5.471	1133.3			
13	50	5.483	2091.0	2071.0	20.17	0.97
14		5.484	2078.7			
15		5.487	2043.4			
16	30	5.485	1467.7	1546.4	65.69	4.25
17		5.490	1628.5			
18		5.495	1543.1			
19	60	5.469	940.6	1042.1	72.83	6.99
20		5.466	1108.0			
21		5.468	1077.7			
22	70	5.467	1890.3	1779.2	78.56	4.42
23		5.470	1721.4			
24		5.471	1726.0			
25	30	5.470	1112.5	1053.1	89.77	8.52
26		5.473	1120.5			
27		5.476	926.2			
28	40	5.479	2271.2	2110.5	167.28	7.93
29		5.479	2180.5			
30		5.482	1879.8			

A summary of the results accompanied by an analysis of variance (ANOVA) can be found in **Table 5.10** and **Table 5.11** respectively. The results are also graphically represented in **Figure 5.10**.

Table 5.10. Summary of results by block from both lab technicians.

		Replicate #1		Replicate #2		
Block	**Flow Quantity (LPM)**	**Order**	**Peak Area**	**Order**	**Peak Area**	**Cell Mean**
Technician #1	30	6	2134.7	9	2078.7	2106.7
	40	3	1037.5	10	1592.4	1314.9
	50	4	1247.5	5	1382.1	1314.8
	60	1	1092.1	7	1214.4	1153.3
	70	2	1028.0	8	1066.1	1047.1
Technician #2	30	5	2071.0	10	2110.5	2090.8
	40	6	1546.4	8	1779.2	1662.8
	50	1	1315.5	2	1305.2	1310.6
	60	3	1157.1	4	1139.5	1148.3
	70	7	1042.1	9	1053.1	1047.6

Table 5.11. ANOVA Table.

Source	**Degrees of Freedom**	**Sums of Squares**	**Means Square**	**F-Ratio**	**p-value**
Flow Quantity	4	2753264.5	688316.1	34.260	<0.0001
Technician	1	20882.0	20882.0	1.039	
Block-Treatment Interaction	4	100446.5	25111.6	1.250	0.3512
Error	10	200909.0			
Total	19	3075502.0			

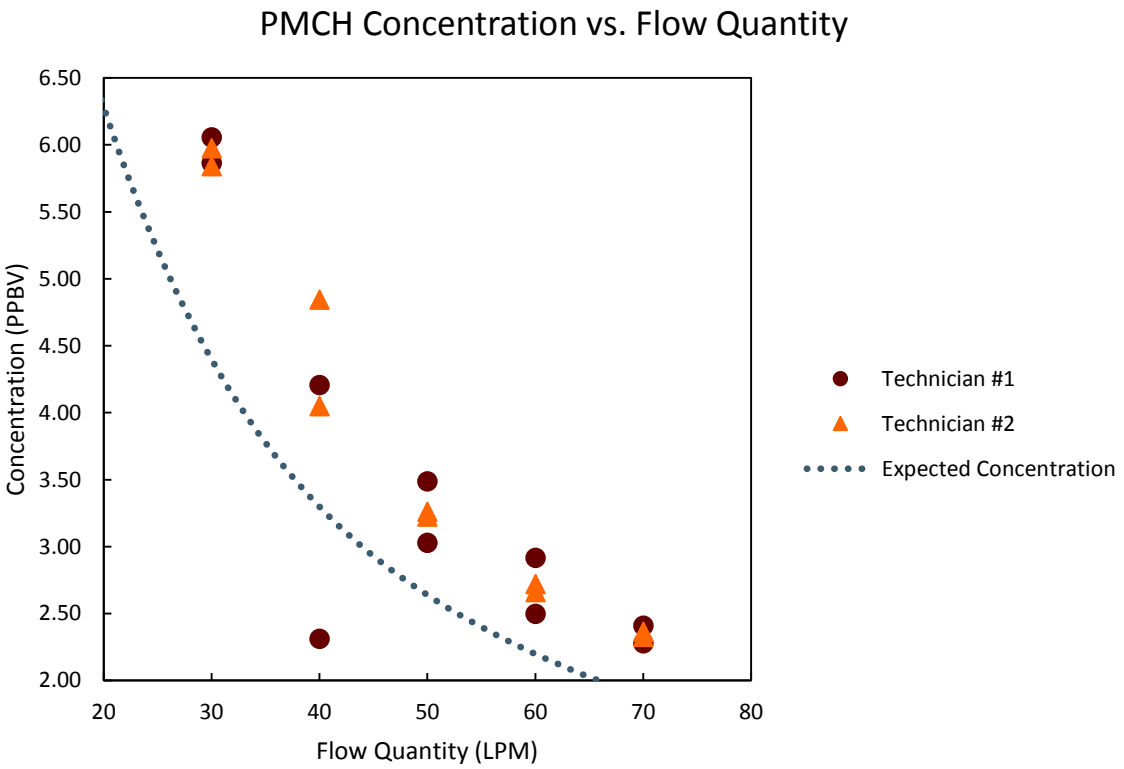

Figure 5.10. Measured PMCH concentration plotted against the associated flow quantity.

Table 5.12 displays the precision of the samples taken at each quantity, which is graphically represented in the previous figure.

Table 5.12. %RSD between replicates at the same treatment level.

Flow Quantity (LPM)	Concentration (PPBV)	%RSD
30	5.93	1.47
40	3.85	24.35
50	3.25	5.02
60	2.70	5.53
70	2.34	2.04

Table 5.13 displays the deviation between the measured PMCH concentration from the sample port and the expected concentrations based on the release rate of the PPRV at the associated flow quantity.

Table 5.13. Expected PMCH concentration compared to measured PMCH concentration.

Air Quantity (LPM)	Expected PMCH Concentration (PPB)	Average Measured PMCH Concentration (PPB)	Difference in PMCH Concentration (PPB)	% Error
30	4.40	5.93	1.54	34.94
40	3.30	3.85	0.55	16.80
50	2.64	3.25	0.61	23.19
60	2.20	2.70	0.50	22.71
70	1.88	2.34	0.46	24.43

5.7 Discussion and Conclusions

The study presented in this paper evaluated the potential of a PPRV assembled by the authors for use as an underground mine ventilation tracer deployment medium. The PPRV consists of a hollow aluminum cylinder with one end opened to the atmosphere and with the other end sealed. Liquid PMCH was stored in the vessel and released over time through a silicone plug pressed flush to the end. The PMCH releases to the atmosphere from the plug at a linear rate directly proportional to temperature. Three release sources were placed at a constant temperature and in a controlled turbulent flow stream to determine their performance under these conditions. A range of air flow quantities from 30 LPM to 70 LPM in increments of 10 LPM was induced to test the predictability and repeatability of the PPRVs. These quantities represent both turbulent and transitional type flows to determine their effect, if any. The PMCH concentration in the flow stream was determined by extracting air samples and then processing those samples through a GC. A detailed description of the experimental design can be found in Section 5.3.

The PMCH concentration measured across each of the replicate is plotted against flow quantity in **Figure 5.10**. A line representing the expected concentration of PMCH at each of the flow quantities is also displayed. The tight grouping of the different replicates at each of the flow

quantities graphically demonstrate high precision at the majority of the sample points. The high sampling precision of both technicians are further demonstrated by the low RSD values. **Figure 5.10** also shows that as the flow quantity enters the transitional zone (i.e. 30 LPM and 40 LPM), the precision of the replicates begins to decrease. This behavior is expected as the molecular weight of PMCH would require a fully developed turbulent flow to facilitate homogeneous mixing of the tracer. Transitional flow displays both laminar and turbulent flow characteristics. As a result, the PMCH shifts between being homogeneous and heterogeneous mixed in the stream.

The ANOVA results displayed in **Table 5.11** show that there is sufficient evidence to suggest that the change in concentration based on peak area was significantly affected by the application of the different air quantities using an alpha value of 0.05. This result also suggests that the release rate of the PPRVs stayed relatively uniform amongst the replicates because a significant difference was only found at the different treatment levels. With a p-value > 0.05, the ANOVA analysis concludes that no significant block-treatment interaction was demonstrated. Thus, any variability in the results caused by the technicians themselves was insignificant and did not affect the results.

The expected PMCH concentration are displayed in **Table 5.6**. These values were determined using the velocity of the volumetric flow of air and the release rate of the sources at 21°C. The release rate of the three PPRVs were recorded in a previous experiment. The difference between the expected concentrations and actual concentrations at each of the flow quantities are shown in **Table 5.13**. Although the errors are on average about 20%, this value only represents a 0.50 PPB shift in concentration. Additionally, given the consistency in the concentration difference, the parallel response of the PPRVs as compared to the expected response, as well as the high sampling and analysis precision, this error is most likely present in the calibration curve. Even so, a 20% deviation based on a calibration curve derived from multiple PPB level serial dilution standards does not represent a significant error.

The low error parallel response, high precision, and highly repeatable results of the analyzed samples demonstrate that the PPRVs did release PMCH at a constant rate. The PPRVs were also

shown to be highly reliable and predictable within the scope of the experiment. According to the response of the PPRVs in the transitional and turbulent flows, homogeneous mixing can be reliably achieved only in a turbulent flow. The PPRVs were therefore found to not only be a viable PMCH release technique but also exceptionally simple to implement. Although these release sources were found to be feasible under controlled conditions, additional complications may present themselves during an actual underground release. As a result, further large-scale field tests must be completed before a final conclusion can be made.

5.8 Bibliography

Dietz, R. N. (1986). Perfluorocarbon tracer technology. Regional and Long-range Transport of Air Pollution, Ispra, Italy, Elsevier Science Publishers B.V.

Dietz, R. N. (1991). Commercial applications of perfluorocarbon tracer (PFT) technology. The Department of Commerce Environmental Conference, "Protecting the Environment: New Technologies - New Markets". Reston, VA.

Dietz, R. N. and E. A. Cote (1982). "Air infiltration measurements in a home using a convenient perfluorocarbon tracer technique." Environmental International **8**: 419-433.

Dietz, R. N., R. W. Goodrich, E. A. Cote and R. F. Wieser (1986). Detailed description and performance of a passive perfluorocarbon tracer system for building ventilation and air exchange measurements. Measured Air Leakage of Buildings. H. R. Trechsel and P. L. Lagus. Philadelphia, PA, American Society for Testing and Materials. **ASTM STP 904:** 203-264.

Fast, J. D., K. J. Allwine, R. N. Dietz, K. L. Clawson and J. C. Torcolini (2006). "Dispersion of perfluorocarbon tracers within the Salt Lake Valley during VTMX 2000." Journal of Applied Meteorology and Climatology **45**(6): 793-812.

Grot, R. A., P. L. Lagus, R. Hyle, R. Ledsky, M. Evans and E. Sutton (1995). Protocol for measuring the air change rate in non-residential buildings, Lagus Applied Technology, Inc.**:** 1-97.

Hartman, H. L., J. M. Mutmansky, R. V. Ramani and Y. J. Wang (1997). Mine ventilation and air conditioning. New York, John Wiley & Sons, Inc.

Heiser, J. and T. Sullivan (2002). The Brookhaven National Laboratory perfluorocarbon tracer technology: a proven and cost-effective method to verify integrity and monitor long-term performance of walls, floors, caps, and cover systems. Long Island, NY, Brookhaven National Laboratory**:** 1-32.

Leaderer, B. P., L. Schaap and R. N. Dietz (1985). "Evaluation of the perfluorocarbon tracer technique for determining infiltration rates in residences." Environmental Science and Technology **19**(12): 1225-1232.

Levin, I., T. Naegler, R. Heinz, D. Osusko, E. Cuevas, A. Engel, J. Ilmberger, R. L. Langenfelds, B. Neininger, C. v. Rohden, L. P. Steele, R. Weller, D. E. Worthy and S. A. Zimov

(2010). "The global SF_6 source inferred from long-term high precision atmospheric measurements and its comparison with emission inventories." Atmospheric Chemistry and Physics **10**(6): 2655-2662.

Maiss, M. and C. A. M. Brenninkmeijer (1998). "Atmospheric SF_6: Trends, sources, and prospects." Environmental Science and Technology **32**(20): 3077-3086.

McNair, H. M. and J. M. Miller (2009). Basic gas chromatography. New Jersey, John Wiley & Sons, Inc.

National Institute of Standards and Technology (2011). Perfluoro(methylcyclohexane), U.S. Secretary of Commerce.

Ravishankara, A. R., S. Solomon, A. A. Turnipseed and R. F. Warren (1993). "Atmospheric lifetimes of long-lived halogenated species." Science **259**(5092): 194-199.

Sandford, G. (2003). "Perfluoroalkanes." Tetrahedron **59**(4): 437-454.

Stymne, H., C. A. Bowman and J. Kronvall (1994). "Measuring ventilation rates in the Swedish housing stock." Building and Environment **29**(3): 373-379.

Thimons, E. D., R. J. Bielicki and F. N. Kissell (1974). Using sulfur hexafluoride as a gaseous tracer to study ventilation systems in mines. Bureau of Mines Report of Investigations, United States Department of the Interior.

Watson, T. B., R. Wilke, R. N. Dietz, J. Heiser and P. Kalb (2007). "The atmospheric background of perfluorocarbon compounds used as tracers." Environmental Science and Technology **41**(20): 6909-6913.

Chapter 6: Development of a perfluoromethylcyclohexane (PMCH) permeation plug release vessel (PPRV) for tracer gas studies in underground mines

ABSTRACT: Perfluoromethylcyclohexane (PMCH) is a member of the perfluorocarbon tracer (PFT) group of compounds. PMCH has shown to be a viable alternative to the widely used tracer gas sulfur hexafluoride (SF_6). This viability stems from the fact that PMCH can be used concurrently with SF_6 while maintaining adequate chromatographic separation and high detection sensitivity during gas chromatographic (GC) electron capture (EC) analysis. However, the release of PMCH in an underground mine ventilation system is challenging due to its physical characteristics. SF_6 exists as a gas at room temperature and pressure and can be accurately released using a variety of means. In contrast, PMCH exists as a volatile liquid at room temperature and pressure, a characteristic that prevents PMCH from being deployed using traditional means. This paper presents a design for a permeation plug release vessel (PPRV) for PMCH. The PPRV is designed to passively deploy PMCH vapor at linear rate as a function of temperature and plug thickness.

6.1 Introduction

Sulfur hexafluoride (SF_6) has been the predominant tracer gas used in underground mine ventilation studies for over 30 years (Thimons, Bielicki, and Kissell 1974). However, the ability of SF_6 to function as the sole tracer is being hindered by two main issues: the increasing scale of mine ventilation systems and the steadily growing background concentration of SF_6 in the atmosphere. In order to support the advance of underground mines, a sympathetic expansion of their ventilation systems must also occur. The sheer scale and complexity modern mines has diminished the analysis power of a single tracer gas. As a result, the effectiveness of SF_6 as a mine ventilation characterization tool has begun to decrease. This issue is compounded by the growing background concentration of SF_6 in the atmosphere.

One of the main characteristics of a tracer gas is low background presence. This property not only reduces the possibility of interference but also allows for the characterization of low velocity flows, such as leakage through a barrier. As the background presence of a tracer increases, the release amount must follow suit in order to maintain an acceptable signal to noise ratio. This increase is the result of two main processes: the popularity of SF_6 as an electrical insulator and the high atmospheric stability of the SF_6 molecule.

SF_6 is widely used to insulate dielectric switchgears and transformers due to its inert nature and high electron affinity. Since its initial industrial production in 1953, the atmospheric concentration of SF_6 has increased by two orders of magnitude. This accumulation of SF_6 is the result of its stability, which equates to an atmospheric lifetime of 3,200 years (Levin et al. 2010, Geller et al. 1997, Ravishankara et al. 1993, Maiss et al. 1996). In order to mitigate the issues of larger ventilation systems and increased background concentrations, recent studies have identified the compound perfluoromethylcyclohexane (PMCH) as a viable supplement for SF_6.

PMCH is classified as a perfluorinated cyclic hydrocarbon. Other compounds in this group classification include perfluoromethylcyclobutane (PMCB) and perfluoromethylcyclopentane (PMCP) (Galdiga and Greibrokk 1997). These compounds are also known as perfluorocarbon tracers (PFT) due to their chemical inertness, low toxicity, and trace level environmental

background presence thus uniquely suiting them for use as tracer gases (Dietz 1991, Watson et al. 2007). Compounds of this type have been widely implemented in heating, ventilation, and air conditioning (HVAC) as well as atmospheric monitoring studies (Dietz 1991) but not yet in the field of underground mine ventilation. In contrast to SF_6, PFTs exist as volatile liquids at room temperature and pressure (National Institute of Standards and Technology 2011). This physical property of PFTs removes one of the great advantages afforded by SF_6, its existence as a gas. As such, SF_6 can be purchased in convenient, standardized gas cylinders and released in a controlled manner using a variety of options (Thimons, Bielicki, and Kissell 1974). Two examples of release options are the flow meter method and the flow controller method.

The flow meter method utilizes an analog or a digital flow meter attached to the gas cylinder. SF_6 is then deployed at a pre-determined volumetric flow rate over time, which can be computed to a mass flow rate over time if necessary. This method offers a significant amount of control and flexibility. The flow controller method utilizes a sophisticated electronic regulator that allows for precise deployment of SF_6 either by mass or by volume depending on the controller. This method provides the greatest accuracy, reproducibility, and control of any readily available release approaches. A controlled tracer release is essential if quantitative data must be generated. However, the established release systems for SF_6 are not applicable to volatile liquids like PMCH. This paper presents a design for a permeation plug release vessel (PPRV) for PMCH. The PPRV passively deploys PMCH vapor at linear rate as a function of temperature and plug thickness. An equation to predict the release rate based on these two variables is provided. Details regarding the PPRV and experimental design are also discussed.

6.2 Background

PMCH is a perfluorinated cyclic hydrocarbon whose chemical structure is composed of perfluoroalkanes (Watson et al. 2007). Compounds of this type are biologically inert, chemically inert, and thermally stable (F2 Chemicals Ltd. 2011). The inert, non-reactive, and non-toxic nature of PMCH makes it an ideal choice as a tracer gas. PMCH is comprised of seven carbon atoms and fourteen fluorine atoms, which gives it a chemical formula of C_7F_{14}. The molecular structure of PMCH is displayed in **Figure 6.1**.

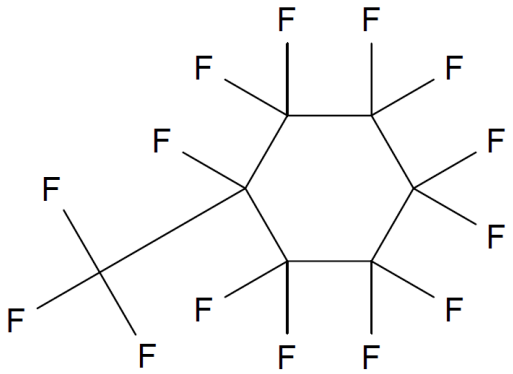

Figure 6.1. Molecular structure of PMCH.

The PMCH molecule is composed of two main parts, which are the cyclohexane ring and the methyl group bonded off to the side. This fully fluorinated molecule has a molecular weight of 350 g/mol and a boiling point of 76°C (169°F). PMCH to exist as a liquid at room temperature and pressure due to its molecular weight. The high volatility of PMCH simultaneously allows it to vaporize even at low temperatures. Once in a vapor state, PMCH, will remain a vapor even through cooler temperatures (National Institute of Standards and Technology 2011). Another advantage of PMCH is its detectability by GC even at low concentrations. This ability stems from PMCH's low ambient background in the atmosphere with concentrations in the low parts per quadrillion (PPQ) (Cooke et al. 2001, Simmonds et al. 2002, Watson et al. 2007) and high electron capture (EC) detection sensitivity (Simmonds et al. 2002). Perhaps the greatest advantage afforded by PMCH is its ability to be simultaneously analyzed with SF_6, which is the standard tracer gas employed in the mining industry. Despite these tracer characteristics, PMCH has not yet been implemented in underground mine ventilation. PMCH, however, has seen widespread use in other fields of study in conjunction with other PFT group compounds.

Building ventilation is one area that has implemented PFTs. PFTs have been used to investigate air infiltration into single family homes using passive PFT permeation sources coupled with passive capillary adsorption tube samplers (CATS) (Leaderer, Schaap, and Dietz 1985, Dietz and Cote 1982) as well as to evaluate the performance of multi-zone deployments of passive PFT sources for categorizing air infiltration, air exfiltration, and air exchanges (Dietz et al. 1986). PFTs have also been used to evaluate ventilation rates in Swedish housing stock as a nation-wide

effort to determine the adequacy of agricultural ventilation systems (Stymne, Bowman, and Kronvall 1994).

In the field of atmospheric tracing, PFTs have been used to characterize down-valley flow, canyon outflow, and interacting circulations on the lower slopes of the Wasatch Front (Fast et al. 2006). They have also been deployed to evaluate air flow patterns in New York City as part of the Urban Dispersion Program to improve wind station placements, to supplement knowledge of contaminant flow patterns, and to update atmospheric flow models (Watson et al. 2006). PFTs have additionally been used in long-term, large-scale investigations of the transport and diffusion of gases over the Alpine topography in Switzerland (Ambrosetti et al. 1998) as well as to evaluate the accuracy of meteorological air quality models under the Metropolitan Tracer Experiment conducted in Washington, D.C. (Draxler 1967).

The aforementioned examples of PMCH applications demonstrate the versatility of this compound as a tracer. Thus, PMCH demonstrates great potential for use as an underground mine ventilation tool. In order to successfully deploy PMCH, the release source must not only be able to perform a controlled release but also withstand the environmental conditions in a mine environment, such as dust and water. This paper presents a design for a permeation plug release vessel (PPRV) for PMCH. The PPRV is designed to passively deploy PMCH vapor at linear rate as a function of temperature and plug thickness. Details regarding the design and execution of the development process are also provided.

The basic concept of the PPRV detailed in this study was initially introduced by Brookhaven National Laboratory (BNL). In order to provide a cursory understanding of how the PPRV source operates, the gas diffusion mechanism must be discussed. The controlled release of PMCH is facilitated by the permeability characteristics of silicone rubber. The passage of a gas through rubber-type mediums such as silicone is a well-documented phenomenon that has undergone extensive study for over 50 years (Barbier 1955, Hammon, Ernst, and Newton 1977, Jordan and Koros 1990, Stern, Onorato, and Libove 1977, van Amerongen 1946, Zhang and Cloud 2006). In silicone rubber, similarly to other rubber-type polymers, gas diffusion occurs in three distinct steps: solution of the gas molecules on one side of the silicone membrane, diffusion

of the gas molecule through the silicone, and evaporation of the gas from the other side (Barbier 1955, Zhang and Cloud 2006). This diffusion through a seemingly impermeable medium can be achieved due to the chemical composition of silicone rubber.

Silicone, or polysiloxane, is a name used to define any compound derived from polymerized siloxanes. Polymerized siloxanes are substances whose molecular structure is created by combining monomers into large chains of alternating silicon (Si) and oxygen (O) atoms. The alternating atoms (e.g. Si-O) have organic groups or hydrogen atoms bonded to the Si atom (Merriam-Webster 2012, Bondurant, Ernster, and Herdman 1999, Velderrain and Lipps 2011, Van Reeth and Wilson 1994, Encyclopædia Britannica 2012). Silicone generally has two methyl groups attached to each siloxane thus producing a polydimethylsiloxane (PDMS) (Bondurant, Ernster, and Herdman 1999, Van Reeth and Wilson 1994). An example of the structural formula for PDMS is displayed in **Figure 6.2**.

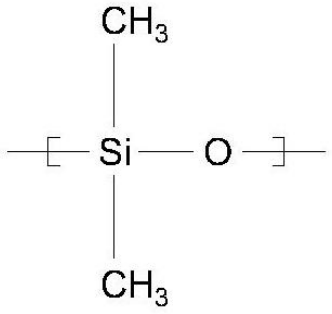

Figure 6.2. Chemical structure of polydimethylsiloxane (PDMS), the basic structure of silicone rubber.

Silicone is typically composed of a long chain, from hundreds to thousands, of repeating PDMS groups thus classifying silicone as a linear polymer (Bondurant, Ernster, and Herdman 1999). In order to form silicone rubber, or silicone elastomer, the polymer chains must be cross-linked through vulcanization. In order to produce silicone rubber, the basic PDMS chemical structure must be slightly altered to facilitate cross-linking (Andriot et al. 2007, Parker Hannifin Corp. 2007, Velderrain and Lipps 2011).

Methyl vinyl silicone (VMQ) is the most common type of silicone rubber. VMQ has the same overall structure as PDMS with some of the methyl groups replaced with vinyl groups to create

the reactive double bond necessary for cross-linking. The structure of the VMQ molecules, which is represented in **Figure 6.2**, allows free rotation around the Si-O bond (Andriot et al. 2007, Parker Hannifin Corp. 2007, Velderrain and Lipps 2011, Van Reeth and Wilson 1994). This chemical property allows the rubber to be highly flexible. This inherent flexibility afforded by the Si-O bond also permits the existence of free volumes within the compound thus allowing for gas permeability. Incidentally, silicone rubber also has the highest permeability of any polymer, which ideally suits this compound for use in the PMCH release source (Zhang and Cloud 2006, Andriot et al. 2007, Parker Hannifin Corp. 2007, Van Reeth and Wilson 1994).

The basic PPRV design consists of a hollow aluminum cylinder with one end of the cylinder open to atmosphere and the other end closed. Liquid PMCH is injected into the aluminum vessel and sealed with an oversized silicone plug pressed flush to the end. The source releases PMCH by allowing the phase change to occur internally. Vapor is produced immediately once the PMCH is exposed to atmosphere due to its high vapor pressure (106 torr at 25°C) (Dietz et al. 1986). The high flow resistance caused by the silicone plug produces a pseudo-closed system that allows the PMCH to reach dynamic equilibrium within the source. This equilibrium produces a steady pressure differential equivalent to the vapor pressure at the ambient temperature between the inside and outside of the vessel. This differential causes the vapor PMCH to slowly diffuse steadily through the silicone plug. This steady release rate result from the combination of a constant pressure front coupled with the fact that the silicone plug can be considered as a constant resistance medium. The permeability of the silicone will remain constant as long as the integrity is maintained and the compression of the plug is not excessive enough to significantly reduce the internal free volumes (Jordan and Koros 1990).

Once the PMCH equilibrates within the plug, vapor PMCH begins desorbing to atmosphere from the plug at a predictable rate directly proportional to temperature (Dietz et al. 1986). Since vapor pressure is directly proportional to temperature and independent of atmospheric pressure, the release rate will remain constant at a stable temperature. The PPRV presented in this paper is based on the overall concept of the BNL source but includes a manner to predict the release rate using VMQ silicone plug thicknesses. A discussion regarding the expected performance of the PPRV over time is also provided.

6.3 Experimental Design

The study presented in this paper examined thirty six PPRVs with varying plug thicknesses and fill level across six temperatures. Barometric pressure and ambient room temperature were also captured as covariates to ensure that these environmental conditions did not significantly affect the experiment. Relative humidity was not captured because the experiment was executed in a laboratory in which the relative humidity was kept constant at 40%. The varying PMCH fill levels were applied to the sources to determine the effect of PMCH depletion over time assuming that a failure of the plug or the shell had not occurred. In order to determine the effect of temperature on release rate, six different temperatures were applied in random time order over the course of the study. This experiment was completed in two main parts: assembling the PMCH release sources and determining the mass flow rate of each release source. The following section details the experimental parameters from preparing the PPRVs to executing the experiment. The PMCH release source components and designs will first be discussed.

The main body of the release vessel is comprised of an aluminum cylinder that is 6.35 cm (2.50 in) in length with an outside diameter (OD) of 0.747 cm (0.294 in). The cylinder itself is comprised of a hollow shell with one end sealed and the other end open to atmosphere. The shell has a wall thickness of 0.0356 cm (0.0140 in) that is consistent throughout the body of the cylinder, which gives an inside length of 6.31 cm (2.49 in) and an inside diameter (ID) of 0.711 cm (0.280 in). A schematic of the aluminum shell is displayed in **Figure 6.3**.

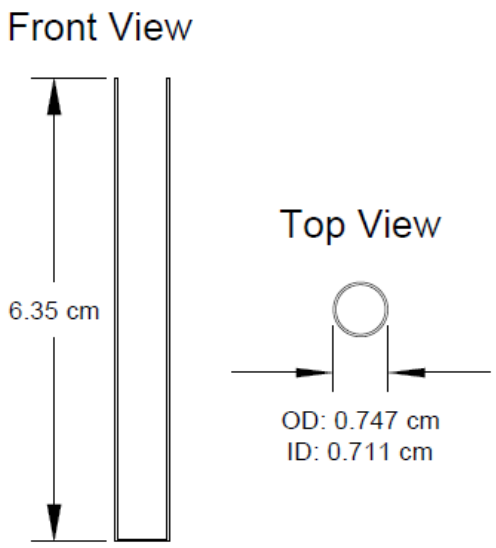

Figure 6.3. Schematic of an aluminum shell used for the PMCH release source.

As such, the shell can contain up to 2.5 mL (0.15 in^3) of liquid PMCH. A slightly oversized VMQ silicone plug with a diameter of 0.699 cm (0.275 in) was inserted into the open end of the aluminum cylinder and pressed flush to the end. Silicone grease was used as a lubricant to facilitate the press-fitting of the plug. The silicone plug serves as the diffusion membrane for PMCH after the liquid volatizes inside the vessel. A cutaway diagram of a completed PMCH source can be seen in **Figure 6.4**.

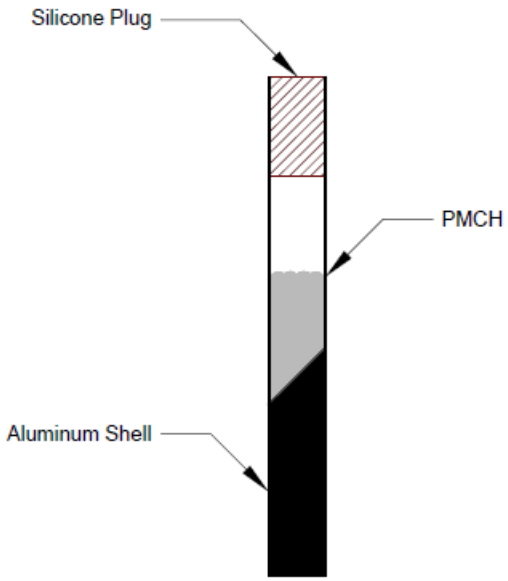

Figure 6.4. Cutaway diagram of a fully assembled PMCH release source.

Four PMCH fill levels, 0.100 mL, 0.275 mL, 0.425 mL, and 0.600 mL, and four plug thicknesses, 0.635 cm (0.25 in), 1.067 cm (0.42 in), 1.473 cm (0.58 in), and 1.905cm (0.75 in), were assigned according to a full factorial design. The fill level and plug thickness increments were divided equally between the two extremes. In previous preliminary studies, a fill level of 0.500 mL was used. A maximum fill level of 0.600 mL was chosen to determine if there was a significant difference in release rate with a greater amount of PMCH. The minimum fill level of 0.100 mL was constrained by the lowest accurate measurement that the chosen liquid tight syringe could achieve. The minimum and maximum plug thicknesses were chosen to represent a range that could be consistently cut and press fitted with high precision.

Two duplicates were created for each unique set of factors (e.g. two PPRVs are created with 0.100 mL of PMCH and a plug thickness of 0.25 in). The only exception was made for the 0.600 mL PPRVs. Three sources were assembled instead of two for the 0.600 mL PPRVs. All 36 release sources were assembled at one time without any personnel substitutions to ensure consistency. A detailed listing of the PPRVs can be found in **Table 6.1**.

Table 6.1. Inventory of PPRVs.

Source No.	PMCH (mL)	Plug Thickness (cm)
1	0.100	0.635
2	0.100	0.635
3	0.275	0.635
4	0.275	0.635
5	0.425	0.635
6	0.425	0.635
7	0.600	0.635
8	0.600	0.635
9	0.600	0.635
10	0.100	1.067
11	0.100	1.067
12	0.275	1.067
13	0.275	1.067
14	0.425	1.067
15	0.425	1.067
16	0.600	1.067
17	0.600	1.067
18	0.600	1.067
19	0.100	1.473
20	0.100	1.473
21	0.275	1.473
22	0.275	1.473
23	0.425	1.473
24	0.425	1.473
25	0.600	1.473
26	0.600	1.473
27	0.600	1.473
28	0.100	1.905
29	0.100	1.905
30	0.275	1.905
31	0.275	1.905
32	0.425	1.905
33	0.425	1.905
34	0.600	1.905
35	0.600	1.905
36	0.600	1.905

The PPRVs were then randomly assigned to one of two 500 mL borosilicate beakers filled with sand resulting in 18 PPRVs per beaker. The sand served as a temperature distribution medium to ensure that all of the sources maintained a uniform temperature as each temperature treatment was applied. These beakers were then placed inside a 20 L water bath capable of maintaining temperatures from ambient room temperature to 100°C with a uniformity of ± 0.2°C, a stability of ± 0.25°C, and a precision of ± 0.1°C. The six chosen temperatures were applied randomly in time over the course of approximately 109 days as shown in **Table 6.2**.

Table 6.2. Temperature treatments.

Time Order	Temperature (°C)
1	35
2	45
3	35
4	25
5	45
6	25
7	30
8	40
9	50
10	50
11	40
12	30

The PPRVs were given 48 hours to equilibrate with each new temperature treatment. After the 48 hour period, the mass of each source was recorded once per day over a period of five days. At the conclusion of the monitoring period, the change in mass per unit time was determined for the final analysis.

The experiment uses a strip-plot design model with two factors and two covariates. The first factor was the combination of plug thicknesses and PMCH fill levels. This factor was applied randomly to the first whole-plot unit of the PPRVs. Each of the 16 treatment combination levels was given two replicates. The one exception was the 0.600 mL PMCH fill level which was assigned three replicates. A similar fill level had already been successfully applied in previous

studies. As a result the 0.600 mL treatment was assigned the extra replicates in order to provide a highly precise base for comparing the effect of the other fill levels.

The second factor was temperature, which was assigned randomly to the second whole-plot unit of time in weeks. Two replicates were used for each of the six temperature treatment levels. The response release rate (i.e. change in PPRV mass per unit time) was obtained using the split-plots. The split-plots were determined using the intersection of the whole-plots. The two covariates, or variables that were present but not directly measured that may impact the response, were ambient room temperature and mean sea level barometric pressure. All factor and covariate terms were assumed to be fixed effects.

Table 6.3 displays a subset of the experiment design. The first and second rows represent PPRV number 10 and PPRV number 8 respectively with their randomly assigned combination of plug thickness and PMCH level. The first and second columns display the temperature randomization, 35°C and 45°C, over the course of Weeks 1 and 2 respectively. The remaining portion of the experiment was a continuation of this table encompassing the remaining sources and treatments listed previously.

Each temperature treatment was applied uniformly across all the plug thickness - PMCH fill level combinations. For example, the water bath was set to 35°C during Week 1 for all sources. No modifications were made to the sources in terms of plug thickness and PMCH fill level as the new temperature treatment of 45°C was applied during Week 2. Thus, each factor is held constant across all levels of the other factor defining a strip plot design. The plug thickness - PMCH fill level combinations were held constant to decrease amount of PMCH needed for the experiment. The application of a more traditional randomized design, such as a split plot design, would have required the manufacture of new PPRVs for each temperature treatment to maintain independent experimental units (EU). This type of experimental design would not have been cost or labor effective according to the constraints of this study. In order to improve the efficiency of time utilization, the temperature treatments were applied in a uniform manner across all PPRVs thus reducing the number of overall trials as well.

Table 6.3. Select subset of the experimental design.

		Factor 2: Temperature	
		Week 1	Week 2
Factor 1: Plug thickness and PMCH fill level	Source 10: PMCH = 0.100 mL Plug = 1.067 cm	Source 10 at 35°C	Source 10 at 45°C
	Source 8: PMCH = 0.600 mL Plug = 0.635 cm	Source 8 at 35°C	Source 8 at 45°C

6.4 Results

The compiled results of the PPRV study are presented in **Table 6.4** to **Table 6.9** and **Figure 6.5** to **Figure 6.9**. The color legends for the graphs are displayed in **Table 6.6** and **Table 6.7**.

Table 6.4. % RSD of PPRVs by plug thickness across each temperature treatment.

	% RSD					
Plug Thickness (cm)	**25°C**	**30°C**	**35°C**	**40°C**	**45°C**	**50°C**
0.635	6.99	11.01	4.35	7.83	5.81	8.87
1.067	16.24	8.93	4.26	8.86	8.61	11.71
1.473	10.96	15.12	10.57	11.79	10.92	16.02
1.905	19.39	9.61	24.07	19.98	12.34	24.52

Table 6.5. % Change in release rate between plug thicknesses across each temperature treatment.

	% Change in Release Rate					
Plug Thickness (cm)	**25°C**	**30°C**	**35°C**	**40°C**	**45°C**	**50°C**
0.635 to 1.067	-32	-34	-36	-37	-36	-39
1.067 to 1.473	-20	-28	-34	-25	-35	-30
1.473 to 1.905	-29	-22	-39	-21	-29	-29

Table 6.6. Color legend for **Figure 6.5** to **Figure 6.8**.

Fill Level (mL)	Color
0.100	
0.275	
0.425	
0.600	

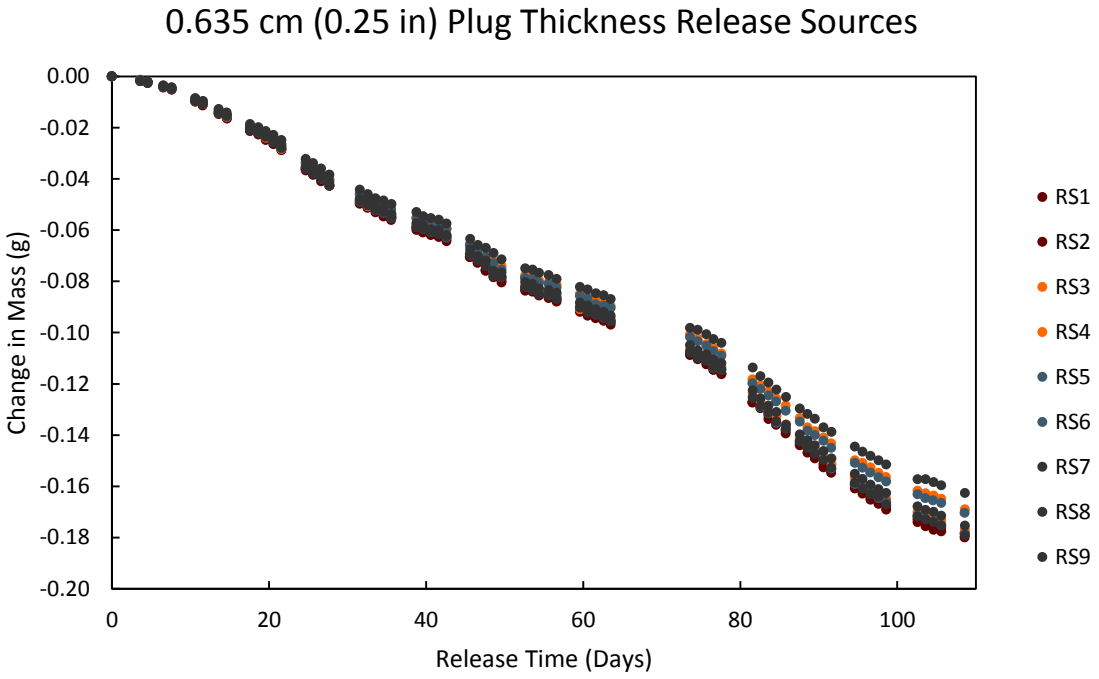

Figure 6.5. The change in mass over time for the 0.635 cm (0.25 in) PPRVs. The PPRVs are grouped by color according to their PMCH fill levels.

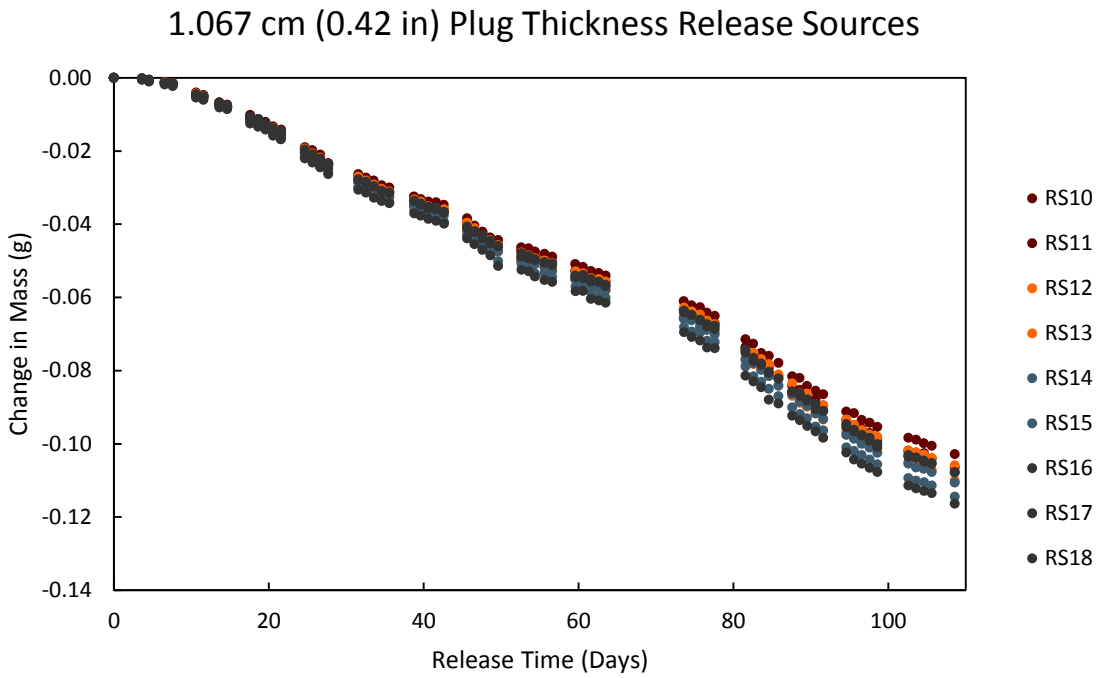

Figure 6.6. The change in mass over time for the 1.067 cm (0.42 in) PPRVs. The PPRVs are grouped by color according to their PMCH fill levels.

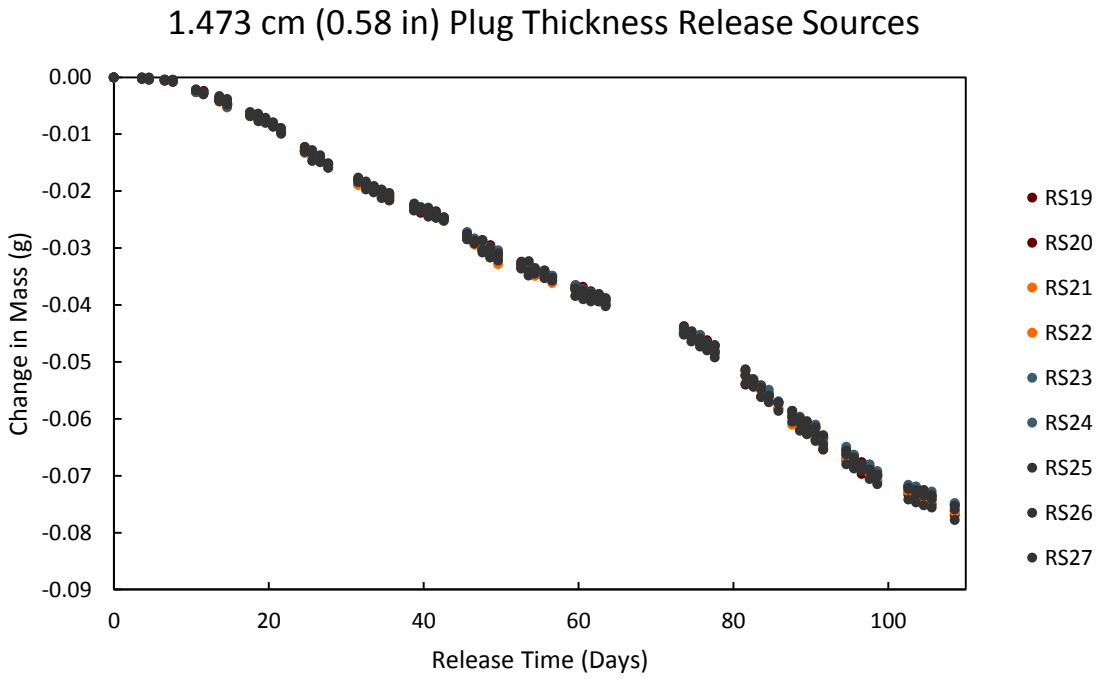

Figure 6.7. The change in mass over time for the 1.437 cm (0.58 in) PPRVs. The PPRVs are grouped by color according to their PMCH fill levels.

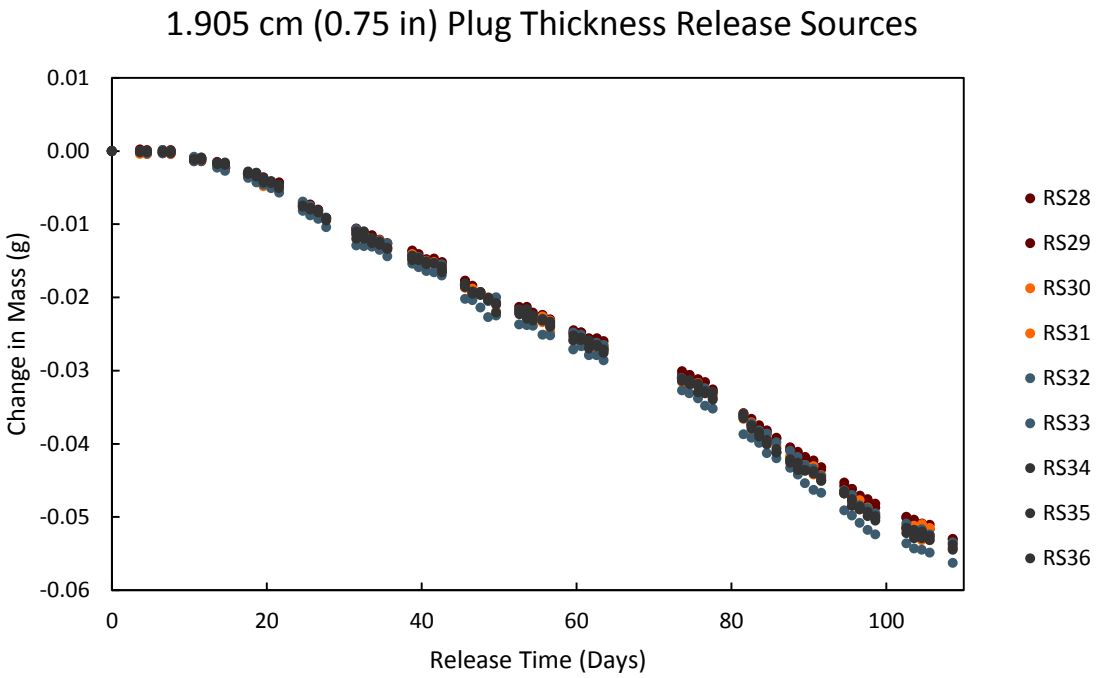

Figure 6.8. The change in mass over time for the 1.905 cm (0.75 in) PPRVs. The PPRVs are grouped by color according to their PMCH fill levels.

Table 6.7. Color legend for **Figure 6.9**.

Plug Thickness (cm)	Color
0.635	
1.067	
1.473	
1.905	

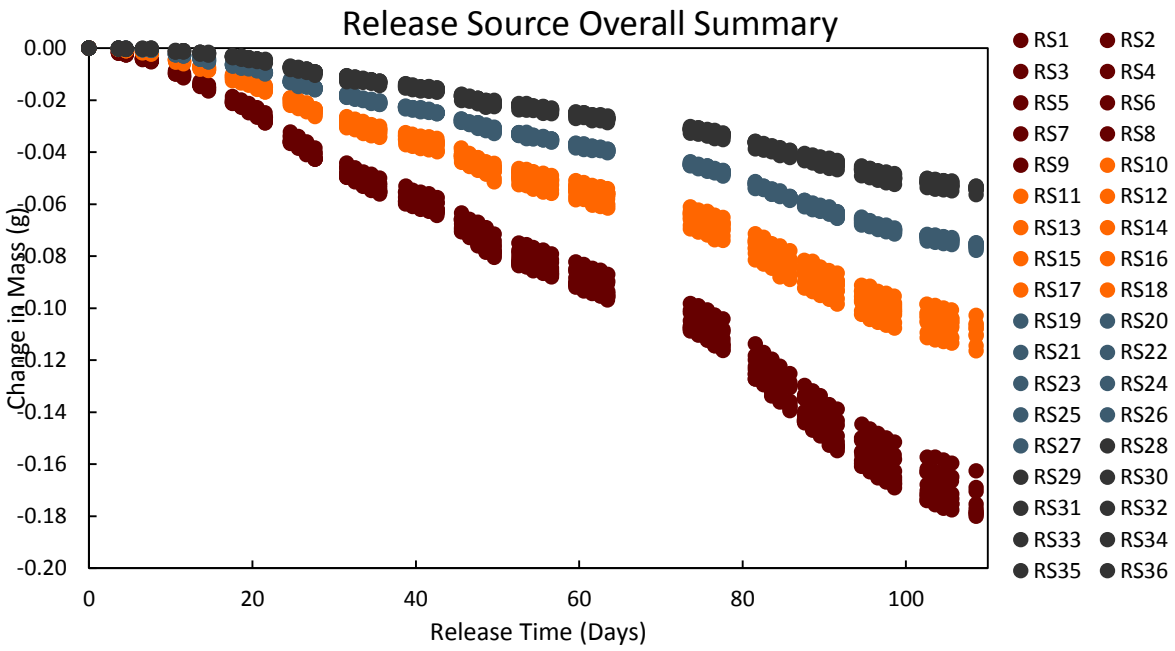

Figure 6.9. The change in mass over time for all PPRVs. The PPRVs are grouped by color according to their plug thicknesses.

Table 6.8 displays the difference between the release rates of the 0.600 mL PPRVs and the release rates of the PPRVs prepared with the 0.100 mL, 0.274 mL, and 0.425 mL fill levels. The 0.600 mL PPRV was selected as a base for comparison based on previous studies.

Table 6.8. % Change in release rate using the 0.600 mL PPRVs as a basis for comparison.

Plug Thickness (cm)	PMCH Fill Level (mL)	% Change					
		25°C	30°C	35°C	40°C	45°C	50°C
0.635	0.100	3.23	6.83	4.72	13.65	6.59	3.21
	0.275	8.62	5.07	3.69	4.51	0.38	4.19
	0.425	5.22	4.15	2.41	4.90	1.37	0.85
1.067	0.100	14.89	2.41	1.35	9.39	2.02	6.20
	0.275	10.01	0.24	5.76	4.07	0.83	1.72
	0.425	7.56	8.21	1.58	7.08	6.73	4.77
1.473	0.100	1.51	17.61	3.23	1.10	1.10	2.91
	0.275	7.60	8.54	6.33	12.15	7.87	14.19
	0.425	5.79	20.96	8.74	0.85	1.92	3.31
1.905	0.100	0.01	12.96	0.14	6.51	5.95	16.80
	0.275	0.73	1.80	6.27	9.50	6.94	6.25
	0.425	4.28	1.53	2.90	2.32	5.91	0.45

The estimated time to complete PMCH depletion in the PPRV according to PMCH fill level, plug thickness, and ambient temperature is presented in **Table 6.9**.

Table 6.9. Estimated lifetime of PPRVs by fill level and plug thickness across all temperature treatments.

PMCH Fill Level (mL)	Plug Thickness (cm)	Time (Years)					
		25°C	30°C	35°C	40°C	45°C	50°C
0.100	0.635	0.44	0.44	0.31	0.24	0.20	0.18
	1.067	0.78	0.62	0.52	0.44	0.34	0.32
	1.473	0.90	0.82	0.75	0.54	0.53	0.41
	1.905	1.23	1.02	1.24	0.72	0.68	0.69
0.275	0.635	1.38	1.18	0.87	0.73	0.59	0.53
	1.067	2.03	1.76	1.32	1.14	0.93	0.85
	1.473	2.27	2.43	2.13	1.68	1.33	1.34
	1.905	3.35	3.11	3.22	2.06	2.12	1.69
0.425	0.635	2.05	1.66	1.36	1.12	0.91	0.79
	1.067	2.62	2.51	2.13	1.82	1.34	1.23
	1.473	3.57	3.37	3.39	2.31	2.26	1.84
	1.905	5.00	4.82	5.45	2.94	3.25	2.46
0.600	0.635	2.75	2.45	1.96	1.67	1.30	1.11
	1.067	3.98	3.83	3.05	2.39	2.02	1.81
	1.473	5.34	5.75	4.36	3.23	3.13	2.51
	1.905	7.36	6.91	7.47	4.06	4.31	3.46

The results of **Table 6.9** are presented graphically in **Figure 6.10** and **Figure 6.11** to illustrate the impact of plug thickness, PMCH fill level, and temperature extremes on the estimated lifetime of the PPRVs.

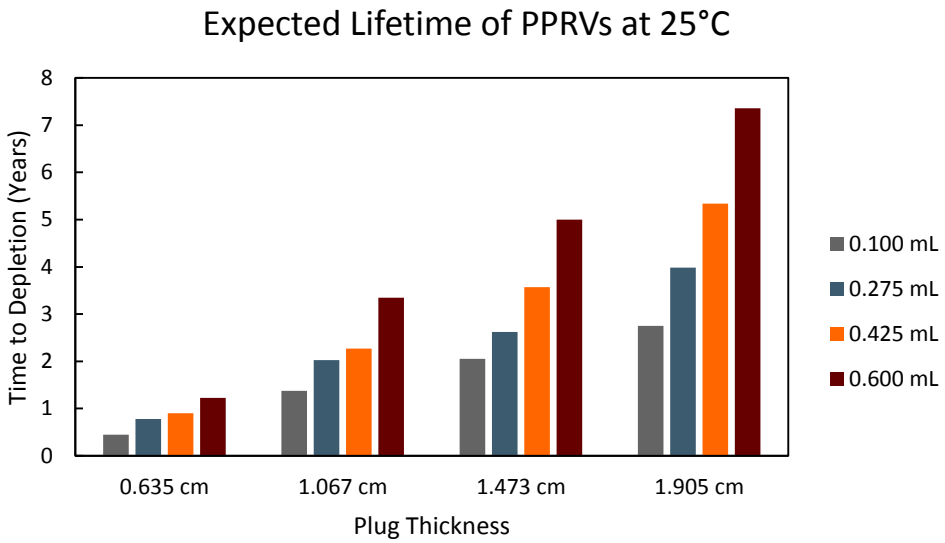

Figure 6.10. Estimated lifetimes of PPRVs at 25°C isothermal compared using PMCH fill level and plug thickness.

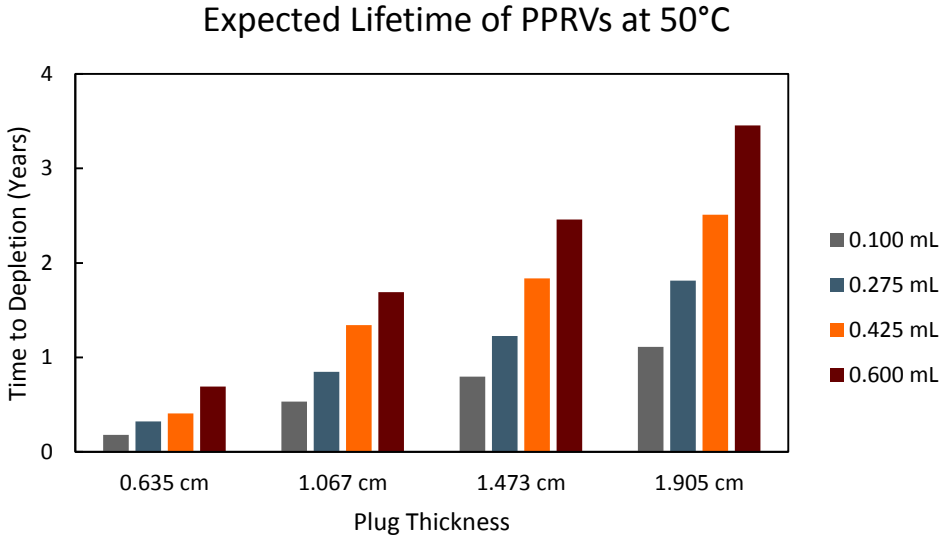

Figure 6.11. Estimated lifetimes of PPRVs at 50°C isothermal compared using PMCH fill level and plug thickness.

The experiment was analyzed as strip-plot design model using SAS Version 9.3. **Table 6.10** displays the Analyses of Variance (ANOVA) table of all fixed effect tests. Note that the denominator degrees of freedom (DOF), 20 or 6, of the whole-plot factors are much smaller than the DOF, 308, of the split-plot factors due to the randomization process used in the study. The interaction effects plot between plug thickness and temperature is displayed in **Figure 6.12**.

Table 6.10. Analyses of Variance (ANOVA) of PMCH release rate.

Effects	Numerator Degrees of Freedom	Denominator Degrees of Freedom	F-value	p-value
PMCH Level	3	20	0.82	0.4994
Plug Thickness	3	20	1070.06	<0.0001
PMCH Level · Plug Thickness	9	20	0.95	0.5076
Temperature	5	6	15.58	0.0022
Temperature · PMCH Level	15	308	0.81	0.6677
Temperature · Plug Thickness	15	308	69.82	<0.0001
Temperature · PMCH Level · Plug Thickness	45	308	0.98	0.5107
Ambient Room Temperature	1	308	0.45	0.5049
Barometric Pressure	1	308	1.17	0.2808

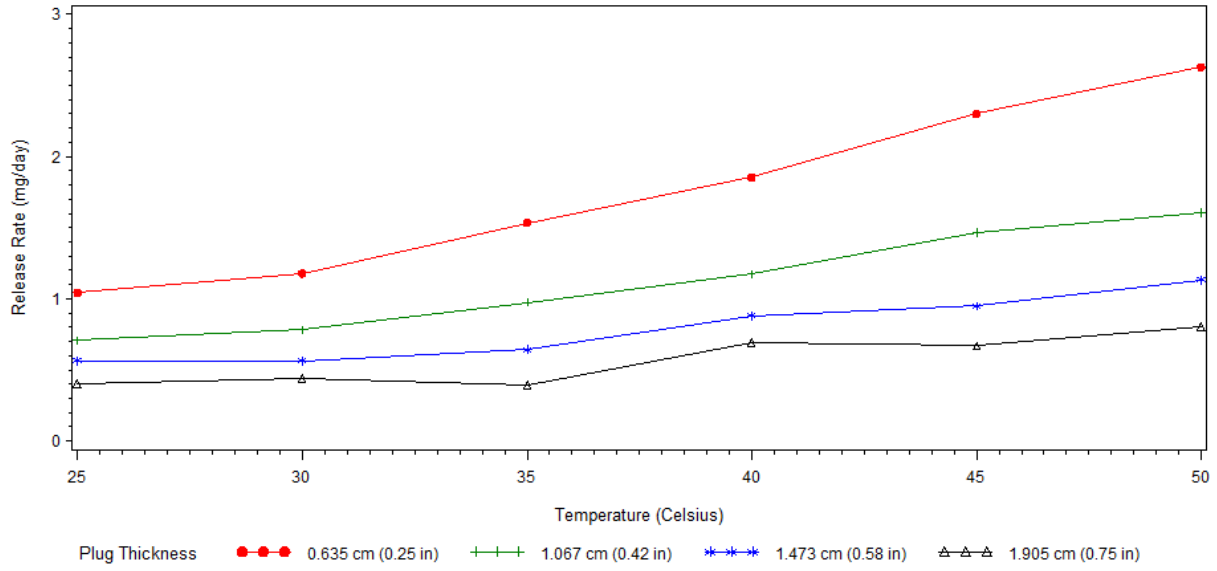

Figure 6.12. Interaction plot of plug thickness and temperature on PMCH release rate where day is defined as 24 hours (i.e. mg/24 hour period).

6.5 Discussion and Conclusions

The results of the PPRV study presented in this paper was successfully able to derive an equation to predict release rate as a function of temperature and plug thickness. **Figure 6.5** through **Figure 6.9** present an overall graphical summary of the PMCH release over the course of the experiment. The graphs clearly show a distinct difference in the PMCH release rate, which is represented by the slope of data points, between difference temperatures. A significant difference can also be seen in **Figure 6.9** between the release rates of sources with different plug thicknesses. These large release rate differences can also be seen in **Table 6.5**.

Table 6.4 displays the % RSDs of the release rates between PPRVs of the same design parameters across all temperature treatments. The precision of the release rates varied from 4% to 25%. The higher % RSDs appear to be concentrated at the two larger plug thicknesses. These slightly elevated % RSDs may indicate that these release sources were assembled inconsistently. However, the low % RSDs reflected by the two thinner plug thicknesses contradicts this source of error considering all of the PPRVs were assembled at once. The sources of the increased variation from the larger plug thicknesses are more likely derived either from the allotted equilibrium time or the time interval between mass change measurements.

The PPRVs were given 48 hours to equilibrate with each new temperature treatment before the mass changes were recorded. If the larger plug thickness sources had not fully equilibrated with the new temperature, the release rate would have been slightly skewed between the beginning and end of the measurement periods. This issue would have been intensified if significant thermal expansion had occurred at the higher temperature. The expansion of the plug along its longitudinal axis would have caused increased compression across the plug's cross-section. Any substantial compression would decrease permeability while increasing equilibrium time. Similarly, the time interval between measurements, about 24 hours, may not have been sufficient to produce a mass difference within the range of sensitivity of the analytical balance. Despite the higher % RSDs, the precision of the PPRVs was still acceptable given the magnitude of the mass changes in question.

Table 6.8 displays the difference in the release rate between the 0.600 mL sources and the sources with the same plug thicknesses across the different fill levels at each temperature treatment. The 0.600 mL fill level was proven in past studies to produce a reliable release rate. However, the effect of PMCH depletion over time was not analyzed. The release rate is expected to naturally deviate once the vapor volume within the PPRV is reduced below a critical level at which time the vapor pressure will be insufficient to maintain a stable rate. In order to identify this critical point, different fill levels were used to represent different time periods within the lifetime of the release source. **Table 6.9** displays the estimated lifetimes of the PPRVs up to an 80% to 95% depletion of its original PMCH volume. Any significant difference between the release rate of the 0.600 mL sources and the release rate produced by the other fill levels would indicate the limit of viability for the PPRVs. As can be seen in **Table 6.8**, the majority of the release rates vary by less than 10% from the release rate of the 0.600 mL PPRVs. Only a few exceptions exist in the table. Based on the inconsistent appearance of the higher deviations, the fill level itself is an unlikely source for this difference. The lack of any repeating pattern suggests that the logging of the mass change at these points contained an error that artificially increased the difference in release rate. As such, the comparison shown in **Table 6.8** indicates that the internal PMCH does not affect the release rate within the constraints of the experiment.

The ANOVA analysis presented in **Table 6.10** indicates with an alpha level of 0.05 that the plug thickness, temperature, and the interaction between these two variables had a significant effect on the PMCH release rate of the PPRVs. The trend between the different plug thicknesses across temperature treatments in **Figure 6.12** shows a rough linear relationship between temperature and release rate. The release rate was found to be directly proportional to temperature and indirectly proportional to plug thickness. Some relatively weak interaction effects, which is represented by the slightly skewed character of the plot, can also be seen in this figure. The weak interaction effects shown in **Figure 6.12** slightly contradicts the conclusion of strong interaction given by the p-value of the effects test in **Table 6.10**. This inconsistency is due to the large sample size coupled with a smaller relative variance between the response from the plug thicknesses and the temperature. This characteristic gives the effects test a higher power to detect differences thus resulting in the conclusion of a more significant interaction. The ANOVA

results regarding the significance of temperature and plug thickness agree with the results presented in **Table 6.5**.

With an alpha level of 0.05, the two covariates, ambient room temperature and barometric pressure, did not have a significant impact on the release rate. The largest concern between these two covariates was barometric pressure. If barometric pressure was found to be a significant effect, it would have needed to be included in the final regression. Theoretically, normal ranges of barometric pressure should not have a significant impact on vapor pressure, the driving force of the PMCH release, which was confirmed by this result. The insignificance of the two monitored covariates confirms that the major environmental factors in the laboratory did not affect the release rate.

PMCH fill level was also found not to have a significant impact on the release rate. The insignificance of the PMCH fill level supports the low variance between PPRVs displayed in **Table 6.8**. This result strongly suggests that the release rate of the sources over time will not be affected by the depletion of PMCH given that the silicone plug and aluminum shell maintains their integrity. The ANOVA analysis supports the conclusion gained from the data in **Table 6.4**. The PPRVs were thus free of any major experimental errors.

Using the significant effects, a regression equation was generated to predict the PMCH release rate as a function of temperature and plug thickness. The coefficient of determination, or model R^2, is 0.94 for fitting the release rate with these two effects and their interaction. In order to improve the accuracy of the prediction, some second order terms were added in this regression equation. Other models involving higher level terms were tested as well. However, the added benefits of the additional terms did not compensate for the increased complexity of the model and the coefficients. The resulting regression equations are provided as follows where R is the release rage in milligrams per day (mg/day), A is the plug thickness in centimeters (cm), and T is the temperature in °C.

$$\mathrm{R} = 0.6681 - 2.3973\left(\frac{A}{2.54}\right) + 0.0383 \cdot \mathrm{T} - 0.0976 \cdot \left(\frac{\mathrm{A}}{2.54}\right) \cdot \mathrm{T} + 0.0006 \cdot T^2 + 3.7104 \cdot \left(\frac{A}{2.54}\right)^2 \quad (6.1)$$

In Equation (6.1), a day is defined as 24 hours. The plug thickness range is from 0.635 cm (0.25 in) to 1.905 cm (0.75 in) and the temperature ranges from 25°C to 50°C. The model R^2 is 0.94, indicating that this equation will accurately predict the release rate of PPRVs manufactured and utilized within the constraints of this study. Although this equation may be extrapolated beyond the plug thicknesses and temperatures defined in this paper, the accuracy of the outputted release rate cannot be guaranteed.

Based on the ANOVA analysis in **Table 6.10** regarding the covariates, Equation (6.1) is accurate through normal variations of barometric pressure such as those created by altitude changes, weather systems, and ventilation flows. Similarly the insignificant impact of PMCH fill level suggests that the PPRVs are viable through 80% to 95% of their estimated lifetimes. **Figure 6.10** and **Figure 6.11** shows that PMCH level does greatly affect the life of the source. Since any loss of silicone plug or aluminum shell integrity will compromise the release rate, the fill level should be tailored to fit the conditions present at the intended release area. For example, certain environmental conditions, such as high ultraviolet exposure, may cause the PPRV to degrade faster. Although this study was able to determine the response of the PPRV based on controlled laboratory conditions, an actual field deployment may elicit a different response. As a result, an underground mine field evaluation of the PPRV will be conducted to determine the performance of the sources in the field.

6.6 Acknowledgements

The authors wish to thank Dr. Russell Dietz, Brookhaven National Laboratory, who has been generous with his time and knowledge of perfluorocarbon tracers and Rudy Maurer Jr., Dyno Nobel, who has been instrumental in supplying the aluminum shells used in this experiment.

This publication was developed under Contract No. 200-2009-31933, awarded by the National Institute for Occupational Safety and Health (NIOSH). The findings and conclusions in this report are those of the authors and do not reflect the official policies of the Department of Health and Human Services; nor does mention of trade names, commercial practices, or organizations imply endorsement by the U.S. Government.

6.7 Bibliography

Ambrosetti, P., D. Anfossi, S. Cieslik, G. Graziani, R. Lamprecht, A. Marzorati, K. Nodop, S. Sandroni, A. Stingele, and H. Zimmermann. 1998. "Mesoscale transport of atmospheric trace constituents across the central Alps: transalp tracer experiments." *Atmospheric Environment* no. 32 (7):1257-1272. doi: 10.1016/S1352-2310(97)00185-4.

Andriot, M., S. H. Chao, A. Colas, S. Cray, F. de Buyl, J. V. DeGroot, A. Dupont, T. Easton, J. L. Garaud, E. Gerlach, F. Gubbels, M. Jungk, S. Leadley, J. P. Lecomte, B. Lenoble, R. Meeks, A. Mountney, G. Shearer, S. Stassen, C. Stevens, X. Thomas, and A. T. Wolf. 2007. "Silicones in industrial applications." In *Inorganic polymers*, edited by R. De Jaeger and M. Gleria, 61-161. Nova Science Publishers Inc.

Barbier, J. 1955. "A study of permeability to gases. Mixtures of natural rubber and other elastomers." *Rubber Chemistry and Technology* no. 28 (3):814-820.

Bondurant, S., V. Ernster, and R. Herdman. 1999. "Safety of silicone breast implants." In, ed S. Bondurant, V. Ernster and R. Herdman. Washington, D.C.: National Academy Press. http://www.nap.edu/catalog/9602.html (accessed 21 OCT).

Cooke, K. M., P. G. Simmonds, G. Nickless, and A. P. Makepeace. 2001. "Use of capillary gas chromatography with negative ion-chemical ionization mass spectrometry for the determination of perfluorocarbon tracers in the atmosphere." *Analytical Chemistry* no. 73 (17):4295-4300. doi: 10.1021/ac001253d.

Dietz, R. N. 1991. Commercial applications of perfluorocarbon tracer (PFT) technology. In *The Department of Commerce Environmental Conference, "Protecting the Environment: New Technologies - New Markets"*. Reston, VA.

Dietz, R. N., and E. A. Cote. 1982. "Air infiltration measurements in a home using a convenient perfluorocarbon tracer technique." *Environmental International* no. 8:419-433.

Dietz, R. N., R. W. Goodrich, E. A. Cote, and R. F. Wieser. 1986. "Detailed description and performance of a passive perfluorocarbon tracer system for building ventilation and air exchange measurements." In *Measured Air Leakage of Buildings*, edited by H. R. Trechsel and P. L. Lagus, 203-264. Philadelphia, PA: American Society for Testing and Materials.

Draxler, R. R. 1967. "One year of tracer dispersion measurements over Washington, D.C." *Atmospheric Environment* no. 21 (1):69-77. doi: 10.1016/0004-6981(87)90272-1.

Encyclopædia Britannica. 2012. silicone. In *Encyclopædia Britannica Online*: Encyclopædia Britannica Inc.

F2 Chemicals Ltd. 2011. Perfluoromethylcyclohexane. Lancashire, United Kingdom.

Fast, J. D., K. J. Allwine, R. N. Dietz, K. L. Clawson, and J. C. Torcolini. 2006. "Dispersion of perfluorocarbon tracers within the Salt Lake Valley during VTMX 2000." *Journal of Applied Meteorology and Climatology* no. 45 (6):793-812.

Galdiga, C. U., and T. Greibrokk. 1997. "Simultaneous determination of trace amounts of sulphur hexafluoride and cyclic perfluorocarbons in reservoir samples by gas chromatography." *Chromatographia* no. 46 (7/8):440-443.

Geller, L. S., J. W. Elkins, J. M. Lobert, A. D. Clarke, D. F. Hurst, J. H. Butler, and R. C. Myers. 1997. "Tropospheric SF_6: Observed latitudinal distribution and trends, derived emissions and interhemispheric exchange time." *Geophysical Research Letters* no. 24 (6):675-678.

Hammon, H. G., K. Ernst, and J. C. Newton. 1977. "Noble gas permeability of polymer films and coatings." *Journal of Applied Polymer Science* no. 21 (7):1989-1997. doi: 10.1002/app.1977.07021072.

Jordan, S. M., and W. J. Koros. 1990. "Permeability of pure and mixed gases in silicone rubber at elevated pressures." *Journal of Polymer Science Part B: Polymer Physics* no. 28 (6):795-809. doi: 10.1002/polb.1990.090280602.

Leaderer, B. P., L. Schaap, and R. N. Dietz. 1985. "Evaluation of the perfluorocarbon tracer technique for determining infiltration rates in residences." *Environmental Science and Technology* no. 19 (12):1225-1232.

Levin, I., T. Naegler, R. Heinz, D. Osusko, E. Cuevas, A. Engel, J. Ilmberger, R. L. Langenfelds, B. Neininger, C. v. Rohden, L. P. Steele, R. Weller, D. E. Worthy, and S. A. Zimov. 2010. "The global SF_6 source inferred from long-term high precision atmospheric measurements and its comparison with emission inventories." *Atmospheric Chemistry and Physics* no. 10 (6):2655-2662. doi: 10.5194/acp-10-2655-2010.

Maiss, M., L. P. Steele, R. J. Francey, P. J. Fraser, R. L. Langenfelds, N. B. A. Trivett, and I. Levin. 1996. "Sulfur hexafluoride - a powerful new atmospheric tracer." *Atmospheric Environment* no. 30 (10):1621-1629.

Merriam-Webster. 2012. siloxane. In *Merriam-Webster.com*: Merriam-Webster.

National Institute of Standards and Technology. 2011. Perfluoro(methylcyclohexane). U.S. Secretary of Commerce.

Parker Hannifin Corp. 2007. Parker O-Ring Handbook. Cleveland, OH: Parker Hannifin Corp.

Ravishankara, A. R., S. Solomon, A. A. Turnipseed, and R. F. Warren. 1993. "Atmospheric lifetimes of long-lived halogenated species." *Science* no. 259 (5092):194-199.

Simmonds, P. G., B. R. Greally, S. Olivier, G. Nickless, K. M. Cooke, and R. N. Dietz. 2002. "The background atmospheric concentrations of cyclic perfluorocarbon tracers determined by negative ion-chemical ionization mass spectrometry." *Atmospheric Environment* no. 36 (13):2147-2156.

Stern, S. A., F. J. Onorato, and C. Libove. 1977. "The permeation of gases through hollow silicone rubber fibers: effect of fiber elasticity on gas permeability." *American Society of Chemical Engineers* no. 23 (4):567-578.

Stymne, H., C. A. Bowman, and J. Kronvall. 1994. "Measuring ventilation rates in the Swedish housing stock." *Building and Environment* no. 29 (3):373-379.

Thimons, E. D., R. J. Bielicki, and F. N. Kissell. 1974. Using sulfur hexafluoride as a gaseous tracer to study ventilation systems in mines. In *Bureau of Mines Report of Investigations*: United States Department of the Interior.

van Amerongen, G. J. 1946. "The permeability of different rubbers to gases and its relation to diffusivity and solubility." *Journal of Applied Physics* no. 17:972-985. doi: 10.1063/1.1707667.

Van Reeth, I, and A. Wilson. 1994. Understanding factors which influence permeability of silicones and their derivatives. *Cosmetics and Toiletries*, 87-92.

Velderrain, M, and N. Lipps. 2011. Guidelines for choosing a silicone based on water vapor transmission rates for barrier applications. In *Moisture permeability of silicone systems*. Carpinteria, CA: NuSil Technology.

Watson, T. B., J. Heiser, P. Kalb, R. N. Dietz, R. Wilke, R. F. Weiss, and G. Vignato. 2006. The New York City urban dispersion program March 2005 field study: tracer methods and results. Upton, NY: Brookhaven National Laboratory.

Watson, T. B., R. Wilke, R. N. Dietz, J. Heiser, and P. Kalb. 2007. "The atmospheric background of perfluorocarbon compounds used as tracers." *Environmental Science and Technology* no. 41 (20):6909-6913.

Zhang, H., and A. Cloud. 2006. The permeability characteristics of silicone rubber. In *38th SAMPE Fall Technical Conference: Global Advances in Materials and Process Engineering*. Dallas, TX: Society for the Advancement of Material and Process Engineering.

Chapter 7: Field test of a perfluoromethylcyclohexane (PMCH) permeation plug release vessel (PPRV) using a dual tracer deployment in an underground longwall mine

ABSTRACT: Perfluoromethylcyclohexane (PMCH) has shown to be a viable alternative to the widely used tracer gas sulfur hexafluoride (SF_6). PMCH and SF_6 were released in a Midwestern underground longwall mine. The operators of this mine graciously allowed full access to an active longwall panel during two stages of its advance, designated as Phase I and Phase II, to perform this study. This paper presents a study designed to determine the feasibility of deploying a PPRV in an underground environment for tracer gas studies. SF_6 was also released in parallel in a full ventilation characterization of the longwall panel to examine the ability of PMCH to compliment SF_6. The results of this study not only showed the PPRV to be a feasible tracer release system in an underground environment but also highlighted the advantages of a dual tracer release.

7.1 Introduction

Sulfur hexafluoride (SF_6) has been the predominant tracer gas used in underground mine ventilation studies for over 30 years (Thimons, Bielicki, and Kissell 1974). However, the ability of SF_6 to function as the sole tracer is being hindered by two main issues: the increasing scale and complexity of mine ventilation systems along with the steadily growing background concentration of SF_6 in the atmosphere (Levin et al. 2010, Geller et al. 1997, Ravishankara et al. 1993, Maiss et al. 1996). In order to mitigate these issues, recent studies have identified the compound perfluoromethylcyclohexane (PMCH) as a viable supplement and compliment for SF_6.

PMCH is a perfluorinated cyclic hydrocarbon and is categorized as a perfluorocarbon tracer (PFT) due to its chemical inertness, low toxicity, and trace level background presence in the environment. These properties make PMCH suitable for use as a tracer gas (Dietz 1991, Watson et al. 2007). Compounds of this type have been widely implemented in heating, ventilation, and air conditioning (HVAC) as well as atmospheric monitoring studies (Dietz 1991) but not yet in the field of underground mine ventilation. PMCH exists as volatile liquids at room temperature and pressure (National Institute of Standards and Technology 2011). This physical property prevents PMCH from being released using conventional techniques designed for gases. Previous studies have presented a permeation plug release vessel (PPRV) designed to convert PMCH from a liquid to a vapor and release it into a flow stream in a controlled manner. Although many laboratory studies have been conducted using the PPRV, it has not yet been utilized in an underground mine. This paper presents the use of a simultaneous, steady-state release of SF_6 and PMCH in a Midwestern underground longwall mine. The purpose of this study was to determine the feasibility of the PPRV as a reliable system to release PMCH and also to examine its ability to compliment SF_6.

7.2 Background

PMCH is a perfluorinated cyclic hydrocarbon whose chemical structure is composed of perfluoroalkanes (Watson et al. 2007). Compounds of this type are biologically inert, chemically inert, and thermally stable (F2 Chemicals Ltd. 2011). The inert, non-reactive, and non-toxic nature of PMCH makes it an ideal choice as a tracer gas. PMCH is comprised of seven carbon atoms and fourteen fluorine atoms, which gives it a chemical formula of C_7F_{14}. The molecular structure of PMCH is displayed in **Figure 7.1**.

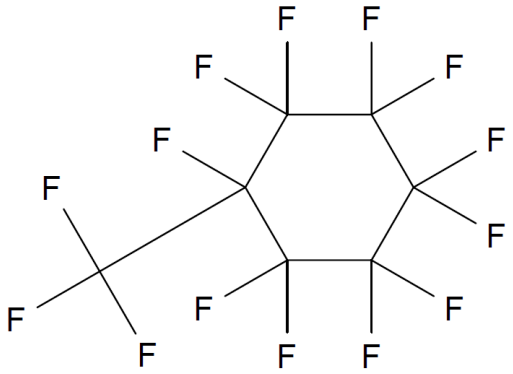

Figure 7.1. Molecular structure of PMCH.

The PMCH molecule is composed of two main parts, the cyclohexane ring and the methyl group bonded off to the side. This fully fluorinated molecule has a molecular weight of 350 g/mol and a boiling point of 76°C (169°F). The volatility of PMCH allows it to vaporize even at relatively lower temperatures. Once in a vapor state, PMCH, will remain a vapor even through cooler temperatures (National Institute of Standards and Technology 2011). Another advantage of PMCH is its detectability by a GC even at low concentrations. This ability stems from PMCH's low ambient background in the atmosphere with concentrations in the parts per quadrillion (PPQ) (Cooke et al. 2001, Simmonds et al. 2002, Watson et al. 2007) and its high detection sensitivity derived from its molecular electronegativity (Simmonds et al. 2002).

The basic concept of the PPRV used in this field study was initially introduced by Brookhaven National Laboratory (BNL). The basic PPRV design consists of a hollow aluminum cylinder with one end of the cylinder opened to the atmosphere and the other end closed. Liquid PMCH is

injected into the aluminum vessel and sealed with an oversized methyl vinyl silicone (VMQ) plug pressed flush to the end. The source releases PMCH by allowing the phase change to occur internally. Vapor is produced immediately once the PMCH is exposed to the atmosphere due to its high vapor pressure (106 torr at 25°C) (Dietz et al. 1986). A schematic of the PPRV used in this field study is presented in **Figure 7.2** and **Figure 7.3**.

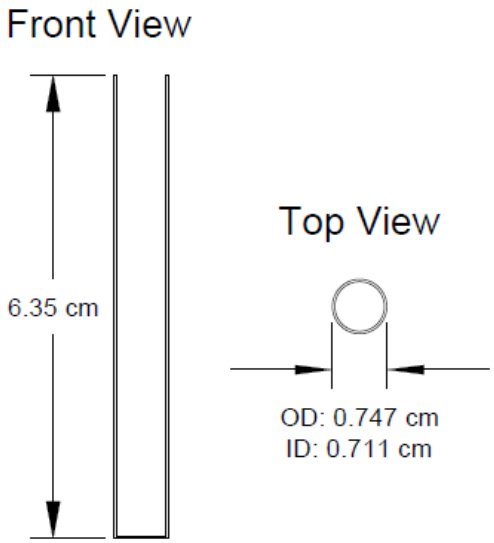

Figure 7.2. Schematic of an aluminum shell used for the PMCH release source.

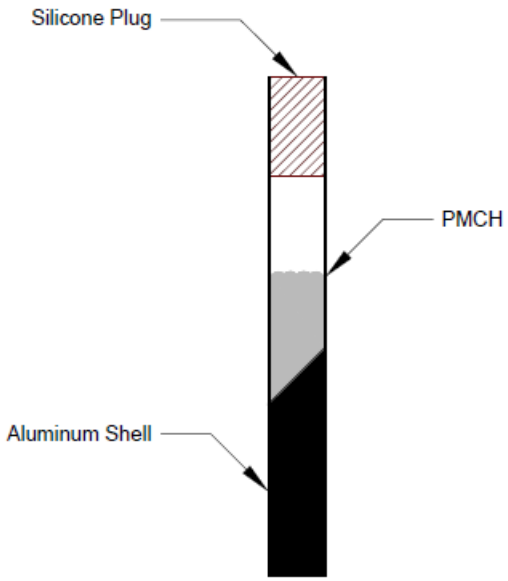

Figure 7.3. Cutaway diagram of a fully assembled PMCH release source.

The high flow resistance caused by the silicone plug produces a pseudo-closed system allows the PMCH to reach dynamic equilibrium within the source. This equilibrium produces a steady pressure differential between the inside and the outside of the vessel equivalent to the vapor pressure produced at the ambient temperature. This differential causes the vapor PMCH to steadily diffuse through the silicone plug. The release rate will remain consistent as a function of temperature as long as the integrity is maintained and the compression of the plug is not excessive (Jordan and Koros 1990).

Vapor pressure is affected most significantly by ambient temperature and is independent of atmospheric pressure. Thus the release rate can be predicted as a function of temperature. The thickness of the silicone plug also greatly affects PMCH diffusion as flow resistance increases with a thicker medium. As a result, a previous long-term study of the PPRV displayed in **Figure 7.3** produced the following equation to compute the release rate of PMCH as a function of temperature and plug thicknesses.

$$\mathrm{R} = 0.6681 - 2.3973\left(\frac{A}{2.54}\right) + 0.0383 \cdot \mathrm{T} - 0.0976 \cdot \left(\frac{\mathrm{A}}{2.54}\right) \cdot \mathrm{T} + 0.0006 \cdot T^2 + 3.7104 \cdot \left(\frac{A}{2.54}\right)^2 \quad (7.1)$$

This paper outlines a study utilizing the PPRV presented in **Figure 7.3** in conjunction with Equation (7.1) to determine the feasibility of deploying this system in an underground environment for tracer gas studies. SF_6 was also released as a part of this study for the full ventilation characterization of the target longwall panel in conjunction with PMCH to examine the ability of PMCH to compliment SF_6. A dual tracer release of this nature in an underground mine has not been attempted prior to this study.

7.3 Longwall Mine Overview

PMCH and SF_6 were released in a Midwestern underground longwall mine. The operators of this mine graciously allowed full access to an active longwall panel during two stages of its advance, designated as Phase I and Phase II for this study. The ventilation around the panel is facilitated using a three entry headgate, a single entry tailgate, a three entry bleeder, and a fringe ventilation path. This mine utilizes a hybridized bleederless ventilation system to provide fresh air to the panel. As such, the tailgate consists of a single return entry that is not connected to the bleeders at the rear of the panel. The fringe ventilation system is another unique aspect of this type of ventilation system. A small amount of intake air is provided to the outside edges of the gob to ventilate any accumulation of gases. This ventilation stream only flows around the outside of the gob and is not designed to penetrate into the gob itself to limit the potential for spontaneous combustion. The fringe ventilation is directed to the rear of the panel where it joins the bleeders through small pipes located in the headgate and the tailgate.

Intake air is delivered through three entries in the headgate. The three intake branches combine to carry fresh air both across the longwall face and into the fringe. The ventilation flow across the longwall face is carried into the tailgate and then exits the mine through the main return. A basic schematic diagram of the ventilation system is displayed in **Figure 7.4**.

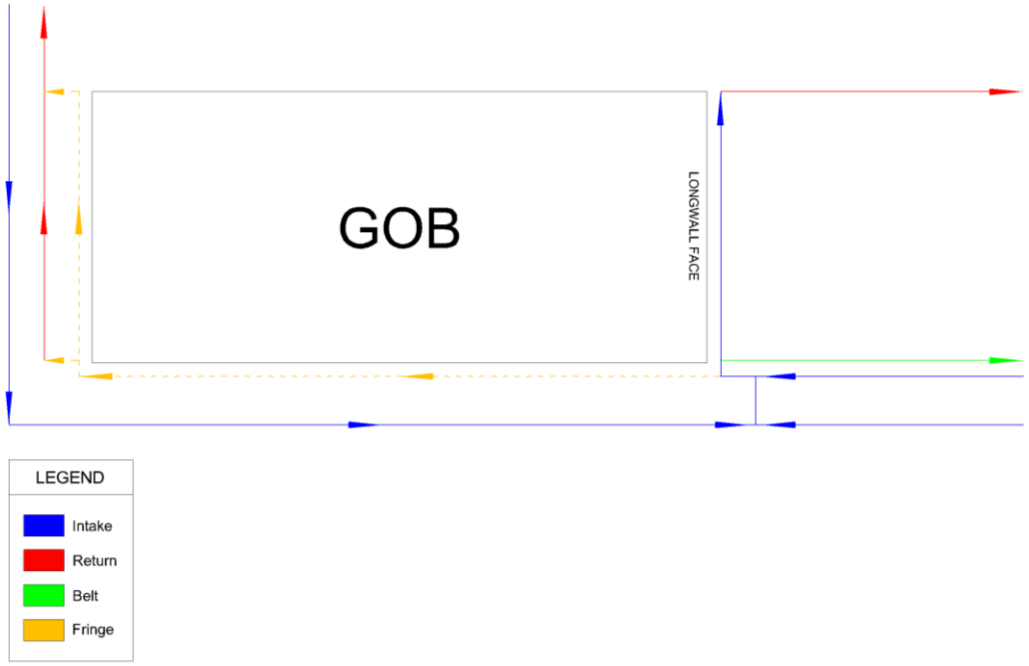

Figure 7.4. Schematic diagram of longwall panel ventilation system.

From the schematic, the three intake branches are delivered to the working face from two different locations: the fresh air intake at the rear of the panel provided by the bleeder man and the dual fresh air intakes from the mine fan. The schematic also depicts the isolation of the gob from any major influx of ventilation flow and the manner in which the fringe ventilation functions. In order to perform the tracer study of this panel, two separate release points and nine monitoring points located in the primary flow areas were chosen for both phases of the experiment.

7.4 Experimental Design

As previously introduced, the tracer study of this panel was accomplished using a simultaneous steady-state release of SF_6 and PMCH. The tracer study was completed in two separate phases, Phases I and II, representing the ventilation system near the start of the panel and near the end of the panel. Phases I and II were executed consecutively with a delay of approximately two months (50 days) between studies. During this delay, the longwall advanced an additional 802 m (2,630 ft) from the Phase I position. The tracer flow around the panel was monitored at nine locations. These nine locations represented all of the primary ventilation branches serving the longwall panel. A description of the release points (RP) and sampling points (SP) are presented in **Table 7.1**.

Table 7.1. Release point and sampling point descriptions.

Station Name	Description
RP1	Bleeder fan intake entry inby the last open crosscut (SF_6)
RP2	Longwall shield adjacent to the tailgate (PMCH)
SP1	Main fan intake entry just outby the face
SP2	Belt entry outby the face
SP3	Fringe entry
SP4	Center of the face
SP5	Headgate bleeder tap
SP6	Tailgate bleeder tap
SP7	Fresh air entry in the bleeders
SP8	Consists of the SP8A, SP8B, and SP8C sampling points representing the three tube bundles in the tailgate
SP9	Tailgate entry outby the face

All of the sampling points were located in open airways except for SP8. SP8 represents the outlet of a tube bundle system consisting of three tubes extending various distances into the gob. These tubes were placed in order to detect any flow communication between the longwall face and the gob. Both phases of the study utilized the same relative locations points located at different absolute locations based on the position of the longwall. The general locations of the release point used for both tracer study phases are graphically represented in **Figure 7.5**. Detailed views of the release and sampling points are presented in **Figure 7.6** and **Figure 7.7**.

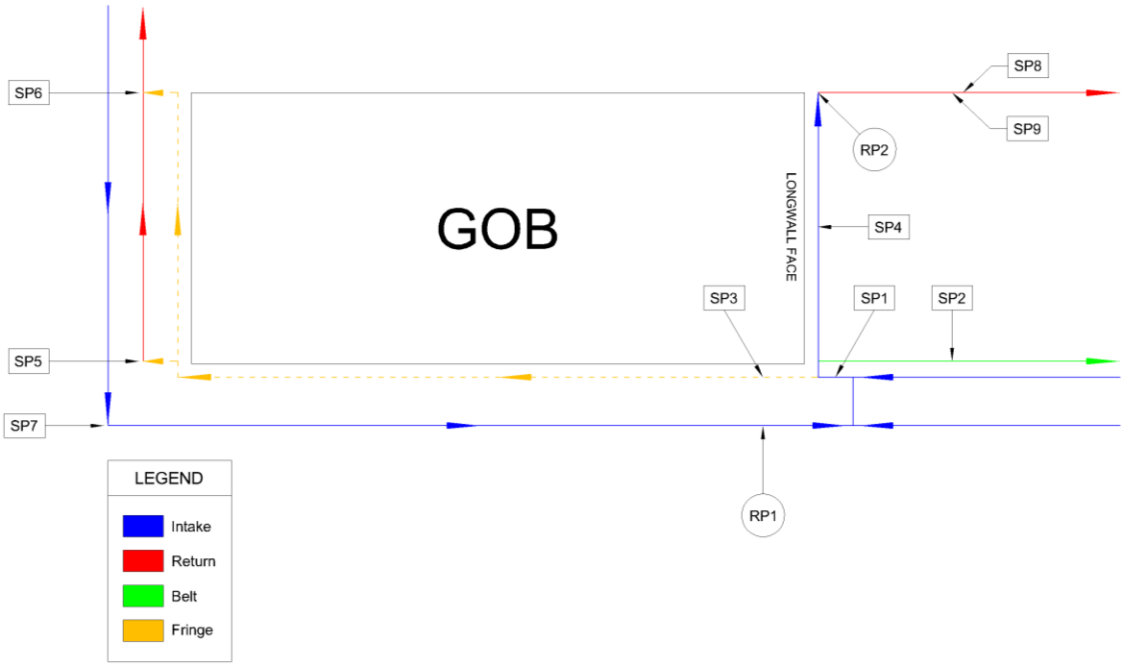

Figure 7.5. Relative locations of release and sampling points for both Phases I and II.

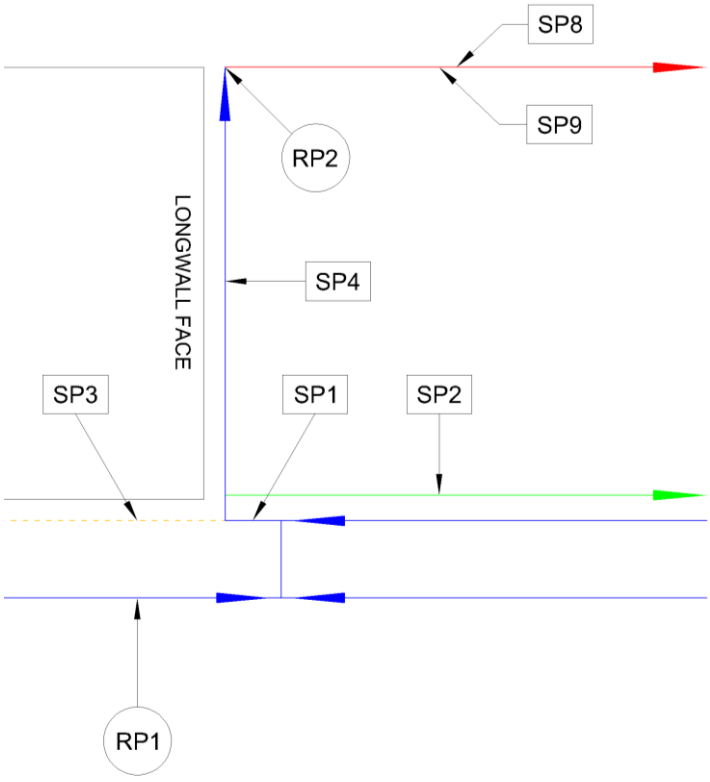

Figure 7.6. Detailed view of the SF6 (RP1) release point and the PMCH release point (RP2) on the longwall face. The SP1, SP2, SP5, SP8, and SP9 sampling points are also displayed.

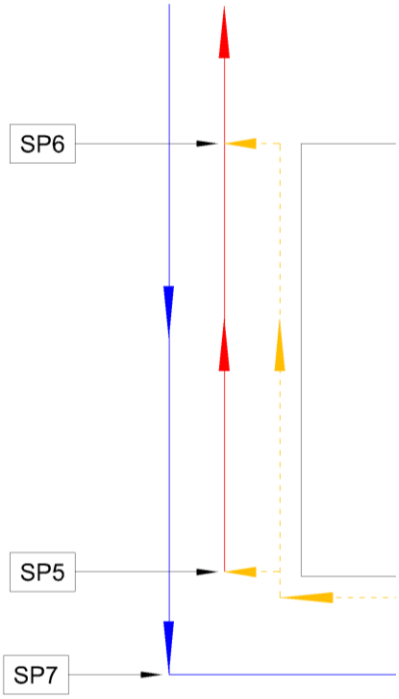

Figure 7.7. Detailed view of the SP5, SP6, and SP7 sampling points.

Figure 7.6 shows that SF_6 was released in the intake entry supplied by the bleeder fan just inby the last open cross-cut while PMCH was released near the tailgate from the last longwall shield. PMCH was released at this location in order to isolate the PMCH release to the single tailgate entry. These two separate release points were chosen not only to determine the performance of the PPRV but to also examine the multi-zone analysis potential of a dual tracer release.

From the assigned intake entry, SF_6 was deployed using a mass flow controller that provided a steady stream of the tracer at 200 standard cubic centimeters per minute (SCCM). A SCC of gas is defined as the mass of the gas that occupies a cubic centimeter of volume at standard temperature and pressure (STP). Assuming ideal gas behavior and a SF_6 density of 6.0380 g/L at a STP of 25°C and 14.696 psia as defined by the manufacturer, the 200 SCCM mass flow is equivalent to 1.21 g/min.

100 PPRVs filled with 0.600 mL of PMCH and press-fitted with 0.635 cm (0.25 in) plugs were placed at the last longwall shield. This number of PPRVs were deployed to provide an adequate concentration of PMCH in the ventilation flow stream to be detected using a GC. For Phase I, the

PPRV bundle was set on an elevated flat area adjacent to the shearer's electrical track. For Phase II, the PPRV bundle was suspended from one of the longwall shield's hydraulic arms. Since the vapor diffusion of PMCH from the PPRV is a function of ambient temperature, the release rate could not be actively controlled. As previously introduced, the release rate is dictated by the following equation.

$$\mathrm{R} = 0.6681 - 2.3973\left(\frac{A}{2.54}\right) + 0.0383 \cdot \mathrm{T} - 0.0976 \cdot \left(\frac{\mathrm{A}}{2.54}\right) \cdot \mathrm{T} + 0.0006 \cdot T^2 + 3.7104 \cdot \left(\frac{A}{2.54}\right)^2 \quad (7.1)$$

As a result, the ambient temperature was monitored throughout the study to provide an average release rate. Barometric pressure and relative humidity were also monitored to record any drastic shifts. However, these two variables are not expected to significantly impact the PPRV.

After the tracer gases were released, air samples were taken at regular intervals for several hours. For Phase I, air samples were taken at 15 min intervals for a six hour period. Although the tracers should have rapidly achieved a homogeneous distribution in the open entries, this time period was allotted to capture SF_6 at SP5 and SP6 in the bleeders. The high resistance, low flow design of the fringe ventilation branch was expected to delay the travel of SF_6 thus increasing the time required to reach a steady-state concentration. As a result, the six hour period was selected in order to accommodate a reasonable amount of tracer travel time. The SP8 tube bundles in this study extended approximately 300 ft, 400 ft, and 500 ft into the gob from the tailgate. The longwall was idled for the entire duration of the Phase I study.

For Phase II, air samples were taken at 30 min or 60 min intervals, depending on the sampling location, for a seven hour period. The original study design called for a 12 hour sampling period to account for the increased linear travel distance in the fringe of approximately 802 m (2,630 ft). However, logistical complications decreased the available time to seven hours. The scheduled study period intersected with the activation of the longwall near the end of allotted time. As a result, Phase II represented six hours of idled longwall ventilation and one hour of active

longwall ventilation. The SP8 tube bundles for this phase extended 200 ft, 300 ft, and 400 ft into the gob from the tailgate.

7.5 Experimental Results

Due to the large amount of data collected for this study, the results are organized in subsections based on study phase and tracer gas.

7.5.1 Phase I SF_6 Results

The Phase I vacutainer samples were analyzed using a gas chromatograph (GC) equipped with an electron capture detector (ECD) for SF_6. PMCH was analyzed using a slightly modified approach that will be discussed in later sections. The GC was installed with a 30 m porous layer open tubular (PLOT) column coated with sodium sulfate deactivated alumina oxide. The column has an internal diameter (ID) of 0.25 mm and a film thickness of 5 µm. **Table 7.2** displays the method parameters used to analyze SF_6.

Table 7.2. GC analytical method for Phase I.

Parameter	**Description**
Sample Injection Size	100 µL
Carrier Gas	He
Injector Temperature	150°C
Split Ratio	30:1
Linear Velocity	35 cm/s
Isothermal Column Temperature	65°C
Detector Temperature	200°C
Make-up Flow	N_2 at 30 mL/min
Total Program Runtime	2.5 min

In order to determine the steady-state concentrations at the sampling points, a calibration curve was generated within the range of the data. The calibration curve is represented by the equation $A = 205.53C + 4414.48$ where A is the GC area count response in µV·min and C is the SF_6 concentration in parts per billion by volume (PPBV). This equation was produced from a set of

laboratory mixed standards interpolated with a regression (R^2) value of 0.96. The calibration curve for Phase I is displayed in **Figure 7.8**.

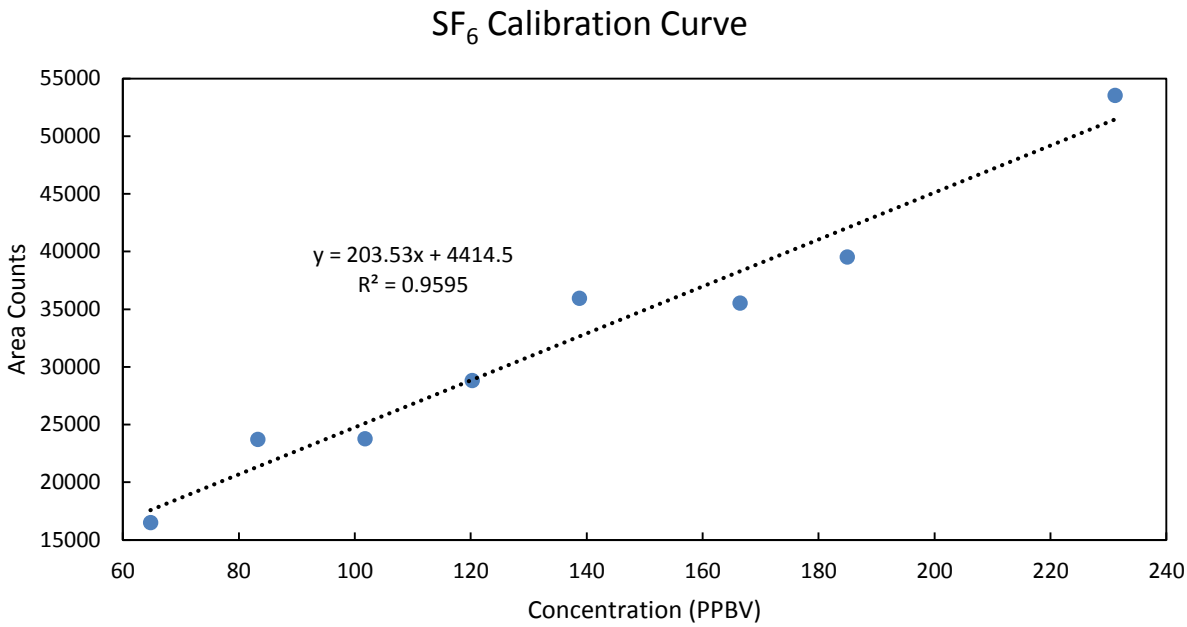

Figure 7.8. SF_6 calibration curve for a concentration range of 64.76 PPBV – 231.14 PPBV.

A chromatogram produced by the GC method outlined in **Table 7.2** is displayed in **Figure 7.9**.

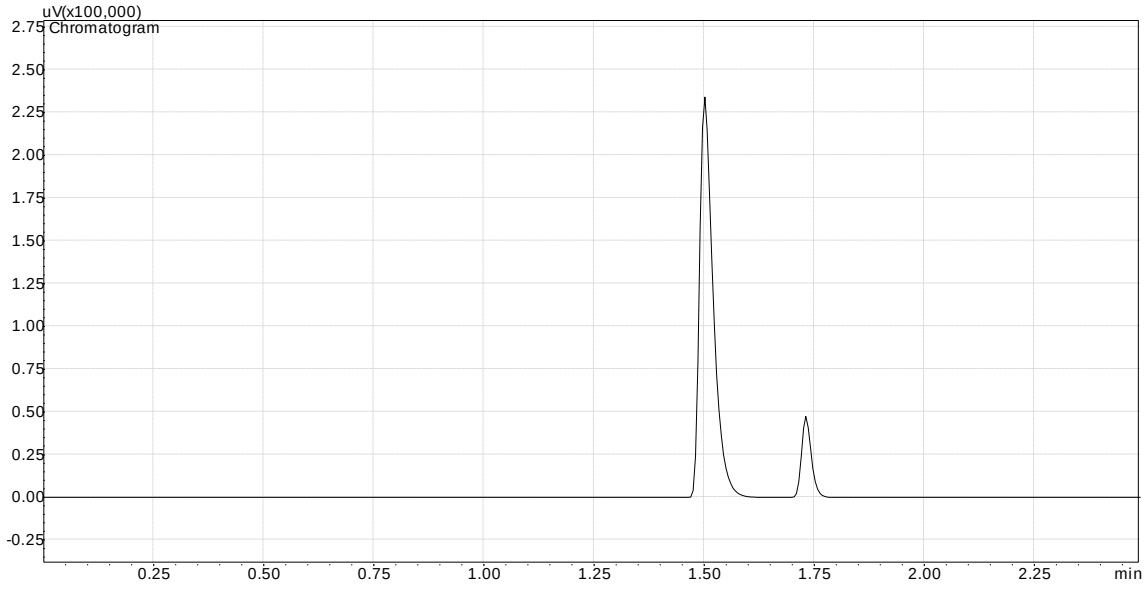

Figure 7.9. Phase I chromatogram displaying the air peak followed by the SF_6 peak.

As expected, the sampling points located in open airways showed the presence of SF_6. The presence of the tracer at these locations confirms that the flow paths represented by sampling points SP1 – SP4, SP5, SP6, and SP9 are directly connected to RP1. These results also confirm that the air is flowing toward these sampling points from this release point. The processed data is displayed in **Table 7.3.**

Table 7.3. Phase I summary of results.

Sampling Point	SF_6 Concentration (PPBV)	% RSD
SP1	159.09	11.45
SP2	168.23	7.91
SP3	167.13	7.18
SP4	173.98	13.43
SP5	152.52	9.57
SP6	173.76	20.83
SP7	0.00	N/A
SP8-1	90.96	125.92
SP8-2	58.85	63.15
SP8-3	67.30	48.68
SP9	140.44	18.38

The % RSD, or percent relative standard deviation, shown in **Table 7.3** is a measure of analysis precision between subsamples at each sampling point. All individual samples were analyzed in triplicate in order to determine % RSD to indicate GC analysis precision. The % RSD between the different sampling points, excluding the SP8 tube bundle, showed an acceptable level of consistency given the concentrations at which the tracer was present. The overall % RSD for all points except the tube bundles was 7%, demonstrating that all locations were sampled consistently and that a similar steady-state tracer concentration was achieved. The results of the tracer analysis are also displayed graphically in **Figure 7.10** through **Figure 7.12**.

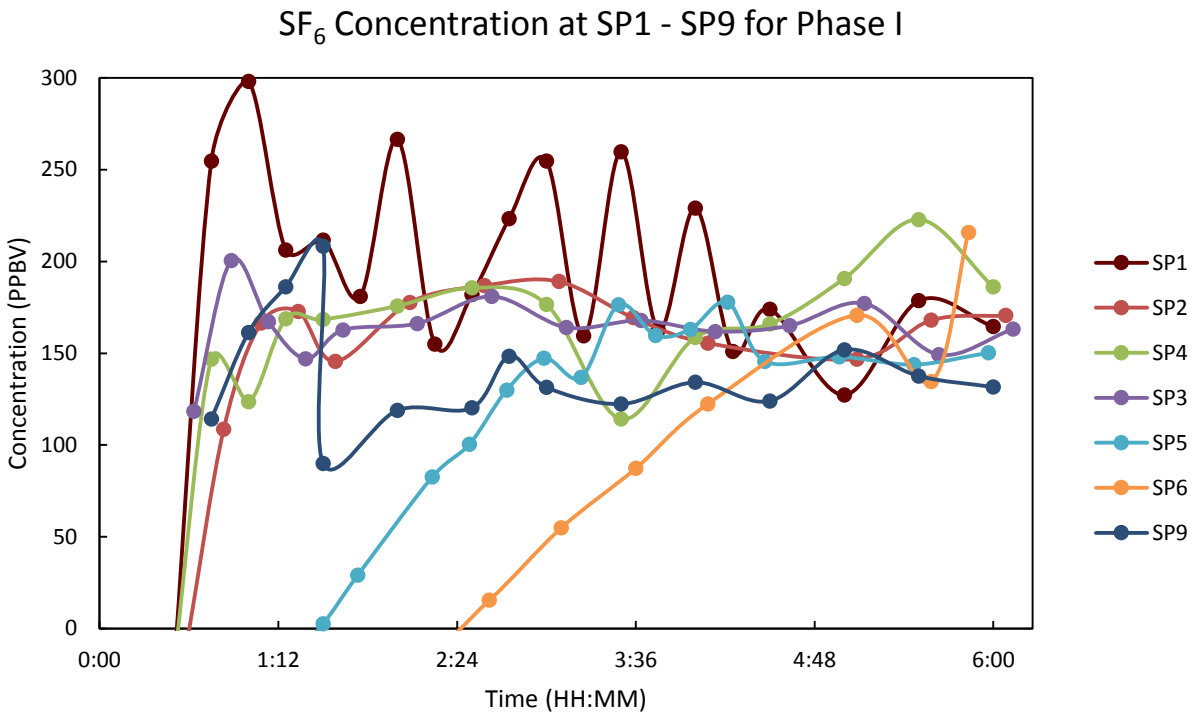

Figure 7.10. SF_6 concentration over time at all sampling points excluding the tube bundle.

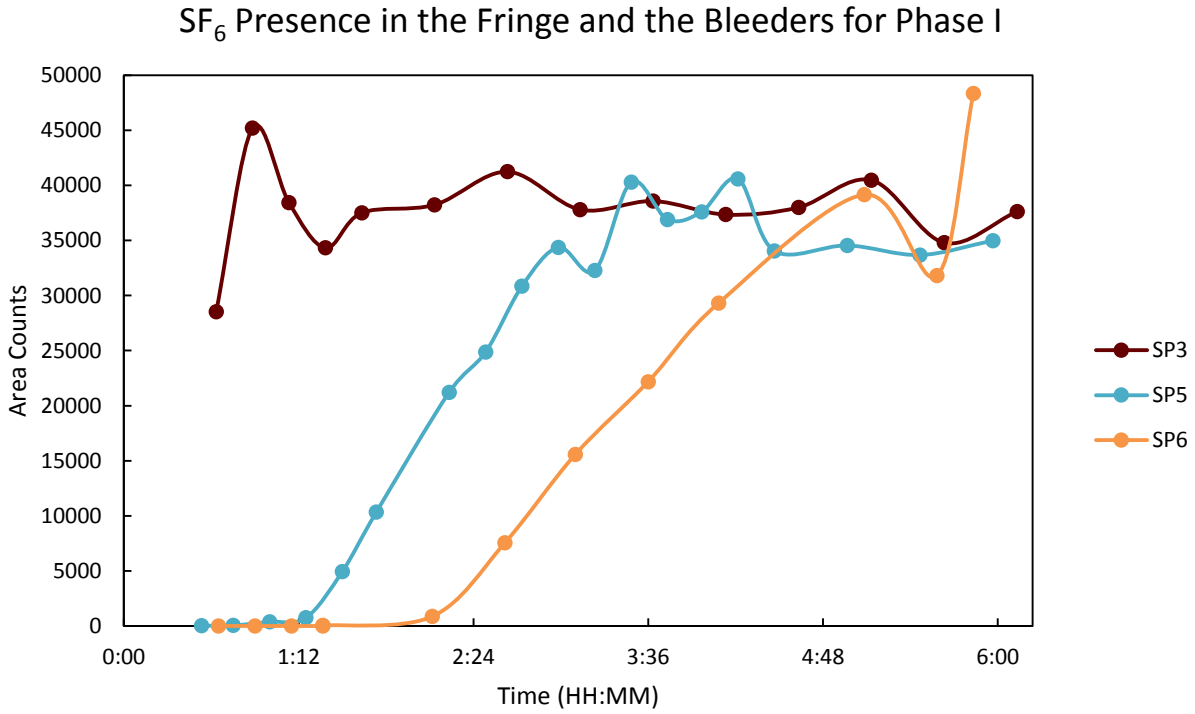

Figure 7.11. SF_6 presence in the fringe and the bleeders. Peak areas are used in this figure to better illustrate the progression of the tracer over time.

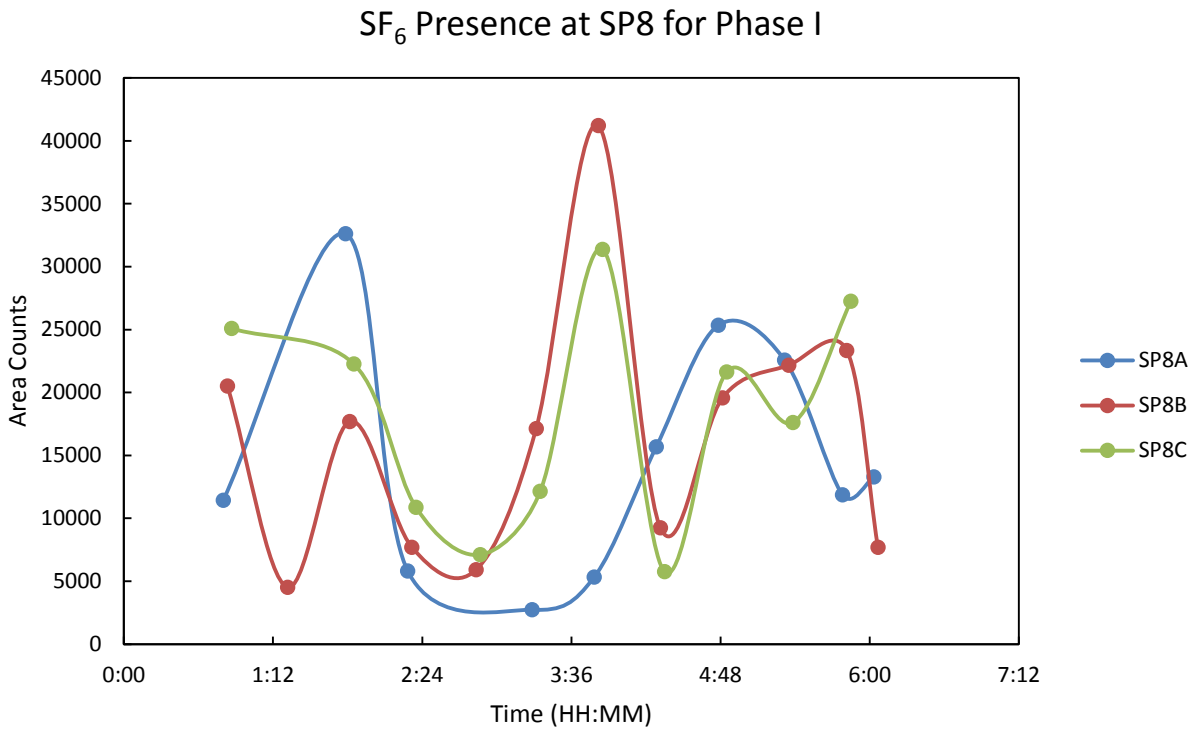

Figure 7.12. SF_6 presence detected in the tailgate tube bundles.

Using the ventilation survey values, which are displayed with their associated point in **Table 7.4**, the volumetric flow of the tracer was determined using the detected tracer concentration at each of the sampling points with the survey data. The volumetric flow of both the air and SF_6 are presented in **Table 7.4**.

Table 7.4. Phase I air and tracer flow quantities.

Location	$\boldsymbol{Q_{Air}}$ (cfm)	$\boldsymbol{Q_{SF_6}}$ (cfm)
RP1	53,600	0.0088
SP1	81,000	0.0129
SP2	19,600	0.0033
SP3	17,000	0.0028
SP5	1,100	0.0002
SP6	3,200	0.0006
SP9	63,000	0.0089

The volumetric flow of SF_6 at RP1 was determined using the ambient atmospheric conditions recorded at SP4 with a 200 SCCM mass flow (SF_6) assuming ideal gas behavior.

7.5.2 Phase I PMCH Results

The average temperature recorded at SP4 was used in Equation (7.1) to determine the average release rate of PMCH. Based on an average temperature of 24°C (75.4°F) and a PPRV plug thickness of 0.635 cm (0.25 in), the release source bundle was expected to produce an average release rate of $7.01 \cdot 10^{-5}$ g/min. Using the surveyed quantity of 1,780 m^3/mi (63,000 CFM) from the tailgate, the steady-state concentration of PMCH at SP9 is expected to be 3.35 PPTV.

Due to the magnitude of the concentration, GC-ECD provided an inadequate detection sensitivity for the samples. As a result, a slightly different analysis technique was developed to quantify PMCH. The vacutainer samples were analyzed using a gas chromatograph (GC) equipped with a single quadrapole mass spectrometer (MS) modified for negative ion chemical ionization (NCI). The chemical ionization gas was methane (CH_4). The GCMS was modified for NCI because traditional electron impact (EI) ionization provided an inadequate detection sensitivity. PMCH has a high electron affinity thereby facilitating the formation of negative ions. Given the soft ionization mechanism of NCI, the preservation of PMCH's negative molecular ion provided an exceptional detection sensitivity.

The NCI-GCMS, identical to the GC-ECD systems described in Section 7.5.1 and Section 7.5.3, was installed with a 30 m porous layer open tubular (PLOT) column coated with sodium sulfate deactivated alumina oxide. The column has an internal diameter (ID) of 0.25 mm and a film thickness of 5 µm. **Table 7.5** and **Table 7.6** display the method parameters used to analyze PMCH.

Table 7.5. GC method used for PMCH analysis.

Parameter	Description
Sample Injection Size	150 µL
Carrier Gas	He
Injector Temperature	150°C
Split Ratio Program	Splitless for 0.50 min and then split at 30:1 to sweep injector port.
Linear Velocity	30 cm/s
Column Temperature Program	50°C initial temperature is held for 0.10 min. Temperature then increases at 40°C/min to 170°C. 170°C is held for 1.00 min. Temperature then decreases at 60°C/min to 120°C. 120°C final temperature is held for 8.07 min.
Total Program Runtime	13.00 min

Table 7.6. NCI-MS method used for PMCH analysis.

Parameter	Description
Interface Temperature	185°C
Ion Source Temperature	195°C
Threshold	260
MS Scan Mode	SIM
SIM Target m/z	350
Scan Time	11.51 min to 13.00 min with an event time of 0.42 sec
Total Program Runtime	13.00 min

The added complexity of the splitless NCI-GCMS method compared to the GC-ECD method was necessary to achieve three primary goals: focusing of the PMCH aliquot within the column, separating the PMCH peak from contaminants with similar molecular weights, and removing background noise through selected ion monitoring (SIM). A chromatogram produced by this method is displayed in **Figure 7.13**.

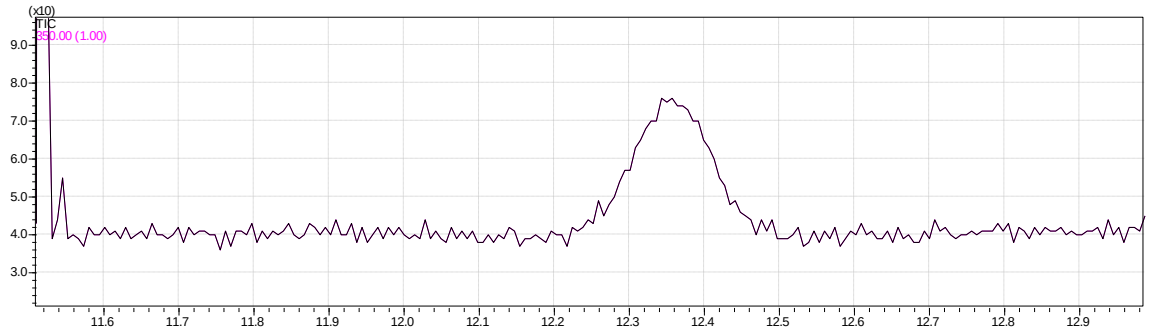

Figure 7.13. Resulting chromatogram from an SP9 injection from Phase II.

In order to determine the PMCH steady-state concentration in the tailgate, a calibration curve was generated within the range of the data. The calibration curve is represented by the equation $A = 71.73C + 33.36$ where A is the area count response in μV·min and C is the PMCH concentration in parts per trillion by volume (PPTV). This equation was produced from a set of laboratory mixed standards interpolated with a regression (R^2) value of 1.00. The calibration curve for Phase I is displayed in **Table 7.7** and **Figure 7.14**.

Table 7.7. PMCH calibration curve data generated using NCI-GCMS.

Concentration (PPTV)	Retention Time (min)	Peak Area	Average Peak Area	% RSD
1.30	12.280	157.0	143.3	6.89
	12.293	139.0		
	12.267	134.0		
1.94	12.264	171.0	177.0	5.20
	12.240	170.0		
	12.256	190.0		
6.48	12.243	521.0	510.0	1.54
	12.237	503.0		
	12.207	506.0		

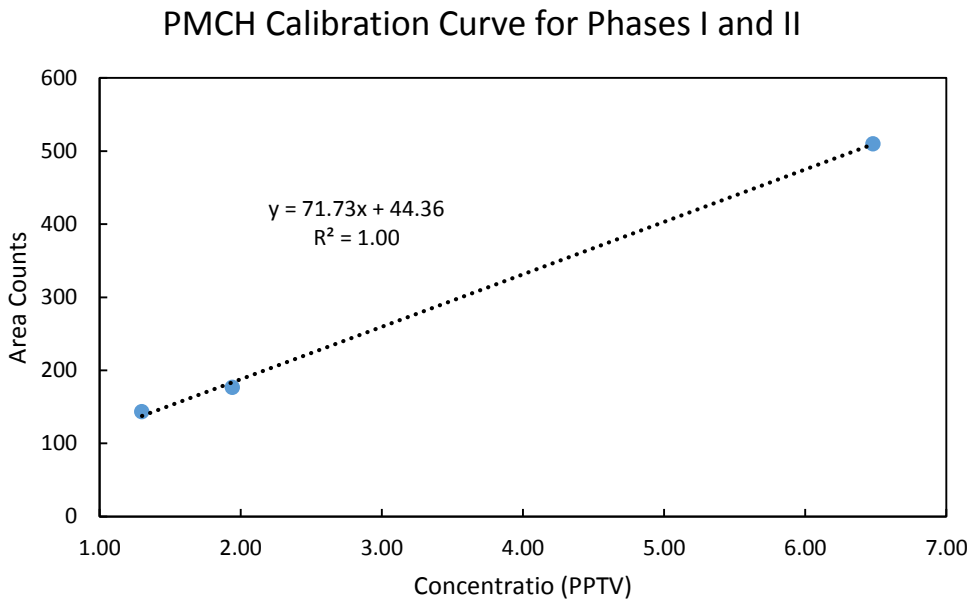

Figure 7.14. PMCH calibration curve generated using NCI-GCMS.

The results of the quantifiable data from the NCI-GCMS analysis of PMCH is displayed in **Table 7.8** and **Figure 7.15**.

Table 7.8. Phase I PMCH quantifiable results.

Sample Number	Time (HH:MM)	Area Counts	PMCH Concentration (PPTV)
SP10-10	2:45	104.7	0.84
SP10-12	3:15	115.7	0.99

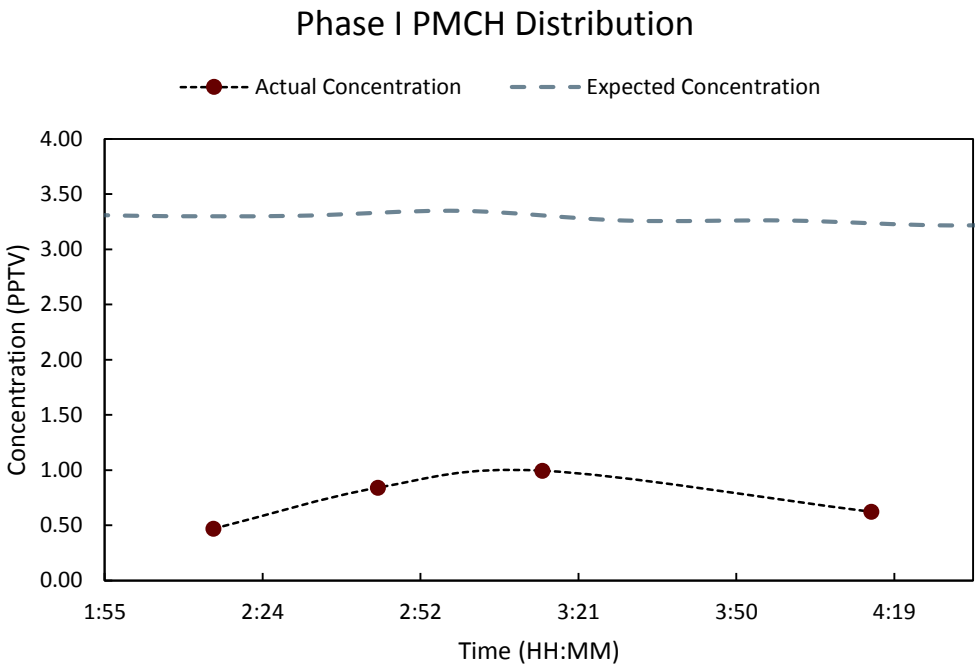

Figure 7.15. Phase I expected and measured PMCH distribution over time.

Only a limited number of points, as seen in **Table 7.8**, are provided due to the unquantifiable signal to noise ratio from many of the PMCH samples. The two points on the extremes in **Figure 7.15** show the estimated concentration of the removed points representing the limit of detection (LOD), about 800 PPQV, for this analysis method. PMCH from the tube bundles was not analyzed to the contamination of the sampling stream as noted by the SF_6 GC results.

7.5.3 Phase II SF_6 Results

The SF_6 vacutainer samples were analyzed using a GC-ECD for Phase II. PMCH was analyzed using a slightly modified approach that will be discussed in later sections. The GC was installed with a 30 m porous layer open tubular (PLOT) column coated with sodium sulfate deactivated alumina oxide. The column has an internal diameter (ID) of 0.25 mm and a film thickness of 5 µm. **Table 7.9** displays the method parameters used to analyze SF_6.

Table 7.9. GC analytical method for Phase II.

Parameter	**Description**
Sample Injection Size	100 µL
Carrier Gas	He
Injector Temperature	150°C
Split Ratio	30:1
Linear Velocity	30 cm/s
Isothermal Column Temperature	50°C
Detector Temperature	200°C
Make-up Flow	N_2 at 30 mL/min
Total Program Runtime	2.5 min

In order to determine the steady-state concentrations at the sampling points, a calibration curve was generated within the range of the data. The calibration curve is represented by the equation $A = 596.52C - 7558.77$ where A is the GC area count response in µV·min and C is the SF_6 concentration in PPBV. This equation was interpolated from a set of laboratory mixed standards with a regression (R^2) value of 0.99. The calibration curve is displayed in **Figure 7.1**.

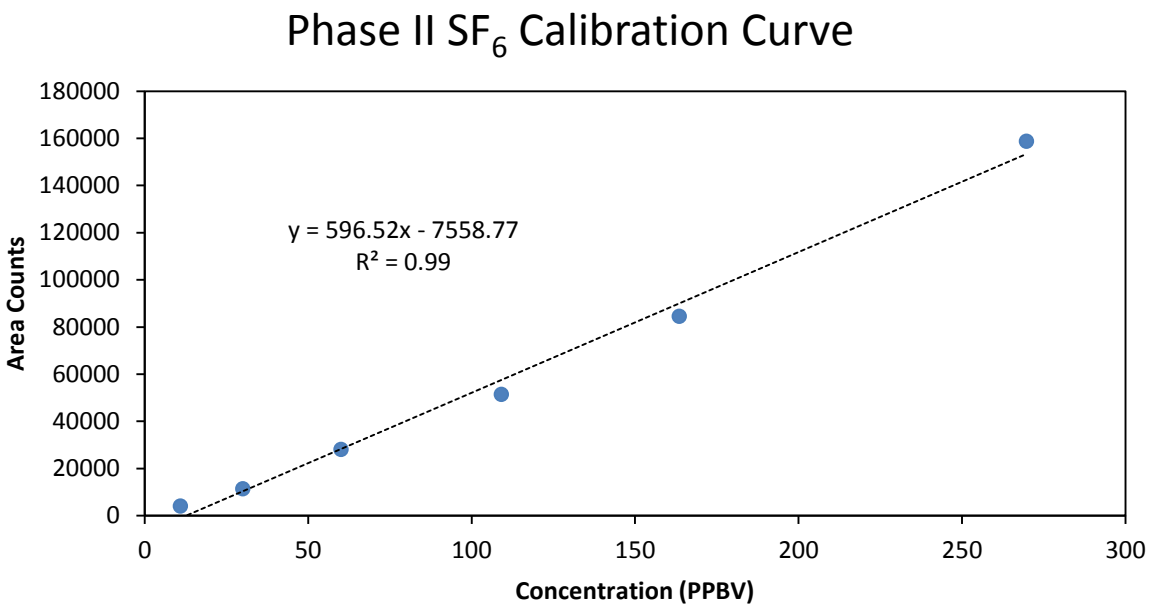

Figure 7.16. SF_6 calibration curve for a concentration range of 11 PPBV – 270 PPBV.

All of the sampling points located in open airways showed the presence of SF_6. The presence of the tracer at these locations confirms that the flow paths represented by sampling points SP1 – SP6 and SP9 are directly connected to RP1. These results also confirm that the air is flowing toward these sampling points from this release point. The processed data is displayed in **Table 7.10**.

Table 7.10. Summary of results for Phase II.

Sampling Point	SF_6 Concentration (PPBV)	% RSD
SP1	85	6.57
SP2	90	5.23
SP3	85	2.97
SP4	87	2.86
SP5	65	3.22
SP6	50	8.21
SP7	0	N/A
SP8-1	67	5.71
SP8-2	17	32.19
SP8-3	18	21.42
SP9	73	5.32

The % RSD between the different sampling points, excluding the SP8 tube bundle, showed an acceptable level of consistency given the concentrations at which the tracer was present. The overall % RSD for all points excluding the bleeder taps and tube bundles was 7%. This precision shows that all locations were sampled consistently and that a similar steady state tracer concentration was achieved, except at those points that were excluded in the computation. The results of the tracer analysis are also displayed graphically in **Figure 7.17** through **Figure 7.20**.

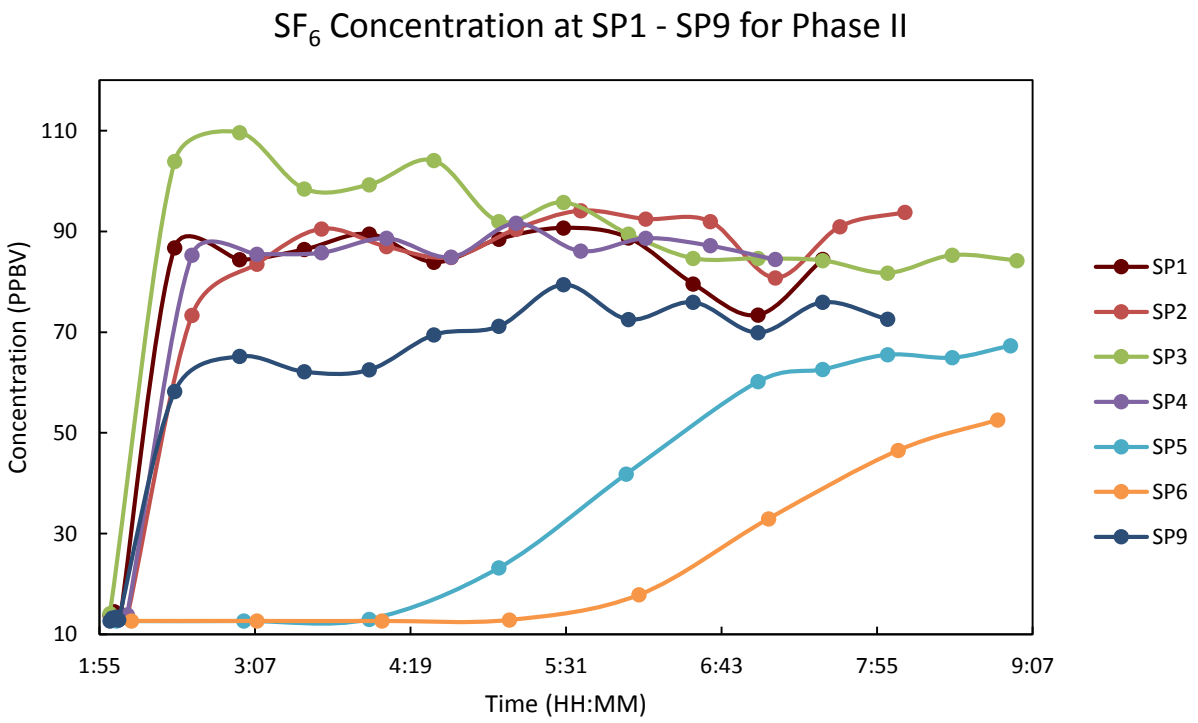

Figure 7.17. SF_6 concentration over time at all sampling points except the tube bundles.

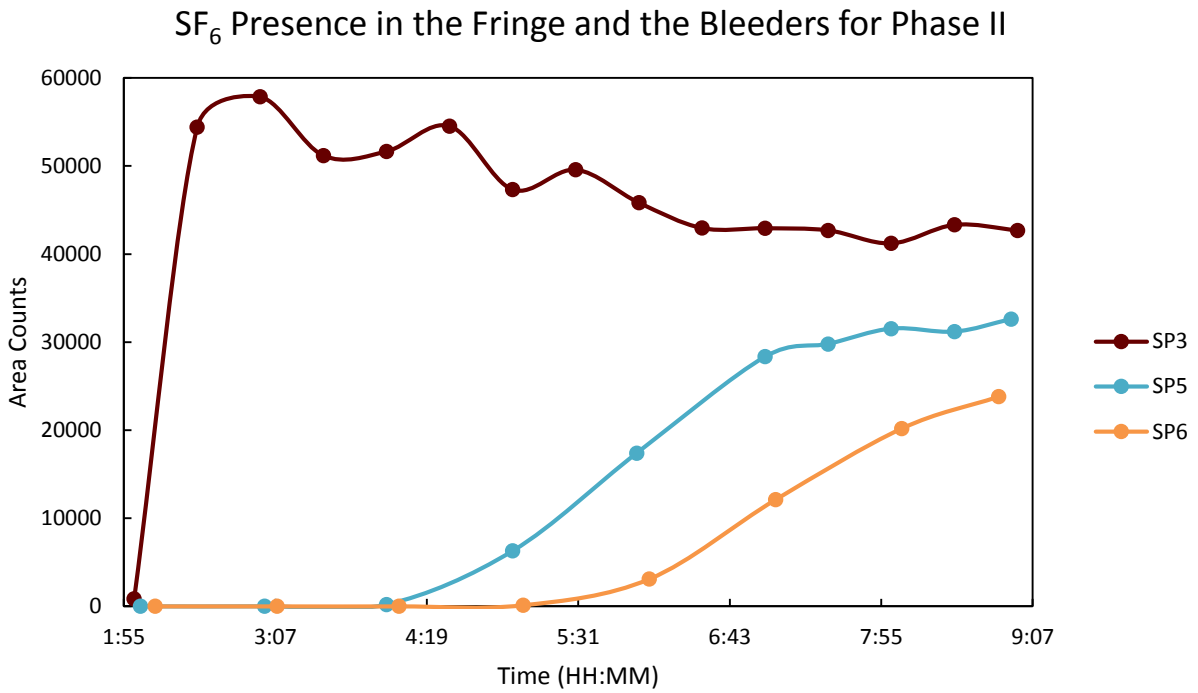

Figure 7.18. SF_6 presence in the fringe and the bleeders. Peak areas are used in this figure to better illustrate the progression of the tracer over time.

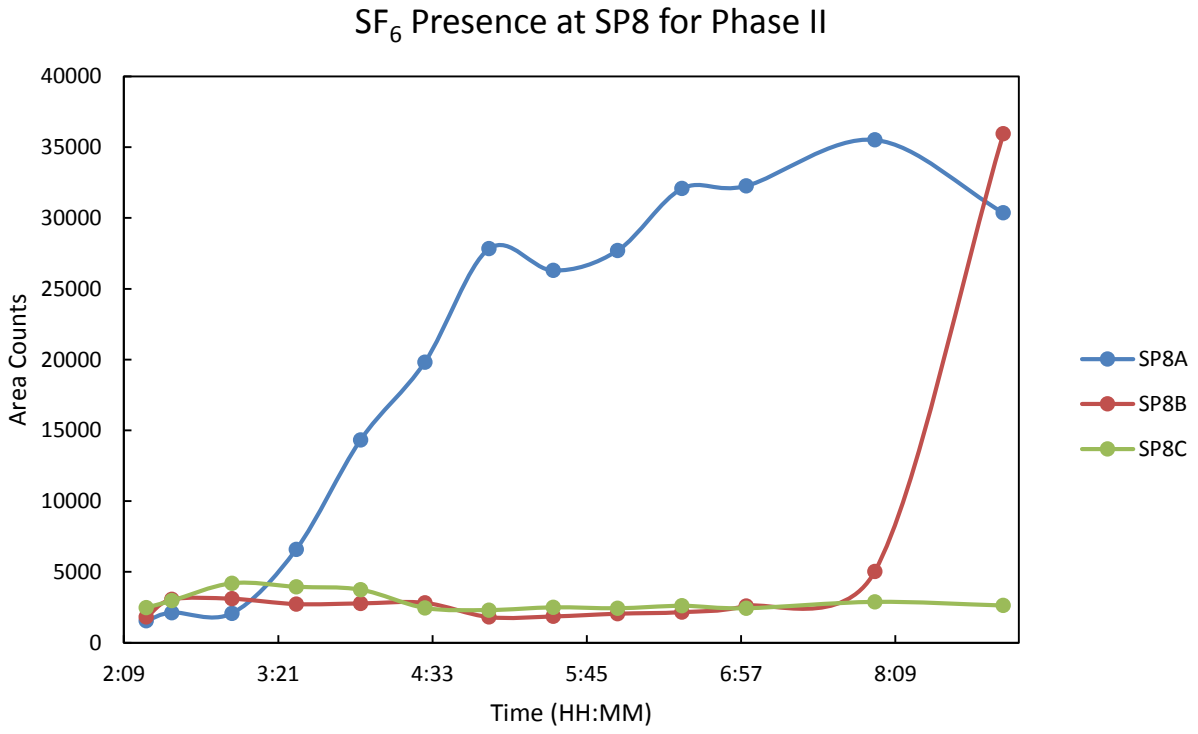

Figure 7.19. SF_6 presence detected in the tailgate tube bundles.

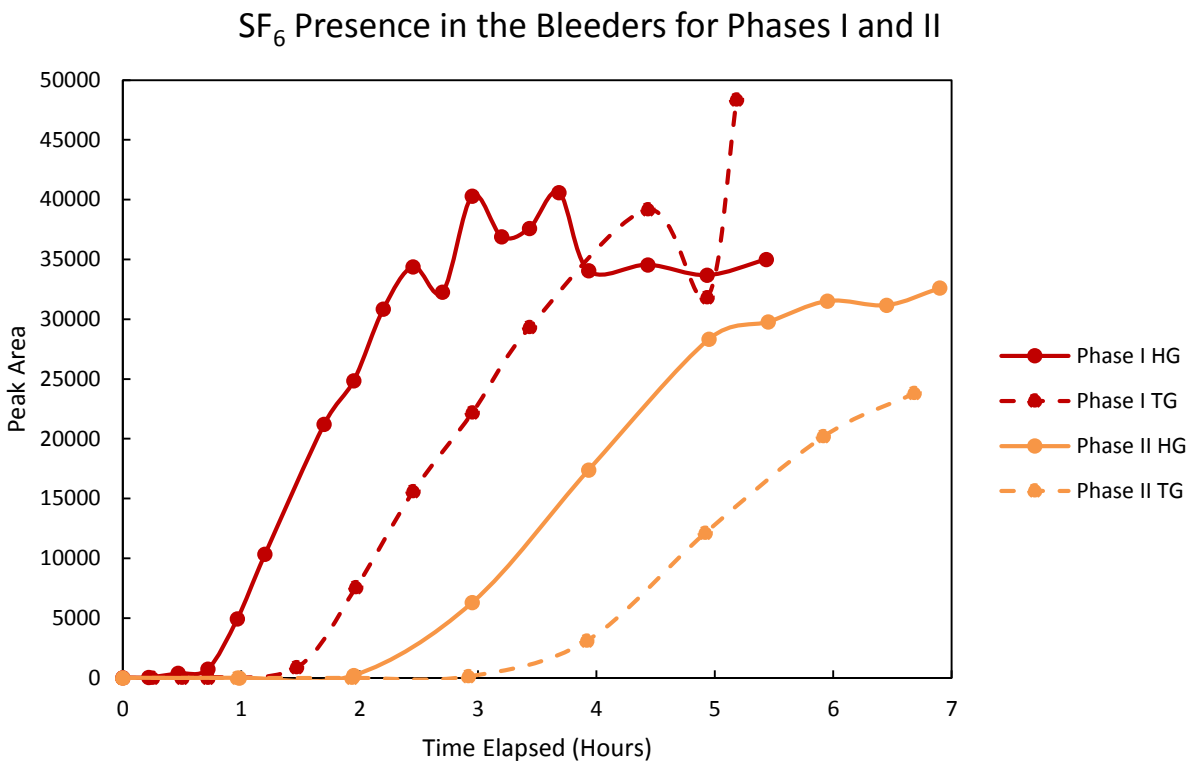

Figure 7.20. SF_6 presence detected at the bleeder taps plotted against time elapsed after tracer release. Results from both Phases I and II are presented.

Using the ventilation survey values, which are displayed with their associated point in **Table 7.11**, the volumetric flow of the tracer was determined using the detected tracer concentration at each of the sampling points with the survey data. The volumetric flow of both the air and SF_6 are presented in **Table 7.11**.

Table 7.11. Phase II air and tracer flow quantities.

Location	Q_{Air} (CFM)	Q_{SF_6} (CFM)
RP1	49,000	0.0113
SP1	84,400	0.0072
SP2	14,400	0.0013
SP3	15,100	0.0057
SP5	1,100	0.0013
SP6	3,300	0.0001
SP9	67,100	0.0005

The volumetric flow of SF_6 at RP1 was determined using the ambient atmospheric conditions recorded at SP1 with a 200 SCCM mass flow (SF_6) assuming ideal gas behavior.

7.5.4 Phase II PMCH Results

The average temperature recorded at SP1 was used in Equation (7.1) to determine the average release rate of PMCH. Based on an average temperature of 21.6°C (70.8°F) and a PPRV plug thickness of 0.635 cm (0.25 in), the release source bundle was expected to produce an average release rate of $6.20 \cdot 10^{-5}$ g/min. Using the surveyed quantity of 1,900 m^3/min (67,100 CFM) from the tailgate, the steady-state concentration of PMCH at SP9 is expected to be 3.60 PPTV.

The vacutainer samples were analyzed using a NCI-GCMS with the same method outlined in Section 7.5.2. The results of the NCI-GCMS analysis of PMCH are displayed in **Table 7.12** and **Figure 7.21**. The SP8 tube bundle data are not presented because the concentration of PMCH was below the LOD. The following data was produced using the same calibration curve outlined in Section 7.5.2.

Table 7.12. Phase II PMCH results.

Sample Number	Time (HH:MM)	Area Counts	PMCH Concentration (PPTV)
SP9-7	2:30	992.3	13.22
SP9-8	3:00	932.0	12.37
SP9-9	3:30	591.3	7.63
SP9-10	4:00	858.7	11.35
SP9-11	4:30	515.0	6.56
SP9-12	5:00	468.3	5.91
SP9-13	5:30	345.0	4.19
SP9-14	6:00	356.0	4.34
SP9-15	6:30	314.3	3.76
SP9-16	7:00	306.7	3.66
SP9-17	7:30	282.0	3.31
SP9-18	8:00	340.0	4.12
SP9-19	8:30	1241.0	16.68
SP9-20	9:00	1531.7	20.73

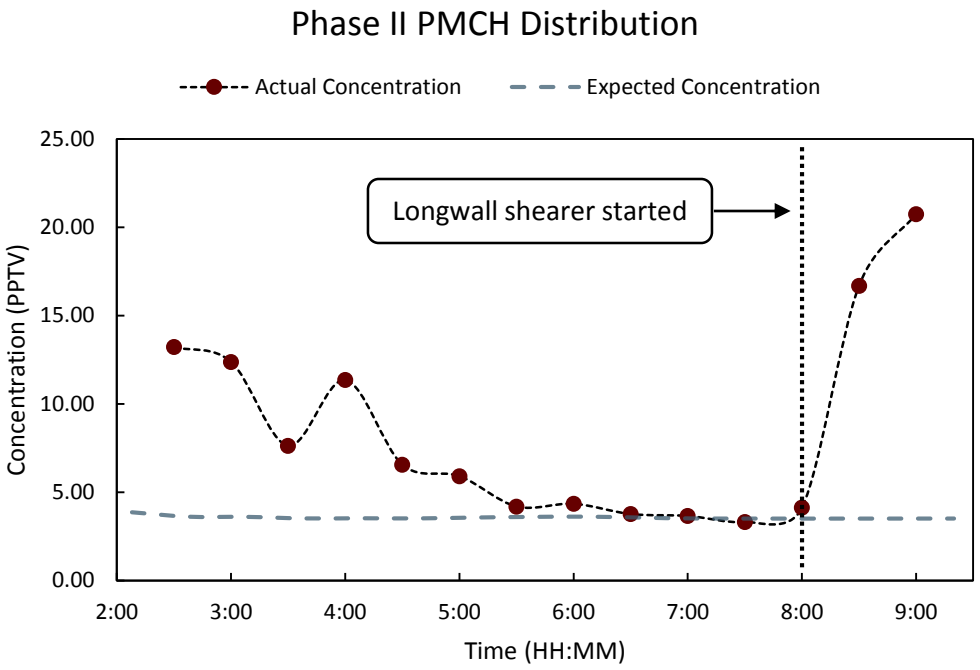

Figure 7.21. Phase II expected and measured PMCH distribution over time.

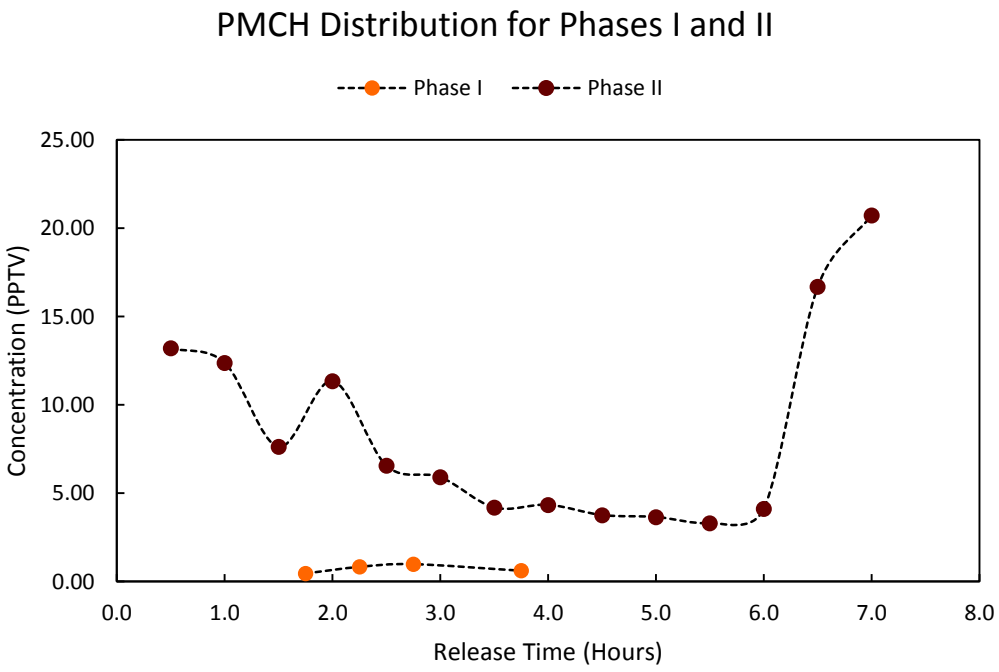

Figure 7.22. Phase I and II measured PMCH distributions over time.

7.6 Discussion and Conclusions

7.6.1 SF_6 Tracer Characterization

The front of the SF_6 stream was immediately apparent at the majority of the sampling points, for both Phases I and II, which can be seen in **Figure 7.10** and **Figure 7.17** respectively. The only exceptions were SP7, which was located in an isolated airway, SP5 and SP6, which were located at the bleeder taps, and the SP8 tube bundles. A discussion of these points is provided later in this section. At the sampling points showing immediate tracer presence, SP1 – SP4 and SP9, the concentration distribution shows that the SF_6 required approximately 30 min to become evenly distributed in the Phase I and II flow streams. This rapid equilibration time demonstrates that the airflow was fully turbulent and traversing the connecting distances quickly. Although air quantities could not be derived from the tracer concentrations at any point other than SP1, the presence of SF_6 coupled with their uniform concentrations at the sampling points demonstrates that the tracer samples were taken in fully developed turbulent flows for both phases of the study. In addition, no significant differences were found between the flow patterns of Phases I and II at the locations represented by SP1 – SP4 and SP9.

Using the concentration of SF_6 at SP1 and the volumetric flow rate of SF_6 from RP1, the airflow quantity at SP1 is calculated to be 55 kcfm for Phase I and 130 kcfm for Phase II. For Phase I, the calculated value was approximately 26 kcfm less than the surveyed airflow quantity of 81 kcfm. For Phase II, the calculated value was approximately 46 kcfm more than the surveyed airflow quantity of 84 kcfm. This discrepancy between the surveyed value and the calculated value of both phases may have resulted from one of three primary reasons: the barometric pressure and temperature readings did not have adequate accuracy, the ventilation survey data contained a discrepancy, or the vacutainer samples were taken at a point in the entry's cross-section with a particularly low SF_6 concentration. Based on the proximity of the sampling point to the air direction change, the physical air sample was most likely taken in an area of layered SF_6 concentrations in the entry for both phases. This conclusion can be inferred from the erratic concentration changes displayed in **Figure 7.10** and **Figure 7.17** for Phases I and II respectively.

The SP1 flow pathway separates into the SP2, SP3, and SP4 flow pathways. From SP1, the average tracer concentration reflects a volumetric SF_6 flow of 0.013 cfm for Phase I and 0.007 cfm for Phase II being delivered from SP1 to the aforementioned branches. These volumetric flows were computed assuming ideal gas behavior of the 200 SCCM mass flow at the recorded environmental conditions. Based on flow conservation, the volumetric tracer flow from SP1 should equal the sum of the volumetric tracer flows from SP2, SP3, and SP4. However, the total flow of the three branches did not balance in terms of quantity for either phase. The Phase I flow is approximately 0.004 cfm greater than the measured tracer flow at SP1. Similarly, the Phase II flow is approximately 0.001 cfm greater than the measured tracer flow at SP1. In order to determine the tracer flow at SP4, the airflow at SP9 was used due to the absence of survey data on the longwall face. These discrepancies equate to an error of 33% and 16% for Phases I and II respectively. The flow discrepancy indicates that SF_6 was added to one of the airflow streams.

The non-conservation of tracer quantity may be the result of leakage from the No. 2 entry to the No. 3 entry that occurred between SP1 and SP3, of an unknown recirculating event at one of the sampling points, or of an error in sampling. Incidentally, a stopping door near SP1 was left open during both studies. This door was located between SP2 and SP3. A short circuit between the No. 2 and No. 3 entries was likely created as a result of the open door. Some of the tracer gas from RP1 would have been diverted into the No. 3 entry prior to reaching SP2. Leakage is thus the most likely explanation of this abnormality. The loss of tracer to SP3 in the airflow stream would have occurred prior to reaching SP2 thus causing an artificially inflated value in the sum of tracer flows from SP2, SP3, and SP4. However, given the low magnitude of the tracer concentration, these errors may not be significant for either phase.

The lack of tracer presence at SP7 for Phases I and II was expected and confirms that this location did not interact significantly with any of the airways directly downwind from the release point. SP7 was the only sampling location at which SF_6 was not detected. Both SP5 and SP6 showed a gradual increase of tracer gas over time. These points were located at the headgate and tailgate bleeder taps respectively. Air is delivered to these taps through the edges of the gob (i.e. the fringe) from the SP3 intake branch. As can be seen in **Figure 7.11**, SP7 and SP8 required approximately four hours and six hours respectively to reach an equilibrium tracer concentration

for Phase I. The time required to reach a steady-state concentration was not captured for Phase II due to logistical complications. Based on the trend in **Figure 7.18**, SP5 and SP6 would have required more than seven hours to reach an equilibrium tracer concentration for Phase II.

The slow increase of tracer concentration over time reflects the low flow, high resistance design of the fringe ventilation system. The arrival time of the tracer front between Phases I and II was approximately 1.5 hours longer for Phase II than for Phase I. This comparison is displayed in **Figure 7.20**. The longer travel time is expected due to the fact that the longwall face had advanced further down the panel thus resulting in a longer distance from the bleeders.

The samples collected from the Phase I 300 ft, 400 ft, and 500 ft tube bundles at SP8 showed the presence of SF_6 but this data is inconclusive. The SF_6 concentrations from the tube bundle are presented in **Figure 7.12**. The random appearance of SF_6 at various magnitudes in the tube bundles suggest the presence of a leak in the tube system. This leak may have been in the tube itself, in the sampling system, or a combination of both. Any one of these three scenarios would have compromised the tracer samples thus contaminating these samples. As such, the results of this study could not identify and inter-zonal interaction between the face ventilation and the gob for the Phase I study.

The samples from the Phase II 200 ft, 300 ft, and 400 ft tailgate tube bundles at SP8 are displayed in **Figure 7.19**. The SF_6 concentrations from the tube bundles does indicate some interaction between the longwall face ventilation and the gob at the 200 ft (SP8A) and 300 ft (SP8B) tube bundles. Although **Figure 7.19** shows that a low concentration of SF_6 was immediately present at each of the tube bundles, a leak in the tube system was not likely given the low SF_6 magnitude and the consistency of the concentration over time. This behavior was reflected by SP8B and SP8C. The double-sided needles used to take the tube bundle samples have a small amount of headspace present in its internal volume. The consistent, low concentration of SF_6 can be attributed to the internal volume of the needle and can be considered as zero SF_6 presence.

The SP8A tube bundle showed a gradual increase of SF_6 over time with the tracer first appearing between two to three hours after the initial release. The increase in tracer concentration and apparent achievement of steady state concentration suggests that the face ventilation did have some flow 61 m (200 ft) into the gob. The lack of significant SF_6 presence at SP8B and SP8C suggests that the interaction with the gob is restricted to a boundary located between SP8A and SP8B. SF_6 does not penetrate deeply enough into the gob to affect SP8C located 122 m (400 ft) into the gob.

A sharp increase in tracer concentration was found at SP8B at the end of the sampling period. This sudden buildup of SF_6 may have been caused by two primary reasons: a collapse in the gob opened a free volume between SP8A and SP8B thus producing a direct flow path between the inlets of these two tube bundles or a failure in the tube bundle/sampling system had occurred. This sharp rise in tracer concentration coincided with the start of the longwall for the morning shift. As such, either scenario was probable.

The SF_6 portion of the tracer study for both studies was free of major errors as reflected by the precision of the data and analysis technique. The qualitative tracer gas data showed that the ventilation flow streams did travel from RP1 to the expected branches. The lack of detectable tracer presence at SP7 confirmed that this point was located in an isolated airway with no communication from the flow streams downwind of RP1. The time required to achieve a steady-state tracer concentration at the sampling points indicated that SP1, SP2, SP3, SP4, and SP9 were located in open, unobstructed airways while SP5 and SP6 were located in areas with low, restricted airflow. Some interaction between the gob and the longwall face ventilation was found for Phase II but not for Phase I. This interaction during Phase II was derived from the SP8 tube bundle system.

7.6.2 PMCH PPRV Evaluation

The PPRVs successfully released a detectable level of PMCH for both Phases I and II. The PMCH analysis results are displayed in Section 7.5.2 and Section 7.5.4. The Phase I results did not provide enough useable quantitative data for a thorough evaluation of the PPRVs. The

majority of the NCI-GCMS data did not provide a sufficient signal to noise ratio for quantification. As a result, only the quantifiable vacutainer samples are presented. However, the presence of PMCH was detected in all of the SP9 tailgate samples. The positive presence of PMCH at an unquantifiable concentration suggests that the PPRVs were located in area of the longwall face that did not allow for homogeneous mixing of the tracer, the SP9 samples had been compromised, or a combination of both. Either event may have occurred given the placement of the sources at a relatively complex area adjacent to the belt conveyor combined with the fact that the samples were not analyzed for several weeks due to equipment complications. Despite the lack of quantitative data provided by Phase I, the presence of PMCH does show that the PPRVs were releasing PMCH.

The Phase II results did successfully provide quantitative data derived from the PPRVs. The NCI-GCMS analysis results are presented in **Table 7.12**. The Phase II PMCH data is also presented graphically in **Figure 7.21**. The distribution of PMCH over time demonstrates that concentration did reach steady-state prior to the activation of the longwall shearer. **Figure 7.21** shows that PMCH required approximately three hours to reach an equilibrium concentration. This increased equilibrium time as compared to SF_6 may have been due to the PPRVs acclimating to the new environmental conditions, the high molecular weight of PMCH, or the manner in which the PPRVs were deployed.

Prior to the study, the PPRVs were transported underground approximately 12 hours prior to the study to allow for temperature acclimation. However, the PPRVs were not placed at the release point. As a result, the temperatures between the two locations may have been sufficiently different to require additional time to reach a steady release rate. In contrast to Phase I, the PPRVs were hung from one of the rear hydraulic arms of the longwall shield for Phase II. The PPRVs were set up in this manner because the Phase II study period intersected with the start of the longwall shearer. As a result, the PPRVs had to be situated in a manner that allowed the bundle to move with the advance of the shield. The rear of the longwall shield did not have a large amount of airflow at the time of the release. The inadequate flow coupled with the high molecular weight of PMCH may have also caused the higher relative equilibration time.

The large spike in tracer concentration occurred just after the start of the longwall shearer. The increase may be been caused by a rise in temperature, a change in ventilation flow, or the opening of a cavity that had been accumulating with PMCH prior to the movement of the shield. Due to the lack of observations at the PMCH release point, the actual cause for the sharp increase is unknown. Despite this unexpected occurrence, the PMCH concentration did achieve and maintain steady-state for approximately three hours.

Based on the surveyed air quantity of 1,900 m^3/min (67,000 cfm), an average temperature of 21.6°C (70.8°F), and an average absolute barometric pressure of 63,400 Pa, the steady-state PMCH concentration was expected to be 3.60 PPTV. The average steady-state concentration measured from the SP9 vacutainer samples was 3.90 PPTV. The difference between the expected and measured concentration equates to an error of 8%. At the PPTV concentration level, an 8% deviation effectively denotes a zero difference between the expected and observed values. Using the detected steady-state concentration of PMCH, the air quantity is calculated to be 1,755 m^3/min (62,000 CFM), which is validated by the results of the ventilation survey.

As such, the PPRVs not only performed according to their design specifications but also supported the ability of Equation (7.1) to predict the release rate of the PPRV. The results of Phase II suggest that the PPRVs will perform as expected in field conditions when placed in an area of adequate turbulent flow. The results of this study also demonstrate the potential of PMCH to supplement SF_6 in tracer gas studies. The location of the SF_6 release point prevented any useful quantitative data to be derived from the tailgate. The location of the PPRVs remediate this problem by providing a secondary release point. Additionally, since SF_6 and PMCH do not interfere with each other when using a GC, these two tracers can be simultaneously analyzed and sampled using the same medium. Given the simplicity of the PPRV, several benefits were realized during the execution of the study. Two of the most prominent advantages were rapid setup and potential for deployment in inaccessible areas, such as the gob. These two advantages were afforded by the simplicity of the PPRV coupled with it passive release mechanism. The PPRV is thus shown to be a feasible system within the parameter of this study for the release of PMCH in underground mine ventilation studies.

7.7 Bibliography

Cooke, K. M., P. G. Simmonds, G. Nickless, and A. P. Makepeace. 2001. "Use of capillary gas chromatography with negative ion-chemical ionization mass spectrometry for the determination of perfluorocarbon tracers in the atmosphere." *Analytical Chemistry* no. 73 (17):4295-4300. doi: 10.1021/ac001253d.

Dietz, R. N. 1991. Commercial applications of perfluorocarbon tracer (PFT) technology. In *The Department of Commerce Environmental Conference, "Protecting the Environment: New Technologies - New Markets"*. Reston, VA.

Dietz, R. N., R. W. Goodrich, E. A. Cote, and R. F. Wieser. 1986. "Detailed description and performance of a passive perfluorocarbon tracer system for building ventilation and air exchange measurements." In *Measured Air Leakage of Buildings*, edited by H. R. Trechsel and P. L. Lagus, 203-264. Philadelphia, PA: American Society for Testing and Materials.

F2 Chemicals Ltd. 2011. Perfluoromethylcyclohexane. Lancashire, United Kingdom.

Geller, L. S., J. W. Elkins, J. M. Lobert, A. D. Clarke, D. F. Hurst, J. H. Butler, and R. C. Myers. 1997. "Tropospheric SF_6: Observed latitudinal distribution and trends, derived emissions and interhemispheric exchange time." *Geophysical Research Letters* no. 24 (6):675-678.

Jordan, S. M., and W. J. Koros. 1990. "Permeability of pure and mixed gases in silicone rubber at elevated pressures." *Journal of Polymer Science Part B: Polymer Physics* no. 28 (6):795-809. doi: 10.1002/polb.1990.090280602.

Levin, I., T. Naegler, R. Heinz, D. Osusko, E. Cuevas, A. Engel, J. Ilmberger, R. L. Langenfelds, B. Neininger, C. v. Rohden, L. P. Steele, R. Weller, D. E. Worthy, and S. A. Zimov. 2010. "The global SF_6 source inferred from long-term high precision atmospheric measurements and its comparison with emission inventories." *Atmospheric Chemistry and Physics* no. 10 (6):2655-2662. doi: 10.5194/acp-10-2655-2010.

Maiss, M., L. P. Steele, R. J. Francey, P. J. Fraser, R. L. Langenfelds, N. B. A. Trivett, and I. Levin. 1996. "Sulfur hexafluoride - a powerful new atmospheric tracer." *Atmospheric Environment* no. 30 (10):1621-1629.

National Institute of Standards and Technology. 2011. Perfluoro(methylcyclohexane). U.S. Secretary of Commerce.

Ravishankara, A. R., S. Solomon, A. A. Turnipseed, and R. F. Warren. 1993. "Atmospheric lifetimes of long-lived halogenated species." *Science* no. 259 (5092):194-199.

Simmonds, P. G., B. R. Greally, S. Olivier, G. Nickless, K. M. Cooke, and R. N. Dietz. 2002. "The background atmospheric concentrations of cyclic perfluorocarbon tracers determined by negative ion-chemical ionization mass spectrometry." *Atmospheric Environment* no. 36 (13):2147-2156.

Thimons, E. D., R. J. Bielicki, and F. N. Kissell. 1974. Using sulfur hexafluoride as a gaseous tracer to study ventilation systems in mines. In *Bureau of Mines Report of Investigations*: United States Department of the Interior.

Watson, T. B., R. Wilke, R. N. Dietz, J. Heiser, and P. Kalb. 2007. "The atmospheric background of perfluorocarbon compounds used as tracers." *Environmental Science and Technology* no. 41 (20):6909-6913.

Chapter 8: Conclusions and Future Work

The study presented in this paper sought to develop a PPRV system that was not only flexible but that allowed for the controlled release of PMCH in an underground mine environment. In order to complete this objective, extensive laboratory and field studies were designed to bring the PPRV from conception to reality. The PPRV development and evaluation study successfully developed a PMCH calibration curve preparation technique for GC, completed an extensive evaluation of potential PPRV designs, deployed a potential PPRV in a small-scale turbulent environment, and completed a field study that validated the final PPRV system. A detailed explanation of each major topic was provided in the preceding chapters.

The multi-dilution calibration curve technique was found to balance level of difficulty with precision thereby producing a viable method for producing PMCH standards. This calibration curve technique proved to be repeatable in the PPRV evaluation studies that followed. The preliminary PPRV designs were found to produce a reliable PMCH release rate and to be free of manufacturing defects. This preliminary study found that plug thickness and temperature significantly affected the release rate. From this data, a comprehensive strip-plot experiment was designed to derive an equation to calculate PMCH release rate as a function of plug thickness and ambient temperature. The results of the final PPRV development study successfully derived an equation to predict release rate as a function of temperature and plug thickness. Additionally, this study confirmed that release rate was independent of both barometric pressure and internal PMCH volume. The PPRV will thus perform consistently across a wide range of elevations and maintain its release rate throughout the majority of its expected lifetime.

In a parallel study, the newly developed PPRVs were evaluated in a controlled turbulent environment. The result of the turbulence experiment showed that the PPRVs were highly precise over a range of flow quantities. Air flows within the transitional characteristic zone were found to cause the PPRV to behave unreliably. Since transitional type flows contain both laminar and turbulent elements, this erratic behavior agrees with the fact that PMCH has a high layering potential from its high molecular weight. Although laminar flows were not included in the evaluation, poor PPRV performance is also expected in the laminar zone due to the inadequate

mixing of PMCH in the flow stream. The final study presented in this paper evaluated the performance of the PPRV in a Midwestern underground longwall mine.

In this field study, the PPRVs performed not only according to their design specifications but also validated the equation derived in the final development study to predict the release rate of the PPRVs. This study also represented the first time that a dual PMCH – SF_6 release has been conducted in an underground mine. The execution of the field study proved to be relatively straightforward when using the PPRVs when compared to SF_6. The simplicity of the PPRV allowed rapid setup of the system. The PPRVs' passive release mechanism also allowed the potential for deployment in inaccessible areas of the mine such as the gob. The results suggest that the PPRVs will perform as expected in an underground mine if the sources are given sufficient time to equilibrate with the environmental conditions. The release sources must also be placed in an area of adequate turbulent flow and be deployed in adequate numbers to satisfy the LOD.

The operating principles of the PPRV show great potential for adaptation to release other similar perfluorocarbon tracers in underground mines. Based on the combined results of this overall study, the PMCH PPRV developed in the preceding chapters was found to be a feasible release system for underground tracer gas studies. This feasibility is, however, limited to the parameters of each of the aforementioned studies. The PPRVs can be enhanced with additional studies designed to develop standard operating procedures (SOP), to examine the effects of release source diameter and plug compression, to examine the effects of sub-ambient temperatures, to investigate the impacts of different underground environments on the PPRV, to explore different techniques for dual tracer releases, as well as to improve trace-level analytical techniques.

The current iteration of the PPRVs would benefit from a comprehensive development of SOPs for tracer studies. The study presented in this paper introduced some recommendations for the use of PPRVs such as suspending the PPRVs in turbulent flow. However, these suggestions were anecdotal in nature and were not formally part of the overall study. A formal study for SOP development would examine the impact of a variety of variables including, but not limited to, different flow path geometries, proximity to ventilation controls, and underground release

locations on the performance of the PPRV. The product of such a study would be to ultimately provide a user's manual for the PPRV along with recommendations on the ideal use of the PPRV based on underground mining conditions.

Given the deployment flexibility of the PPRV, the available release options are indefinite. As a result, a formal SOP study may benefit from being separated into two parts, a broad spectrum exploration of release scenarios to determine significant factors along with an in-depth study of these significant factors. Although numerous experimental designs are available for such a study, any future experiments should at least include performance as a function of PPRV placement at different locations in an entry's cross-section, of PPRV placement in different mining areas such as various longwall faces, continuous miner sections, smooth entries, rough entries, overcasts, etc., and of PPRV proximity to abrupt flow path changes such as a turn, a contraction, an expansion, etc. The interactions of the different placement options should also be included for a more robust study. SOP development should include a discussion regarding the limitations of the PPRVs based on the LOD of various analytical techniques, the flow quantity, and the type of flow. Additionally, a cost-benefit analysis of the PPRV vs. the traditional SF_6 release should be given in order to provide recommendations for when the PPRV may be used in place of SF_6 and when the PPRV may be used in conjunction with SF_6.

One of the limitations of the PPRV is the relatively low release rate when compared to traditional release systems. In order to provide an adequate PMCH concentration with typical underground flow quantities, the PPRV introduced in this study should either be deployed in parallel with other PPRVs or be analyzed using a technique with a sufficient LOD. An increase in PPRV diameter may, however, be another manner in which the PMCH release can be increased. Future studies should examine the effect of this design variable as well as its interaction with plug thickness and temperature on the PPRV's release rate. Increasing the PPRV diameter would result in a sympathetic increase in the exposed surface area of the plug. Greater surface area at a given plug thickness is expected to increase the release rate because of the higher volumetric flow potential. In conjunction with PPRV diameter, the range of temperatures can be expanded to include sub-ambient temperatures to interpolate a wider range of operating conditions. Due to the unknown effect of diameter on the PMCH release rate, close attention should be given to the

data produced by PPRVs with a high diameter to plug thickness ratio. As the release rate increases, a critical point will be reached at which the loss of PMCH through the plug exceeds the rate at which PMCH vaporizes. If this critical point is reached, a vapor pressure equilibrium cannot be maintained and would result in an unsteady release rate.

Further development of the PPRV would benefit from an investigation regarding the impact of different environmental conditions on the integrity of the PPRV. The study presented in this paper showed that the PPRV's release rate would remain consistent throughout at least 90% of the PPRV's estimated lifetime. This long-term viability can only be maintained if the integrity of both the silicone plug and aluminum shell is not breached. The environmental conditions in underground mines can be extremely harsh with dripping water, suspended dust, and nebulized industrial chemicals. A formal study on the long-term effects of such environmental condition on the overall integrity of the PPRV would provide further insight into the operating constraints of the PPRV.

The field evaluation of the PPRV presented in this paper represents the first time that both PMCH and SF_6 have been simultaneously released in an underground mine. As a result, the application of multiple tracers as a mine ventilation characterization tool has not yet been extensively explored. The multi-zone analysis ability afforded by multiple tracers has great potential to enhance the analysis of mine ventilation systems. In addition to the steady state dual release presented in this paper, numerous other quantitation techniques also exist, such as the pulse releases and tracer decay release methods. Although these additional quantitation methods have already been extensively studied in HVAC, further research is needed to translate these models for use in underground mines.

The detection of PMCH and SF_6 in this study was accomplished by sampling the tracer remotely and analyzing the sample later using a GC. This manner of tracer gas analysis has been used numerous times in analog studies and has a well-established protocol. However, this method has two main drawbacks, increased probability of sample contamination and delayed results production. Although vacutainers have shown high sample stability, contamination can still occur through a reduction of stopper integrity through exposure to ultraviolet light and

destruction of the vacutainer itself. The probability of either scenario grows with sample idle time (i.e. the time between sampling and analysis). Sample idle time is an inherent part of underground mine ventilation tracer gas analysis regardless of the analytical technique. Although rapid analysis is not essential to routine tracer gas studies, sample idle time does become a significant factor during emergencies. In order to remove this element, a real-time analytical system can be developed. Incidentally, such a system would also reduce the possibility of sample contamination through the removal of the vacutainer. Although the nature of such future research may seem daunting, current strides in GC technology, such as the micro-ECD, shows great potential for application in manner. The aforementioned suggestions for future work do not represent the full scope for such research but do represent endeavors that maximize the degree of PPRV improvement while minimizing the level of difficulty.